

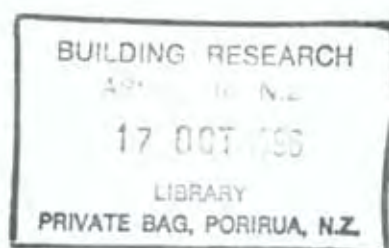


STUDY REPORT

No. 65 (1996)

MODELLING FIRE BEHAVIOUR OF METAL PIPE PENETRATIONS THROUGH CONCRETE WALLS

Stuart J. Thurston



The work reported here was funded jointly by the Building Research Levy
and the Foundation for Research, Science and Technology from
the Public Good Science Fund.

Preface

This report on a project carried out at the Building Research Association of New Zealand describes the computer modelling of heat flow near metal pipe penetrations as they pass through concrete walls. Experimental measurements to verify predictions are presented. The purpose of the project was to reduce the need for full-scale testing and to enable greater extrapolation of test results.

Acknowledgements

The author acknowledges financial support for this project from the Building Research Levy and the Public Good Science Fund of the Foundation for Research Science and Technology. The author wishes to thank the manufacturers of the seals tested, who all donated their products free of charge. Their names and products are listed in Appendix B.

Readership

This report is intended for fire engineers, architects, designers, manufacturers, codewriters and other researchers into the fire resistance of penetrated elements.

MODELLING FIRE BEHAVIOUR OF METAL PIPE PENETRATIONS THROUGH CONCRETE WALLS

BRANZ Study Report SR65

S.J. Thurston

REFERENCE

Thurston, S.J. 1996. Modelling fire behaviour of metal pipe penetrations through concrete walls. Building Research Association of New Zealand. Study Report SR65, Judgeford, Wellington.

KEYWORDS

Concrete; Fire Resistance; Fire Properties; Walls; Mathematical Modelling; Pipes; Seals; Testing; Temperature Measurements; Penetrations.

ABSTRACT

The objective of this project was to model the behaviour of pipe penetrations as they pass through fire-rated concrete walls so that the amount of full-scale testing required can be reduced, greater extrapolation of results can be made, and non-standard fire scenarios can be considered.

The development of a (NISA) computer model to simulate heat flow in a pipe-penetrated concrete wall during a fire is described, and comparisons are made between predictions and experimental results.

The results of two full-scale fire tests using a total of 14 pipes and over 200 thermocouples are presented. These tests were performed to provide a database to assist the modelling. Variables were pipe diameter and thickness, pipe material and seal type.

Contents

Page No.

1.	INTRODUCTION.....	1
1.1	Objective.....	1
1.2	Study Outline.....	1
1.3	Codes and Standards.....	1
1.3.1	New Zealand Building Code requirements	1
1.3.2	Relevant Standards (called up by NZBC Approved Document C3/AS1)	3
1.4	The "Red" Book.....	3
1.5	Types of Pipe Systems.....	3
1.5.1	Plastic pipes.....	3
1.5.2	Metal pipes	4
1.6	Fire Stopping of Services.....	4
1.6.1	Function required	4
1.6.2	Materials commonly used for sealing service penetrations.....	4
1.6.3	Commercially available fire-stop systems	5
1.6.4	Research findings	5
1.7	Computer Models	6
2.	EXPERIMENTAL PROGRAMME	7
2.1	Overview.....	7
2.2	Pipe and Seal Details	8
2.3	Concrete Used for Testing	15
2.4	Fire Exposure Method	15
2.5	Temperature Measurement	15
3.	OBSERVATIONS AND RESULTS	19
3.1	Observations	19
3.2	Furnace Temperatures.....	23
3.3	Verification of Pipe Surface Temperatures.....	26
3.4	Experimental Results	26
3.4.1	All thermocouple results	26
3.4.2	Limit of 180 °C temperature rise.....	26
3.4.3	Thermocouples at "A"	31
3.4.4	Thermocouples at "E"	32
3.4.5	Temperature profiles	32
3.4.6	Radiation guard temperatures.....	33
4.	FINITE ELEMENT (NISA) ANALYSIS.....	33
4.1	Program.....	33
4.2	Assumed Concrete Properties.....	34
4.3	Assumed Steel Properties	36
4.3.1	Thermal conductivity	36
4.3.2	Specific heat	36
4.3.3	Density	36
4.4	Assumed Copper Properties.....	37

4.5	Assumed Lightweight Concrete Properties	37
4.6	Assumed Gypsum Filler Fire-Stop Properties	37
4.7	Assumed Air Properties	37
4.8	Assumed Boundary Conditions	38
4.8.1	Standard fire resistance test	38
4.8.2	Radiation	38
4.8.3	Convection	39
5.	COMPARISON OF EXPERIMENTAL RESULTS WITH NISA PREDICTIONS	39
5.1	Ignoring Heat Flow Within the Pipes	39
5.2	Modelling Heat Flow Within the Pipes	46
6.	CONCLUSIONS	49
6.1	From Research	49
6.2	From Experimental Comparisons	49
6.3	From Comparisons of Predicted and Measured Temperatures	50
7.	RECOMMENDATIONS	50
8.	REFERENCES	50
Appendix A:	Time History Temperature Plots	53
Appendix B:	Proprietary Products Used	76
Appendix C:	Methodology For Performing NISA Analysis	77
Appendix D:	Measured Temperature Profiles Along Pipes	88

FIGURES

Page

Figure 1.	Wall Casting Bed	7
Figure 2.	Wall Storage During Concrete Aging.....	8
Figure 3.	Pipe and Thermocouple Locations	9
Figure 4.	Photographs of Test Walls Installed in Furnace	7
Figure 5.	Separation Distance Between Pipes.....	11
Figure 6.	Details of Seal Construction	13
Figure 7.	Thermocouples Associated With Pipe No. 9	16
Figure 8.	Typical Instrumentation Near Pipe Junction With Wall "Cold" Face.....	17
Figure 9.	Crack Patterns Which Developed in Wall During Fire Testing	19
Figure 10.	Depths of Concrete Spalling Measured on Exposed Face of 175 mm Thick Wall After Test (mm)	20
Figure 11.	Photograph of Concrete Spalling on Exposed Face of 175 mm Thick Wall.....	21
Figure 12.	Comparison of Measured Furnace Temperatures and ISO 834 Curve	24
Figure 13.	Comparison of Thermocouple and Probe Temperatures on Pipe	25
Figure 14.	Temperature Development at "A" on Pipes 1,2,3 & 4	27
Figure 15.	Temperature Development at "A" on Pipes 1,2,8 & 12	27
Figure 16.	Temperature Development at "A" on Pipes 5,6,7 & 14	28
Figure 17.	Temperature Development at "A" on Pipes 9,10,11 & 13	28
Figure 18.	Temperature Development at "E" on Pipes 1,2,3 & 4	29
Figure 19.	Temperature Development at "E" on Pipes 1,2,8 & 12	29
Figure 20.	Temperature Development at "E" on Pipes 5,6,7 & 14	30
Figure 21.	Temperature Development at "E" on Pipes 9,11 & 12	30
Figure 22.	Comparison of Predicted and Measured Temperatures at P1A and P1E (First Material Assumptions).....	40
Figure 23.	Comparison of Predicted and Measured Temperature Profiles Along Pipe 1 (First Material Assumptions).....	40
Figure 24.	Comparison of Predicted and Measured Temperature at P1A and P1E (Second Material Assumptions).....	41
Figure 25.	Comparison of Predicted and Measured Temperature Profiles Along Pipe 1 (Second Material Assumptions)	42
Figure 26.	Comparison of Predicted and Measured Concrete Temperatures.....	43
Figure 27.	Comparison of Predicted and Measured Temperatures at P4A and P4E..	44
Figure 28.	Comparison of Predicted and Measured Temperature Profiles Along Pipe 4	45
Figure 29.	Comparison of Predicted and Measured Temperature at Pipe 4 at Mid Wall Thickness	46
Figure 30.	Comparison of Measured and Predicted Temperatures Along Pipe 4	48

TABLES

Page

Table 1.	Details of Pipes and Seals.....	12
Table 2.	Description of Seals Used.....	14
Table 3.	Seal Backing Rods and Seal Age at Testing.....	14
Table 4.	Measured Concrete Properties	15
Table 5.	Thermocouple Labelling System	18
Table 6.	Observations During Test on 100 mm Thick Wall.....	22
Table 7.	Observations During Test on 175 mm Thick Wall.....	23
Table 8.	Time to Reach 180° Temperature Rise.....	31
Table 9.	Volumetric Enthalpy as a Function of Temperature.....	35
Table 10.	Assumed Steel and Copper Thermal Properties	36

1. INTRODUCTION

Fire compartments are used to limit the risk of fire spread in buildings. Compartments are formed by floors and walls that resist the spread of fire. The most likely points for spread of fire between compartments are the openings created for people and services.

1.1 Objective

The objective of this project is to model the behaviour of pipe penetrations as they pass through fire-rated concrete walls so that the amount of full-scale testing required can be reduced, greater extrapolation of results can be made, and non-standard fire scenarios can be considered.

Over the past few years considerable effort by various manufacturers has been invested in developing proprietary fire-sealing systems designed to ensure that the performance of fire separations is not prejudiced due to inadequate detailing of services which pass through floor/ceiling systems or walls. This concern is also reflected in the New Zealand Building Code Approved Documents (BIA, 1992), where tested fire-stopping systems are required. There is a need for guidelines or methods of extending test results to cover situations other than those tested since it is very difficult to test all the combinations of wall thickness, pipe diameter, gap size etc. These guidelines may enable manufacturers testing new systems to economise on the range of combinations they need to test, and will also provide a sound basis for the test laboratory in providing assessments of variations to tested systems.

1.2 Study Outline

The research reported here considers pipe penetrations passing through cast concrete walls and masonry block walls. Lightweight construction has not been considered. Results from an experimental program were compared with results obtained from a computer model. It was intended that the model would be used to develop guidelines for varying pipe material, pipe wall thickness, pipe diameter, and concrete wall thickness. However, inadequacies in the model became apparent as the study progressed and it was considered unsuitable for this function in its current form. Experimental measurements collected with the purpose of verifying the model are of use in themselves and can be used for verification purposes in any future model developments.

1.3 Codes and Standards

1.3.1 New Zealand Building Code requirements

The relevant part of the New Zealand Building Code (Building Regulations 1992) with regard to pipe penetrations of fire walls is C3.3.3 which states:

“Fire separations shall:

- (a) Where openings occur, be provided with fire resisting closures to maintain the integrity of the fire separations for an adequate time, and
- (b) Where penetrations occur, they shall maintain the fire resistance rating of the fire separation.”

The acceptable solution C3/AS1, Section 6, outlines a solution to meet these requirements.

Section 6.0, C3/AS1, states that fire stops shall be used around penetrations to maintain the continuity and effectiveness of fire separations, and that fire stops are required to have a Fire Resistance Rating (FRR) of no less than that of the fire separation within which they are installed, and they shall be tested in accordance with paragraph E7.0 of Appendix E of the Annex to the Fire Safety Documents (BIA, 1992).

Appendix E7.1 (Fire Resistance) of the Annex to Fire Safety Documents C2,3,4/AS1 states that:

“Primary and secondary elements, closures and fire stops shall be assigned a fire resistance rating (FRR) when tested to:

- AS 1530: Methods for Fire Tests on Building Materials and Structures- Part 4: Fire Resistance Tests of Elements of Building Construction; or
- NZS/BS 476: Fire Tests on Building Materials and Structures- Part 20 to 22. Test Methods and Criteria for the Fire Resistance of Elements of Building Construction.”

Note: BS 476 Part 20 to 22 (BSI, 1987) does not have a specific standard for fire resistance testing of penetration seals and fire stops. The Standard used in New Zealand is AS 1530.4 (SA, 1990).

Requirements of Appendix E7.2 (Fire Resistance) further state that:

“Fire stops shall be tested:

- (a) In circumstances representative of their use in service, paying due regard to the size of expected gaps to be stopped, and the nature of the fire separation within which they are to be used, and
- (b) In accordance with AS 4072 Part 1 Service Penetrations and Control Joints.”

1.3.2 Relevant Standards (called up by NZBC Approved Document C3/AS1)

1. Australian Standard AS 4072 Part 1 (SA, 1992). This Standard sets out requirements for sealing systems (testing, interpretation of test results, installation and certification) at the following locations:
 - (a) around penetrations through separating building elements which are required to have a fire resistance level or, if applicable, a resistance to the incipient spread of fire; and
 - (b) at control joints between building elements which are required to have a fire-resistance level.
2. Australian Standard AS 1530 Part 4 (SA, 1990). This details testing requirements for determination of the fire resistance of construction joints and penetration seals under one or more of the following criteria:
 - **Integrity**
Failure shall be deemed to occur when cracks, fissures or other openings develop through which flames or hot furnace gases can pass to the unexposed side of the penetrated element.
 - **Insulation**
Failure shall be deemed to occur when the temperature of any of the relevant thermocouples attached to the unexposed face of the test specimen rises by more than 180°C above the initial temperature. AS 4072.1 (SA, 1992) specifies the location of these thermocouples to be 25 mm from the edge of the hole in the wall (see Figure 7 for location of these thermocouples labelled as P9A and P9D) and 25 mm along the pipe from the unexposed face (also on Figure 7, as P9E and P9F). It is interesting to note that the Australian Building Code (BCA, 1990) (clause C3.15) waives the insulation requirements for pipes.

1.4 The "Red" Book

The "Red" Book (ASFPCM, 1993) provides a summary of the generic types of seal systems which are available. It also gives information about the suitability of the various seals for different applications.

1.5 Types of Pipe Systems

1.5.1 Plastic pipes

From the experience of testing pipe penetrations at BRANZ, the limitation on fire resistance of plastic pipes is usually the result of destruction of the pipe in the fire compartment. This provides a path for hot gases to flow along the pipe causing the pipe to collapse on the unexposed side, thereby allowing the fire to enter the adjacent compartment.

1.5.2 Metal pipes

In BRANZ experience, fire resistance of metal pipes is usually limited by temperature rises at the unexposed wall face as a result of conduction of heat along the pipe. If all gaps around pipes are adequately sealed then, unless they melt or fracture, metal pipes do not allow escape of flames and combustion products from a compartment containing a fire.

It has been shown (Keough et al. 1976) that metal pipes (cast iron and copper) which have their ends open in the test furnace show temperature rises at the unexposed face which exceed AS 1530 Part 4 (SA, 1990) criteria in about two or three minutes. This is due to hot gases flowing along the pipe. This is unlikely to occur in most installations, but can result where the intensity of the fire is sufficient to melt the pipe walls or where the pipe is damaged by either physical means or as a result of thermal expansion loading of pipe joints during the fire.

Tests carried out in France and reported by Martin (1983) found that metal pipes with diameters less than 60 mm satisfied the heat insulation requirements for two-hour fire tests. In contrast, pipes with diameters of 110 mm and larger reached excessive temperatures at times significantly less than two hours.

1.6 Fire Stopping of Services

1.6.1 Function required

The primary purpose of any fire-stopping method is to seal gaps around a service penetrating a fire-resistant element of construction, to ensure that the passage of flames and hot gases is prevented. There are several desirable attributes, outlined in ASFPCM (1993), that fire-stopping methods and materials should have:

- a) the seals must maintain their integrity in a fire. Loss of integrity could be caused by burning, melting, warping, or cracking due to thermal expansion;
- b) materials should have a simple composition and be easy to install. The installation procedure should be easily reproducible so that the quality of fire-stops is uniform;
- c) cavities should not occur in the sealant or around the penetrating service;
- d) sealants should have a degree of flexibility, combined with load-bearing ability, so that the service can vibrate or undergo small lateral displacements without the seals losing their integrity;
- e) seals should permit easy removal of the service from the penetration.

1.6.2 Materials commonly used for sealing service penetrations

from Martin (1983)

- a) silicone foam fire stop
- b) cement mortar
- c) asbestos wool (no longer used)
- d) intumescent mastics
- e) sleeving of PVC pipe

- f) vermiculite containing cement or vermiculite containing gypsum plaster
- g) ceramic fibre

Other methods (ASFPCM, 1993) include:

- a) room-temperature vulcanising silicone mastics and gels
- b) board materials such as high density mineral wool, calcium silicate, and compressed vermiculite
- c) bags containing an inert or reactive (intumescent) filling material

1.6.3 Commercially available fire-stop systems

A number of patented designs which effectively stop the passage of flames and smoke through fire-resistant barriers are available. Those marketed in New Zealand must comply with the New Zealand Building Code (BIA, 1992) and thus should have been tested by the various manufacturers under similar conditions.

1.6.4 Research findings

Martin (1983) provides an excellent literature overview on the subject and recommends that all penetrations of fire-resistant walls, floors and ceilings must be fire stopped with a material or materials that will have the same fire resistance as the structure in which they are installed. It is most important that these seals are maintained in good condition at all times.

As noted above, to avoid spread of fire, AS 1530 Part 4 (SA, 1990) limits temperature rise on the unexposed side of the wall to 180 °C. Parker et al. (1975) tried to ascertain the danger of fire outbreak caused by hot pipes by placing cotton pads and crumpled newspapers in contact with metal pipes that had reached 500 °C and found no examples of ignition of these combustibles. He concluded that the 180 °C insulation criterion should not apply to services unless it could be demonstrated that a significant fire hazard existed.

Parker et al. (1975) carried out a comprehensive study of the fire resistance of plasterboard walls and ducts containing plastic and metallic plumbing. Nine metallic plumbing installations were tested, consisting of stacks of cast iron, galvanised iron and copper pipes of 50 to 100 mm diameter with 12 mm diameter metal branch pipes. All of these installations successfully withstood more than 60 minutes of fire testing exposure without reaching any of the failure criteria of flame-through, excess surface temperature rise (of wall or duct) or smoke penetration. The authors recommended that the maximum temperature rise criterion should not include branch pipe temperatures, unless it can be demonstrated that they significantly increase fire hazard. Carey (1977) provides discussion to the paper and suggests that adequate firestopping is of greater importance in preventing passage of smoke and flame.

Keough et al. (1976) investigated the fire resistance of uPVC, cast iron and copper pipes penetrating a fire-resisting concrete floor. Pipes of nominal diameters 80 to 100 mm were tested with pipe ends within the furnace either open (thereby venting furnace gases along the bore of the pipe) or sealed (simulating continuous pipework passing through the fire compartment). In the former case, uPVC pipes burnt through the slab within 30 minutes while metal pipes exhibited pronounced heat transfer, causing them to fail the AS 1530 Part 4 thermal insulation criteria in 2 minutes, compared to 16 minutes for uPVC pipes. With the sealed pipes, heat transfer was markedly less and failure of metal pipes by temperature rise was extended to approximately 30 minutes.

Brown and Burn (1980) investigated 50 and 100 mm diameter copper and cast iron pipes penetrating a 100 mm thick concrete slab. They concluded that levels of heat transfer along 100 mm cast iron, copper and brass plumbing pipes penetrating a concrete slab into a model furnace were similar. They considered that the radiation levels emitted from these pipes in up to 2 hours of testing were insufficient to ignite typical combustible building materials held at distances greater than 225 mm from the pipes. However, at 15 mm separation distance, ignition could occur in less than 1 hour. The authors also studied a number of flexible stoppings which demonstrated the ability of horizontal building elements to maintain the fire-resisting performance.

1.7 Computer Models

Hunter and Farin (1981) attempted to provide a model to enable test results to be interpreted and extrapolated. From their study Hunter and Farin proposed a model for electric cable penetrations based purely on heat transfer by conduction. Since the response of the penetration is insensitive to cable spacing, wall conductivity and the convective heat transfer coefficient into the unexposed room, Hunter and Farin concluded that the common factor was simple heat conduction alone.

2. EXPERIMENTAL PROGRAMME

2.1 Overview

Fire exposures were carried out on two concrete walls to AS 1530.4 (SA 1990) with furnace temperatures conforming to ISO 834 (ISO, 1975). Each wall had seven pipe penetrations and used steel or copper pipe types and various fire protection sealing systems. Temperatures were monitored with approximately 100 thermocouples in each wall.

Each wall incorporated a steel reinforcing grid made from 12 mm diameter deformed steel. High tensile wires (1.4 mm diameter) were strung across the moulds to support thermocouples, at pre-determined depths.

The walls were cast horizontally on a plywood sheet supported on a concrete floor within an edge steel frame. The steel frame was used to lift the wall and attach it to the furnace. In some instances collapsible steel sheet, and in others removable plastic cylinders were located in the moulds to form circular holes in the concrete at planned pipe penetration locations (see Figure 1).



Figure 1. Wall Casting Bed

After casting and floating, the concrete was left in the mould and covered with plastic sheeting for 6 days to facilitate concrete curing. Concrete cylinders were cast in plastic pipes, of the same thickness as the wall, and were stored under the same conditions as the wall, to measure concrete density and moisture content representative of the wall.

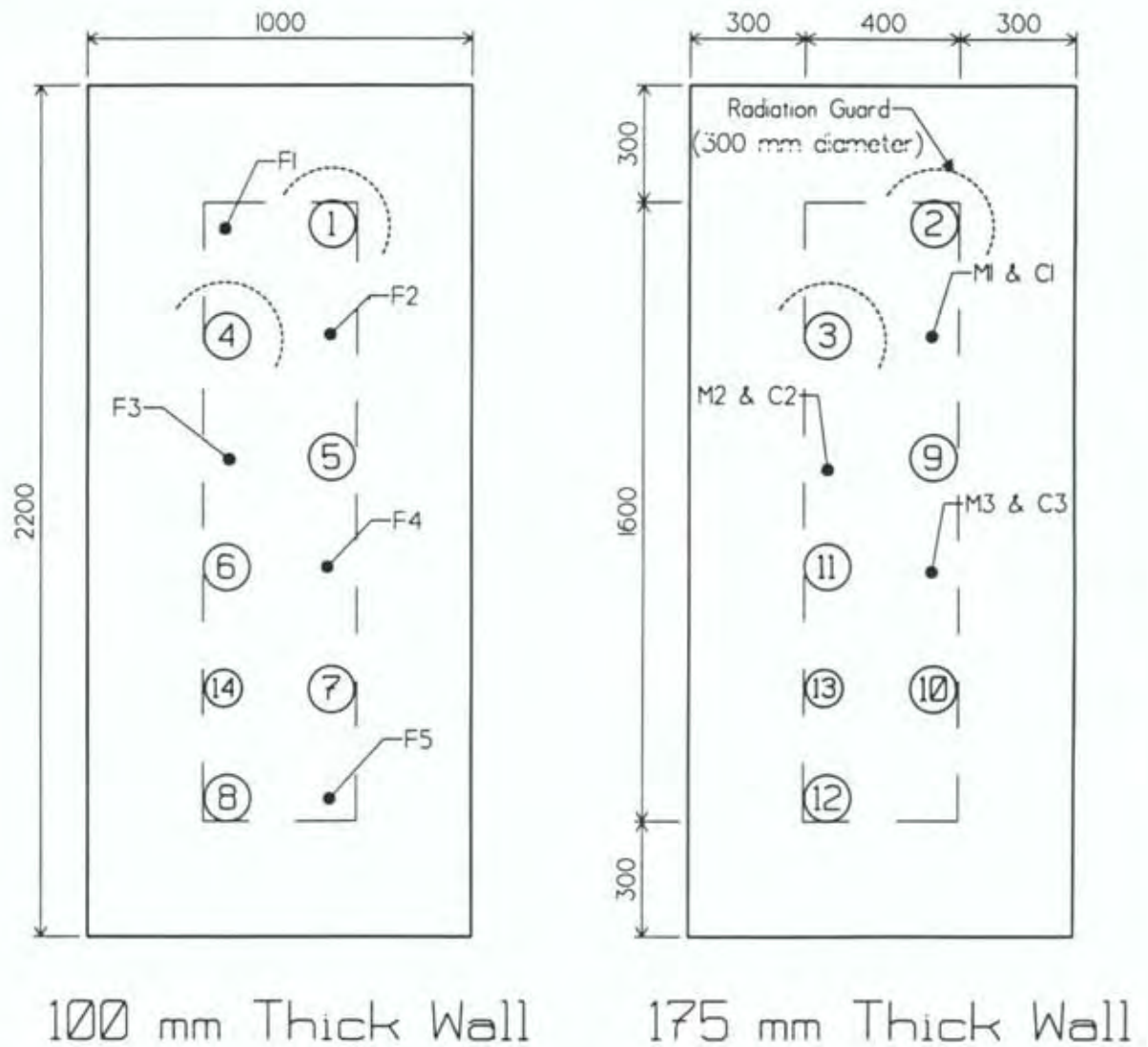
The walls were stored vertically, spaced from each other (see Figure 2), until installed in the furnace for testing.



Figure 2. Wall Storage During Concrete Aging

2.2 Pipe and Seal Details

The general layout of the pipes in the walls is shown in Figure 3 and Figure 4. The pipes and penetrations were at least 300 mm from the wall edges, as required by AS 1530.4 (SA 1990). The separation distance between pipes is given in Figure 5. The pipes extended 100 mm into the furnace and were sealed at the exposed end. They protruded 2 metres through the wall and were structurally supported on a steel frame. The relationship between pipe number, pipe material (steel or copper), pipe size, pipe wall thickness, concrete hole diameter and concrete wall thickness is given in Table 1. Table 1 also gives a key to the seal type used on each pipe. Generic details of the seal corresponding to the key are given in Table 2. Names of seal manufacturers and seal brand names are given in Appendix B. Where backer rods (see Figure 6) were used to form the seals, the details are given in Table 3.



Note

Thermocouples shown above were used in both walls

Those with prefix F were on the hot face

Those with prefix C were on the cold face

and those with prefix M were embedded at mid concrete depth.

Legend

⑧ Pipe location and identifying number

●^{F5} Thermocouple location and identifying symbol

Figure 3. Pipe and Thermocouple Locations

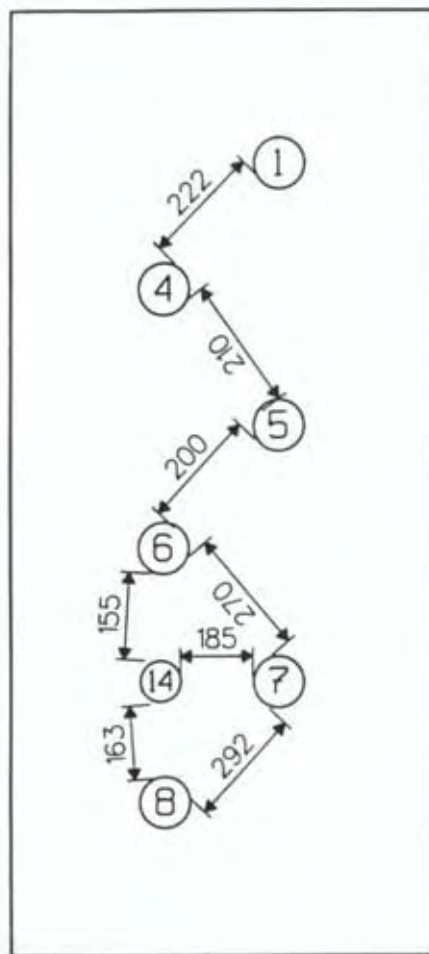


(a) 175 mm Thick Wall

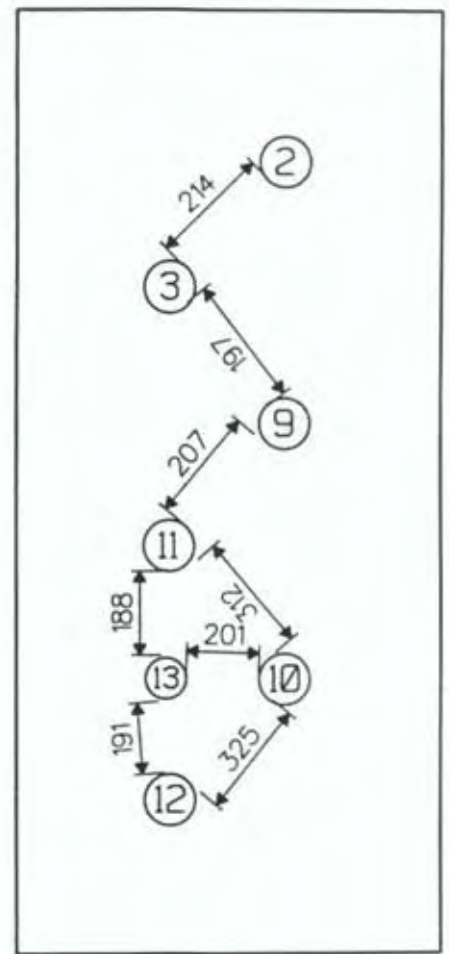


(b) 100 mm Thick Wall

Figure 4. Photographs of Test Walls Installed in Furnace



100 mm Thick Wall



175 mm Thick Wall

Note:

Distances shown are from edge to edge of holes formed in the concrete.

Figure 5. Separation Distance Between Pipes

Table 1. Details of Pipes and Seals

Pipe No.	Pipe Material	Wall Thickness (mm)	Pipe Outside Diameter (mm)	Diameter of Hole in Concrete (mm)	Concrete Thickness (mm)	Steel Mesh Radiation Guard	Pipe Seal Type	
							Hot Face	Cold Face
1	Steel	2.1	101.7	200	100	Yes	E	E
2	Steel	2.0	101.7	200	175	Yes	E	E
3	Steel	8.0	101.5	200	175	Yes	E	E
4	Copper	1.6	104.8	200	100	Yes	E	E
5	Steel	2.0	101.7	140	100	No	-	A
6	Steel	2.0	101.8	160	100	No	-	B
7	Steel	2.0	101.5	120	100	No	C	C
8	Steel	2.0	101.5	140	100	No	D	D
9	Steel	2.0	101.6	160	175	No	-	B
10	Steel	2.0	101.6	121	175	No	B	-
11	Steel	2.0	101.6	148	175	No	F	F
12	Steel	2.0	101.6	140	175	No	D	D
13	Steel	3.3	25.3	126	175	No	E	E
14	Copper	1.25	34.4	126	100	No	E	E

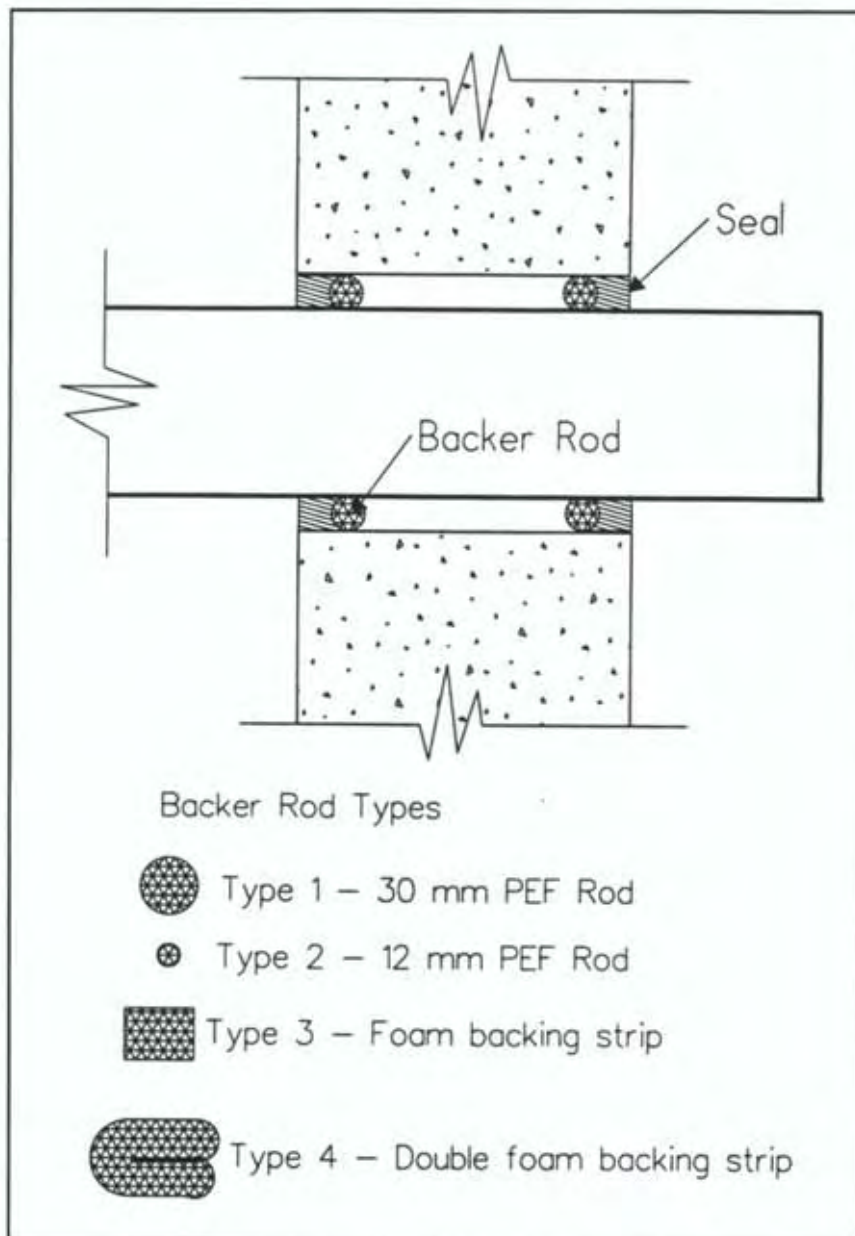


Figure 6. Details of Seal Construction

Table 2. Description of Seals Used

Seal Type	Description
A	Intumescent seal used on one face only
B	Two pack formulation - polyurethane-based seal, not intumescent, used at one concrete face only
C	Acrylic intumescent seal used on both concrete faces
D	Gypsum-based filler. Entire cavity between concrete and pipe filled
E	Lightweight cement composition. Entire cavity between concrete and pipe filled
F	Intumescent seal, used at both concrete faces

Table 3. Seal Backing Rods and Seal Age at Testing

Pipe No.	Seal Type	Age at Testing (Weeks)	Average Clearance (mm) **	Depth of Seal (mm)	Backing Rod Type *
5	A	6	18.1	25	3
6	B	6	29.1	30	4
7	C	7	9.3	9	2
9	B	7	29.2	30	4
10	B	7	9.8	10	3
11	F	8	23.3	12	1

Legend

- * 1 30 mm diameter PEF rod
 2 12 mm diameter PEF rod
 3 Polymer foam backing strip, size 27 mm high x 36 mm wide. Turns to charcoal and crumbles on burning.
 4 As 3 but bent double. Size before bending 27 mm high x 55 mm long.
 ** = Distance between pipe and concrete wall.

For some pipes (as defined in Table 1), a radiation guard was used around the pipe on the unexposed side of the wall. This was a 450 mm long semi-circular cylinder of steel mesh as shown in Figure 3 and Figure 8.

2.3 Concrete Used for Testing

The concrete was mixed on site using a concrete mixer. The aggregate was supplied by Firth Concrete Products and was originally obtained from the Winstone Belmont Quarry. The mix was made using the volume ratio 1 cement: 6 aggregate. Concrete moisture contents and density measurements are given in Table 4.

Table 4. Measured Concrete Properties

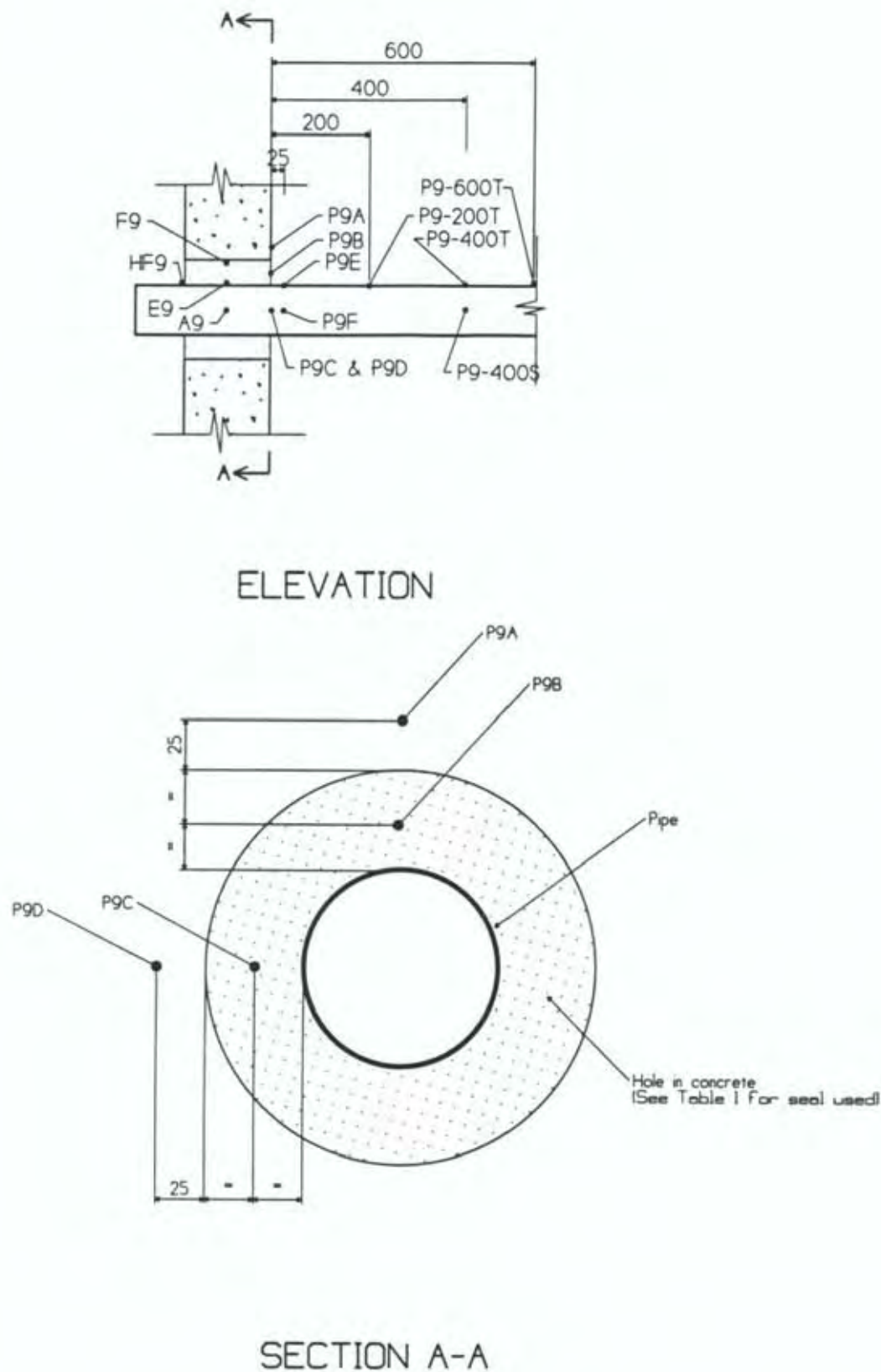
Wall Thickness (mm)	Moisture Lost During Curing %	Final Wet Density kg/m ³	Moisture Content by Weight at Test %	Concrete Age at Testing (Weeks)
100	1.64	2374	5.04	13
175	1.22	2379	6.35	14

2.4 Fire Exposure Method

The concrete walls were tested in the 1.0 m by 2.2 m diesel-fired pilot furnace at BRANZ laboratories, Judgeford (Figure 6). Fire exposures were carried out in July 1994.

2.5 Temperature Measurement

A description of the thermocouple labelling system used is given in Table 5 and a listing of all thermocouples used is given in Table A.1 and A.2 of Appendix A. The location and referencing symbols of thermocouples either embedded in the concrete, or placed on the concrete surface, are shown in Figure 3. Thermocouples associated with particular pipes (e.g. Pipe 9) are shown in Figure 7. The symbols for thermocouples at pipe locations other than Pipe 9 are the same as given in Figure 7, except replace the "9" in the pipe label with the relevant pipe number.



Note: A shorthand notation of "A" and "E" is used for thermocouples P9A and P9E respectively.

Figure 7. Thermocouples Associated With Pipe No. 9

Particular attention is given to thermocouples P9A and P9E in this report. When referring to these particular thermocouples for any general pipe, a shorthand notation of "A" and "E" respectively is used.

Thermocouples were also put on radiation guards (where used) and these are identified by the letter "G" in the thermocouple label. For instance, a label P3-G25S refers to a thermocouple on the radiation guard around Pipe 3, 25 mm from the unexposed concrete face, and on the side (i.e. "S") rather than the top (i.e. "T") of the guard (See Figure 8).

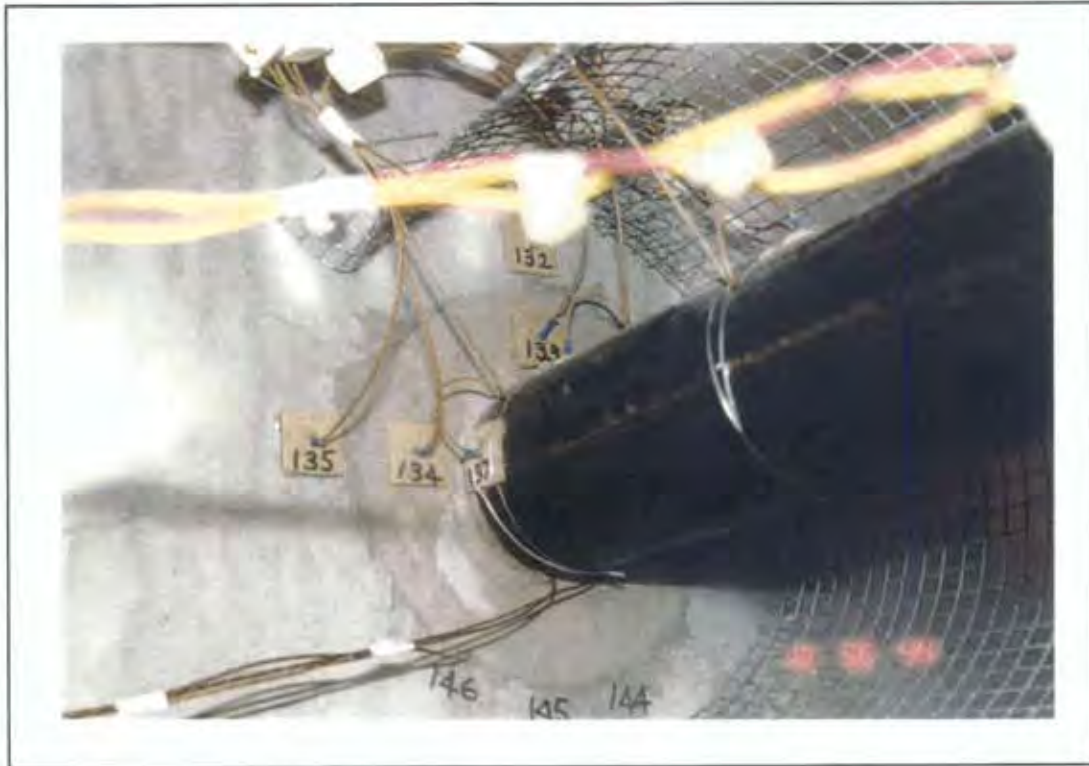


Figure 8. Typical Instrumentation Near Pipe Junction With Wall "Cold" Face

Thermocouple types were all Type K chromel/alumel thermocouples. Disk type thermocouples with pads were used on the pipes and unexposed wall face. "Quick tips" were used on the exposed face and embedded in the concrete.

Time history plots of all thermocouple readings are presented in Appendix A, each plot being identified by the labels as described above.

The thermocouples were connected to a Hewlett-Packard HP 3497 data acquisition unit (DAU) capable of monitoring the 100 thermocouple channels used every 60 seconds. The DAU was controlled by a Hewlett-Packard series 9000 computer.

Table 5. Thermocouple Labelling System

Thermocouple Label *	See Figure Number	Description
General Thermocouples		
F1-F5	3	Thermocouples on concrete exposed face
M1-M3	3	Thermocouples embedded in the concrete at wall mid-depth
C1-C3	3	Thermocouples on concrete unexposed face
FA1-FA4	-	Within the furnace distributed in a vertical plane 100 mm from the exposed concrete face
AAIR		Ambient air temperature
Thermocouples Associated with Particular Pipes		
HF9	7	Located at junction of pipe and exposed wall surface
A9	7	In the air in the middle of the pipe at wall mid-depth
E9	7	On the pipe surface at wall mid-depth
F9	7	On the concrete hole surface at wall mid-depth
P9A	7	On the concrete surface on the unexposed side of the wall 25 mm above the edge of the concrete hole
P9B	7	At mid-thickness of the seal above the pipe on the unexposed side of the wall
P9C	7	At mid-thickness of the seal to the side of the pipe on the unexposed side of the wall
P9D	7	On the concrete surface on the unexposed side of the wall 25 mm to the side of the edge of the concrete hole
P9E	7	On the top of the pipe, 25 mm from the unexposed concrete face
P9F	7	On the side of the pipe, 25 mm from the unexposed concrete face
P9-200T	7	On the top of the pipe, 200 mm from the unexposed concrete face
P9-400T	7	On the top of the pipe, 400 mm from the unexposed concrete face
P9-400S	7	On the side of the pipe, 400 mm from the unexposed concrete face
P9-600T	7	On the top of the pipe, 600 mm from the unexposed concrete face
P9-G25T	-	Top of the fire guard, 25 mm from the unexposed concrete face
P9-G25S	-	Side of the fire guard, 25 mm from the unexposed concrete face
P9-G400T	-	Top of the fire guard, 400 mm from the unexposed concrete face
P9-G400S	-	Side of the fire guard, 400 mm from the unexposed concrete face

Legend

* The symbols above are for thermocouples at Pipe 9. For other pipe locations use the same label as given above, except replace the "9" in the pipe label with the relevant pipe number.

3. OBSERVATIONS AND RESULTS

3.1 Observations

Observations noted during testing of the 100 and 175 mm thick walls are given in Table 6 and Table 7 respectively. The observations refer to what was visible on the unexposed face except for comments on concrete spalling on the exposed face (which could be seen through furnace observation windows). No damage was detected other than that noted in these tables.

Figure 9 shows the crack patterns that developed in the two test walls. More water was observed coming through the unexposed (i.e. cold) face of the 175 mm thick wall than the 100 mm thick wall. Concrete spalling on the exposed (i.e. hot) face of the 175 mm thick wall was far more extensive than on the 100 mm thick wall (see Figures 9 -11). At the end of the test it was noted that many (dull red) globules of a light, aerated substance had formed on the exposed surface, presumably from melting of some component of the concrete aggregate which had bubbled and migrated to the surface.

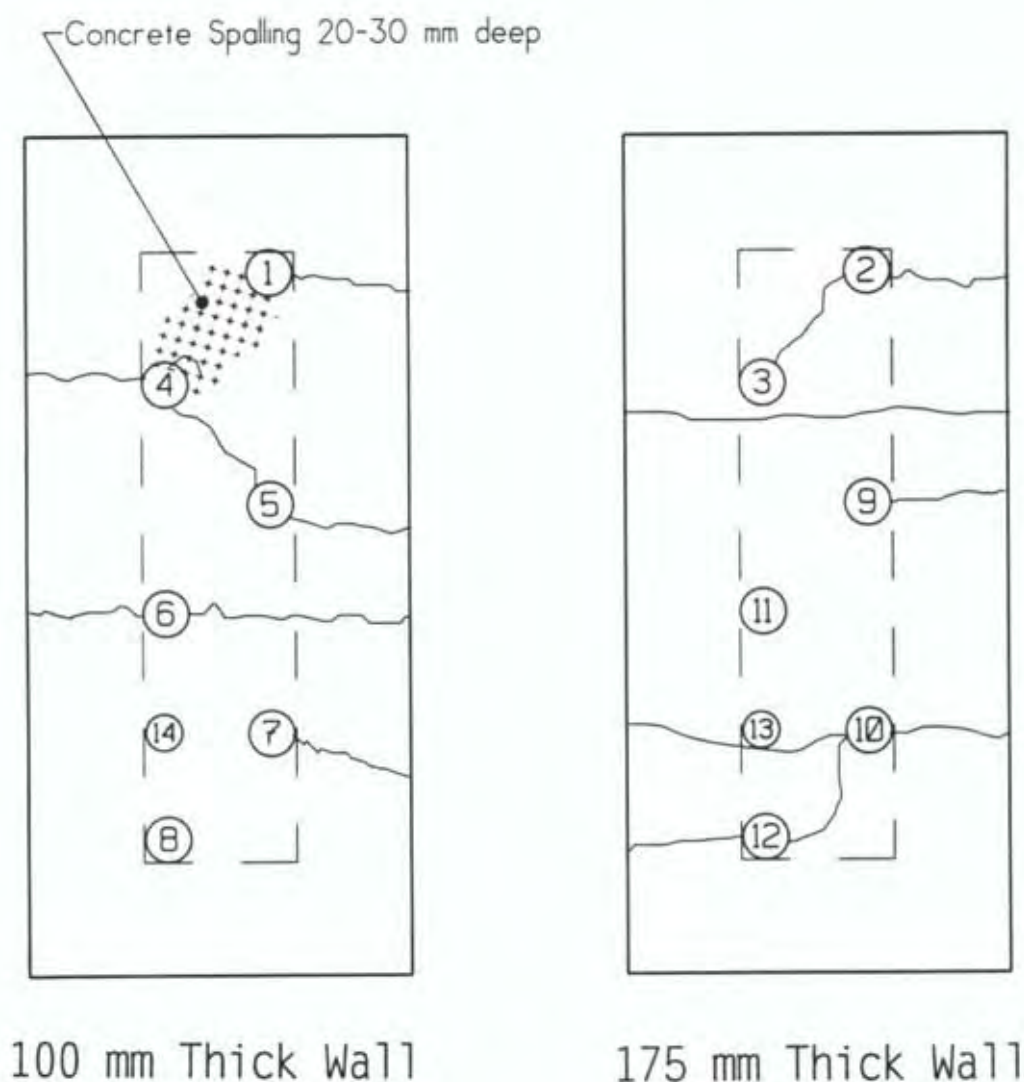
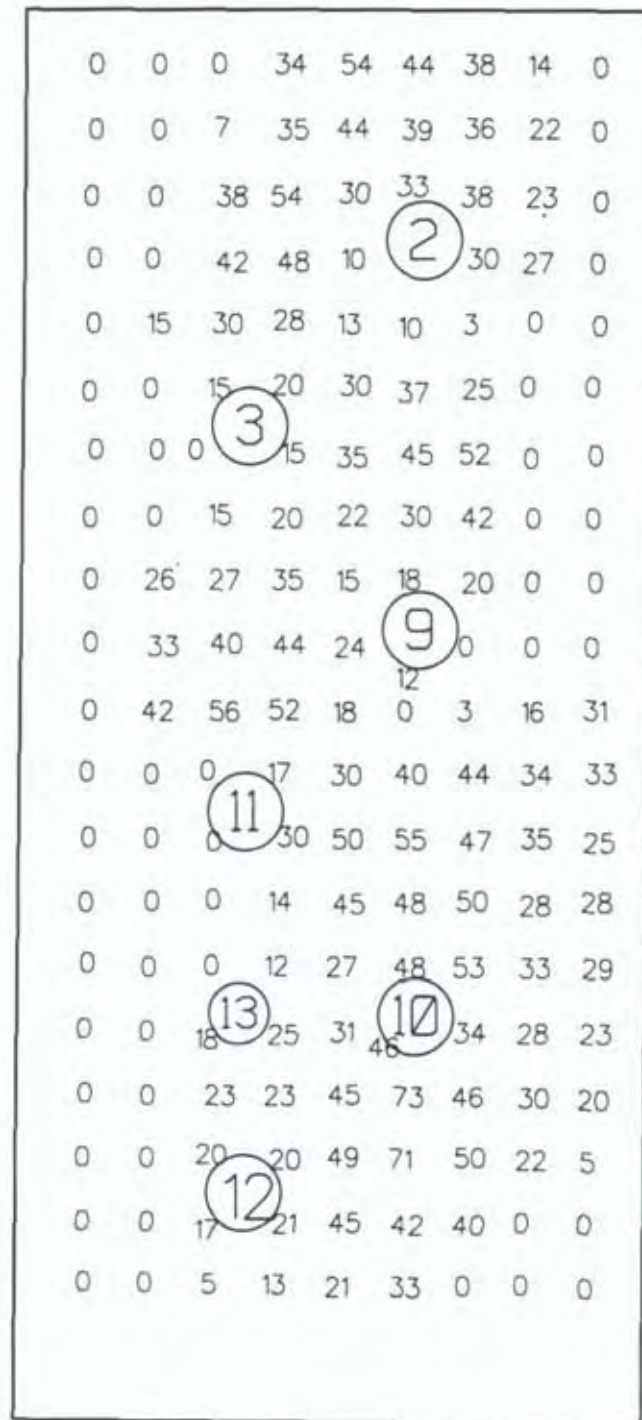


Figure 9. Crack Patterns Which Developed in Wall During Fire Testing



175 mm Thick Wall

Figure 10. Depths of Concrete Spalling Measured on Exposed Face of 175 mm Thick Wall After Test (mm)



Figure 11. Photograph of Concrete Spalling on Exposed Face of 175 mm Thick Wall

Table 6. Observations During Test on 100 mm Thick Wall

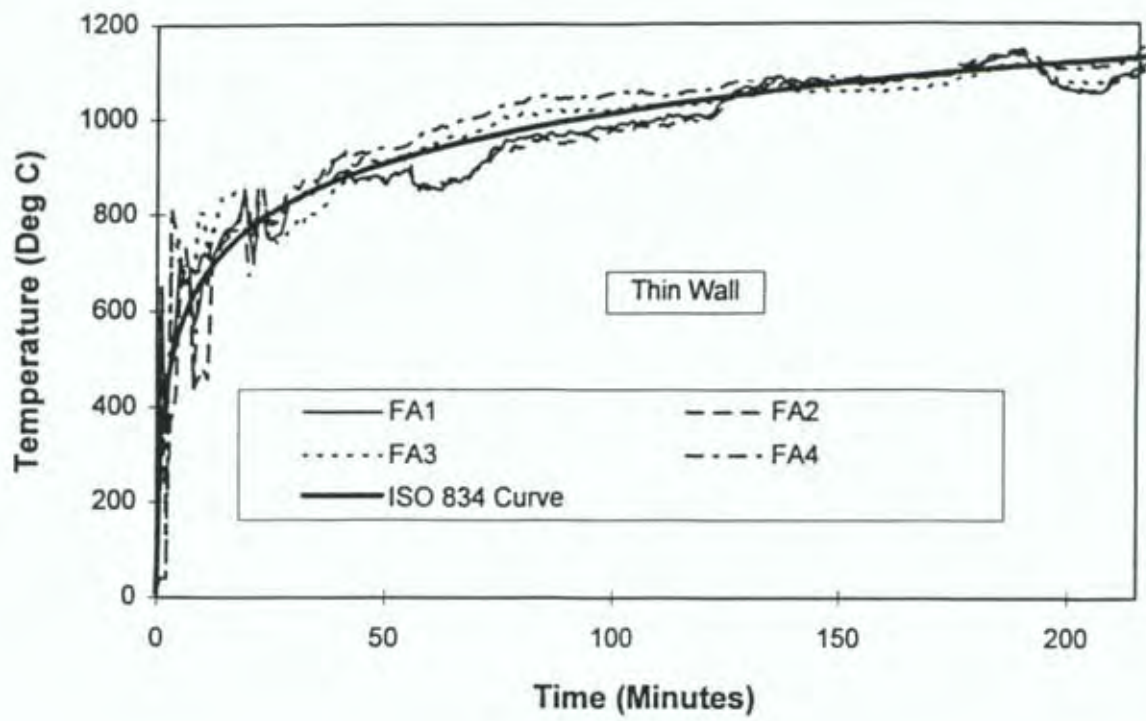
Time (Minutes)	Observations
14	Steam/smoke emitted through top of seal on Pipe 7 and through the ends of most pipes.
16	Development of crack in concrete passing through Pipe 6 (see Figure 9). Concrete spalling on exposed face 20 - 30 mm deep x 200 mm wide linking top of Pipe 4 with bottom of Pipe 1.
19	Full development of cracks as shown in Figure 9. Water seeping through cracks and running down unexposed wall face.
34	Resin in seal at Pipe 6 (at unexposed face) became fluid and left granular filler. Slight swelling of seal at Pipe 5.
45	Resin in seal at Pipe 6 pouring out of hole. Water stopped seeping out of concrete cracks, but steam being emitted.
55	Seal at Pipe 5 protruding 20 mm and cracking up.
73	Steam coming out of seal on Pipe 6 through 8 mm radial gap.
74	Ignition at seal at Pipe 6. Gap between concrete and pipe stopped with ceramic fibre to allow test to continue.
80	Concrete now dry on unexposed face.
90	Seal at Pipe 5 stopped intumescent. It had become a dry brittle texture that fell off on touching.
100	Fine cracks developed in seal on Pipe 8.
230	Copper Pipe No. 4 burnt through on hot face and smoke poured through.

Table 7. Observations During Test on 175 mm Thick Wall

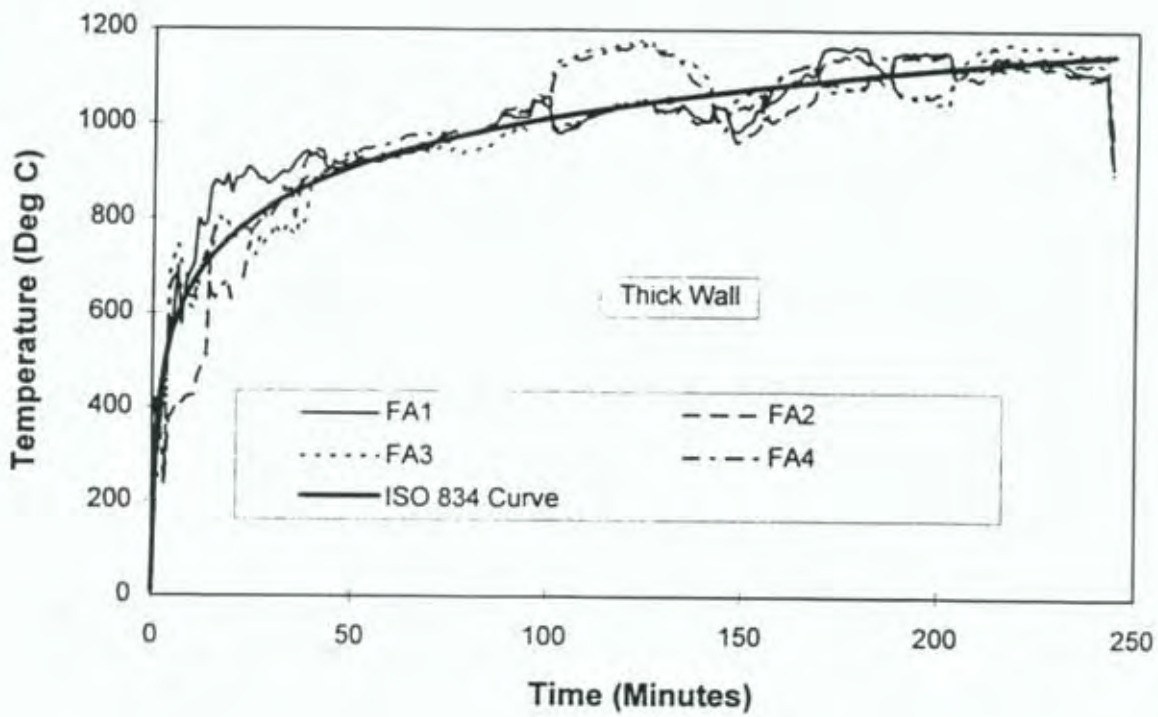
Time (Minutes)	Observations
5	A loud noise of concrete spalling occurred. Spalling on exposed face detected directly above Pipe 2.
9	Smoke/steam being emitted from end of pipes.
14	Fire breaking out of seal at Pipe No. 10. Seal was covered with ceramic fibre insulation to allow test to continue.
17	Spalling, about 15 mm deep, near Pipe 10.
19	First concrete cracks (two) appeared.
25	Water seeping from cracks.
36	Spalling continuing, but intermittent. Water flowing through concrete cracks.
65	Less water being emitted from cracks, but continuous steam. Dry patches appearing on unexposed face.
78	Seal at Pipe No. 9 going liquid. Seal pulling back from pipe and turning brown at edge.
83	Seal at Pipe 11 protruding out of pipe by about 5 mm.
120	Water stopped being emitted from cracks. Pipe 11 seal pulled back from pipe and swollen.
132	Tiny gap at seal of Pipe 9 through which furnace glow was visible.
137	Flames burst through Pipe 9. Stopped with ceramic fibre.
145	Unexposed concrete face dry, except cracks showing moisture at edge.

3.2 Furnace Temperatures

The measured furnace temperatures closely followed the ISO 834 Curve (ISO, 1975), as shown in Figure 12 on the next page.

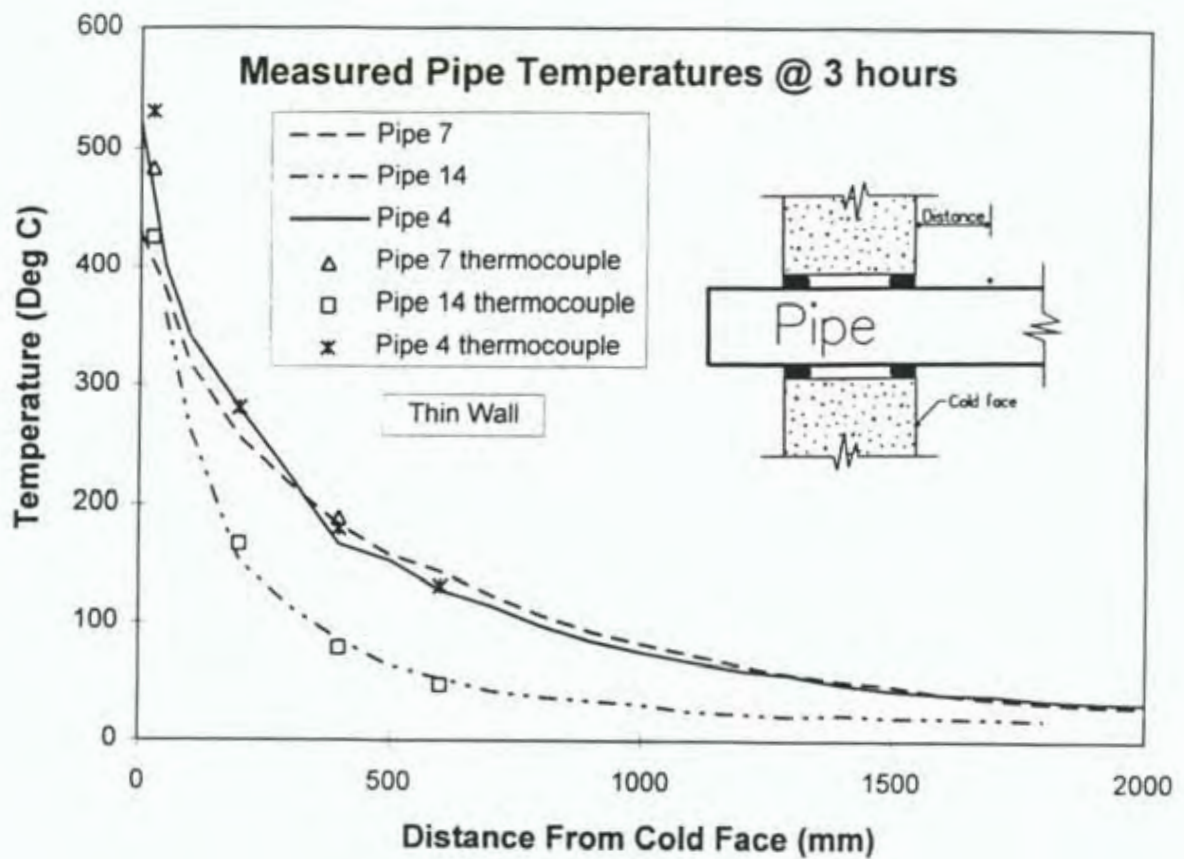


(a) 100 mm Thick Wall

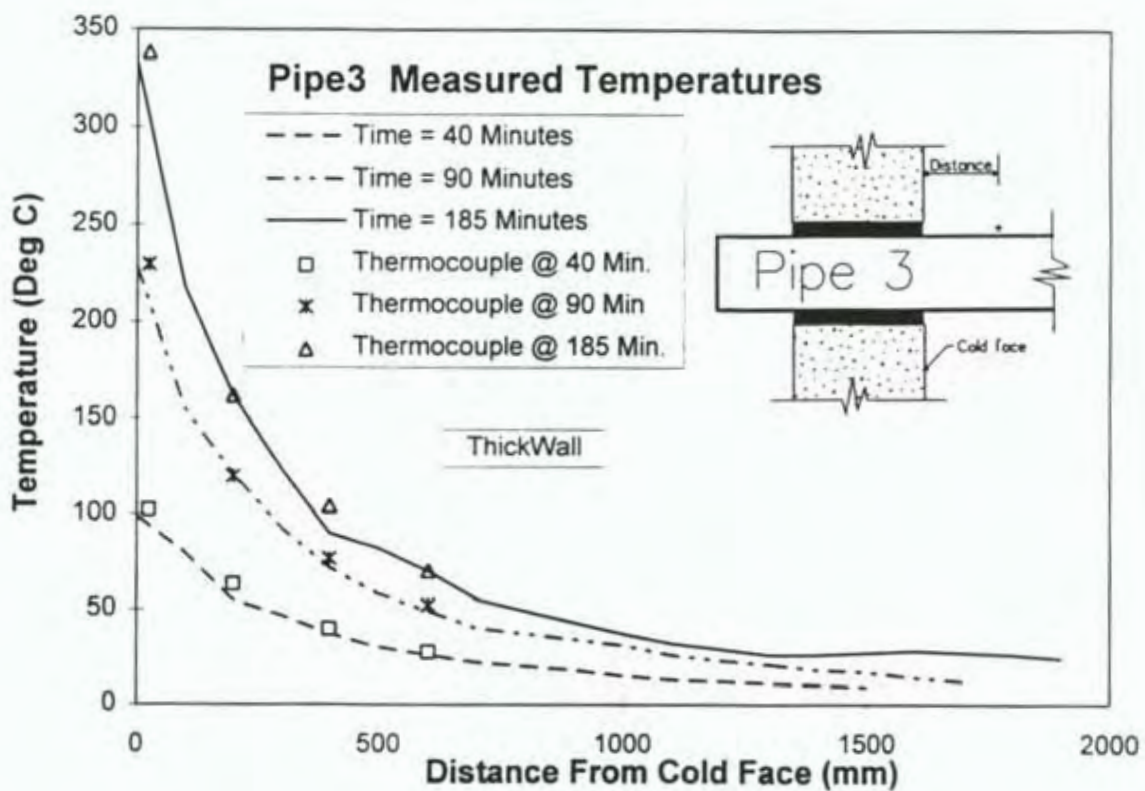


(b) 175 mm Thick Wall

Figure 12. Comparison of Measured Furnace Temperatures and ISO 834 Curve



(a) 100 mm Thick Wall



(b) 175 mm Thick Wall

Figure 13. Comparison of Thermocouple and Probe Temperatures on Pipe

3.3 Verification of Pipe Surface Temperatures

An X-80 Thermo Tester roving probe was used to measure “spot” pipe surface temperatures. Figure 13(a) compares the temperature profiles along the pipes as recorded with the probe to those recorded with thermocouples for three pipes in the 100 mm thick wall. Figure 13(b) compares temperature profiles along Pipe 3 at three selected times in the 175 mm thick wall. Agreement in all instances is within 7% which in the author’s opinion, indicates that the thermocouple pad has relatively small effect on local temperatures.

3.4 Experimental Results

3.4.1 All thermocouple results

Temperature time history plots for all thermocouples are given in Appendix A. Many of these plots exhibit “flat portions” (i.e. plateaus) at about 100 °C temperature. Water changes state from liquid to gas (i.e. steam) at this temperature, absorbing a large amount of energy (latent heat) in the process. A summary of the temperature rises for all thermocouples is also given in Table A.1 and A.2 of Appendix A.

3.4.2 Limit of 180 °C temperature rise

As discussed in Section 1.3.2 the insulation requirements stipulated in AS 1530.4 (SA 1990) limit temperature rise to 180°C at thermocouple locations P9A, P9B and P9E of Figure 7. When referring to these particular thermocouples for any general pipe, a shorthand notation of “A” and “E” respectively is used in this report. A time history plot for all gauges at location “A” on the concrete is given in Figures 14-17, and for gauges at location “E” on the steel in Figures 18-21. Table 8 lists the time to reach 180°C temperature rise for all these thermocouples. Note that the temperatures (within the first hour) at these locations would have been significantly influenced by water running down the unexposed face.

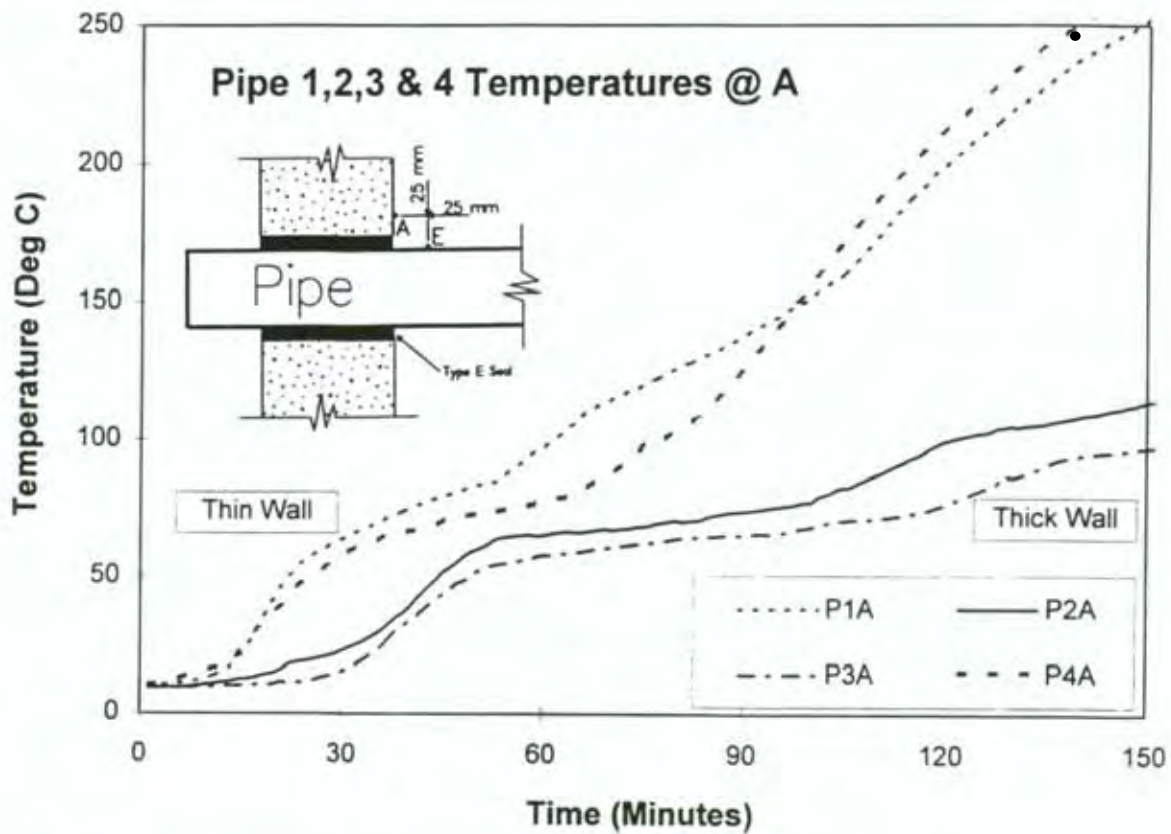


Figure 14. Temperature Development at "A" on Pipes 1,2,3 & 4

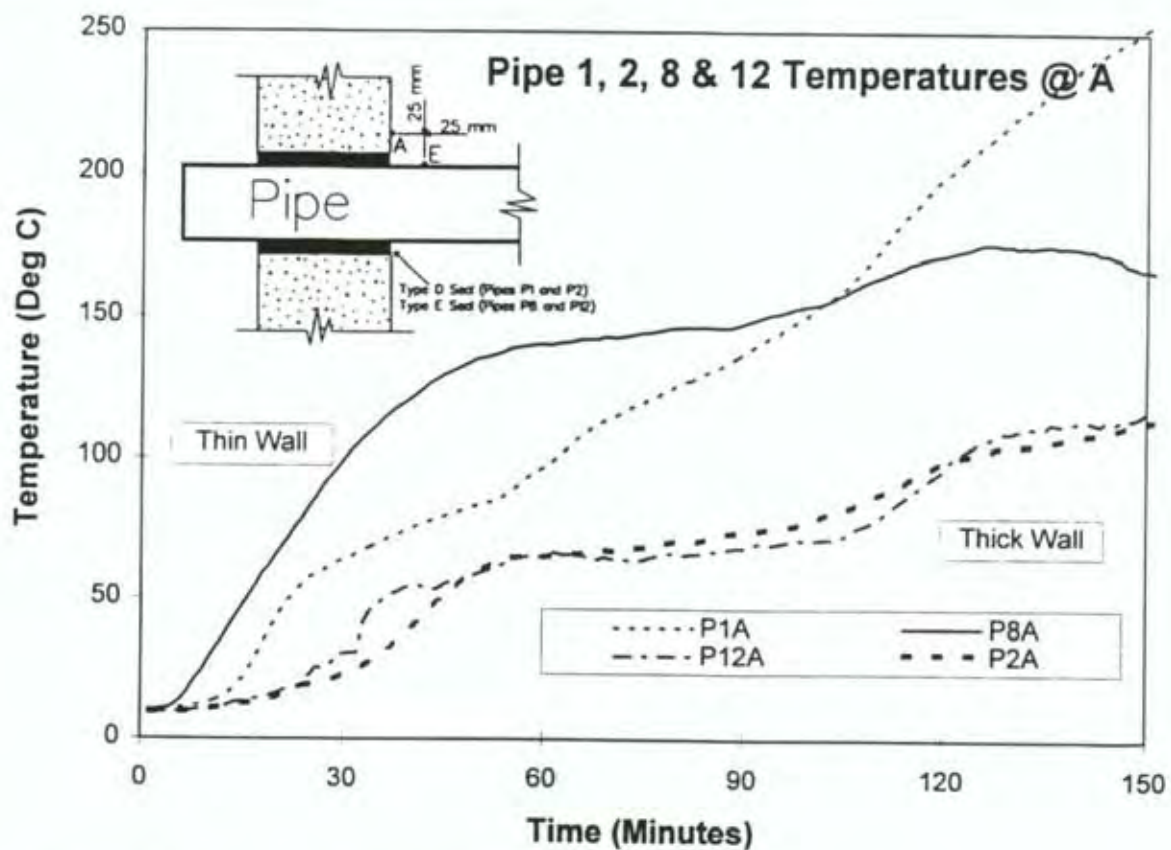


Figure 15. Temperature Development at "A" on Pipes 1,2,8 & 12

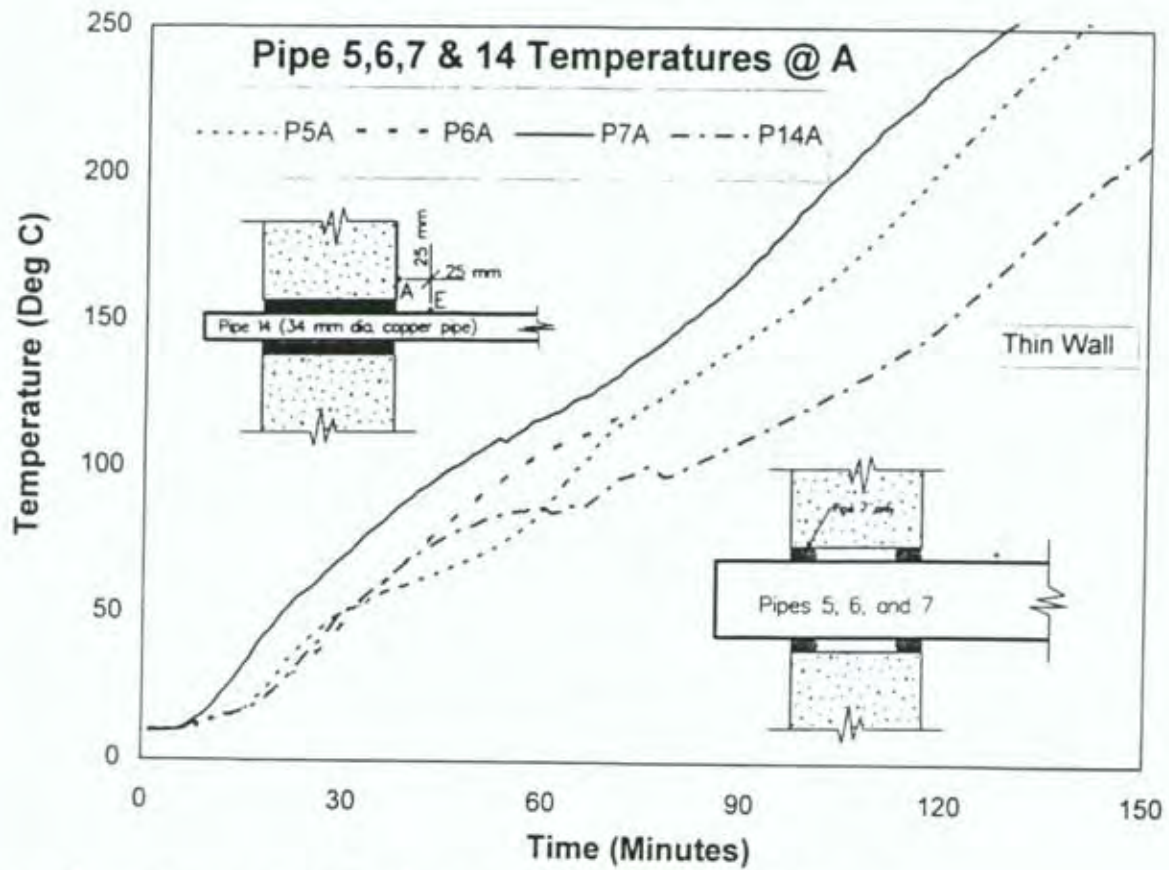


Figure 16. Temperature Development at "A" on Pipes 5,6,7 & 14

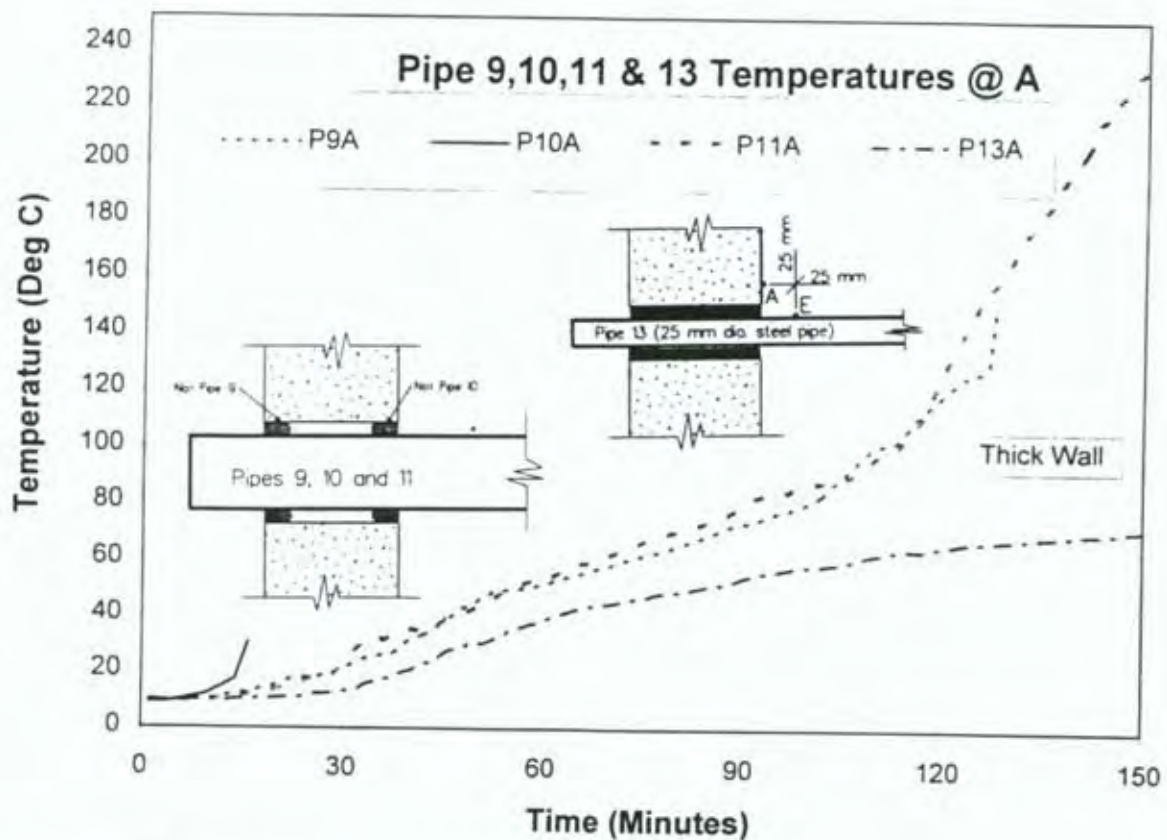


Figure 17. Temperature Development at "A" on Pipes 9,10,11 & 13

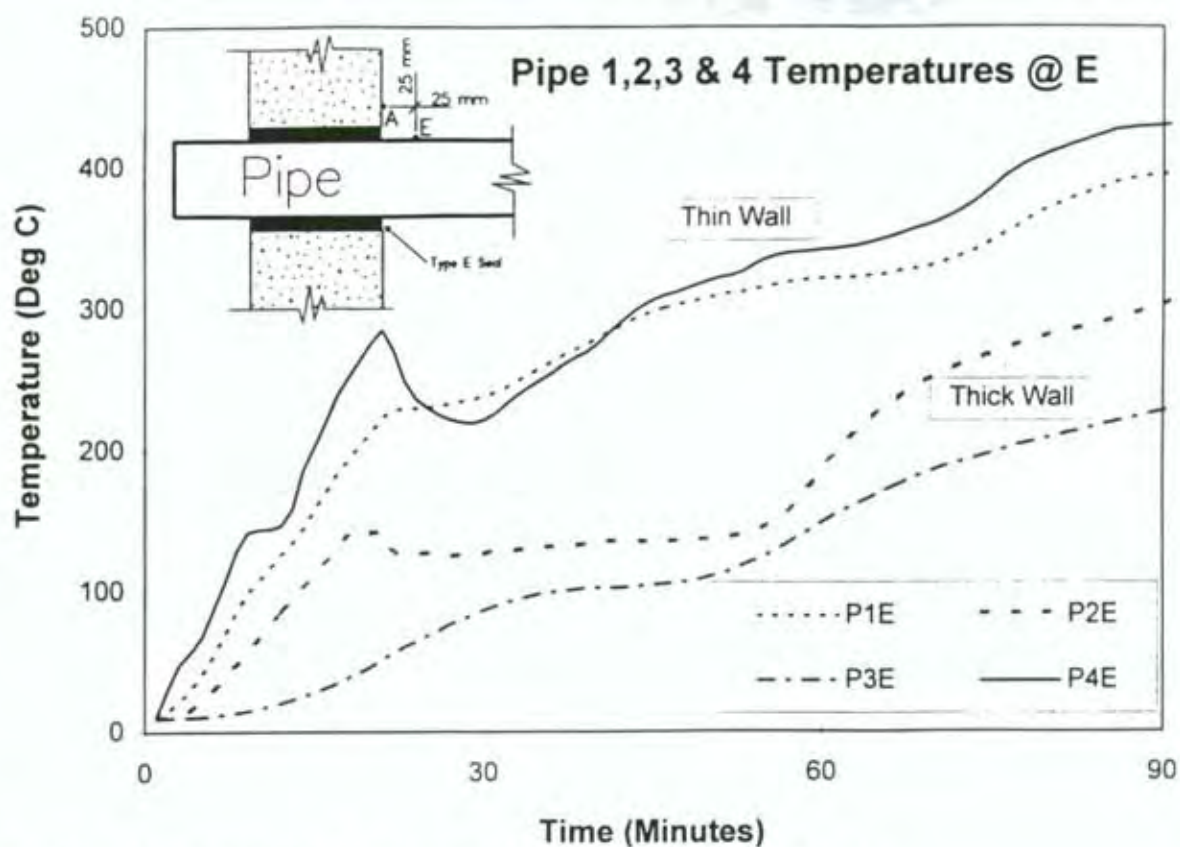


Figure 18. Temperature Development at "E" on Pipes 1,2,3 & 4

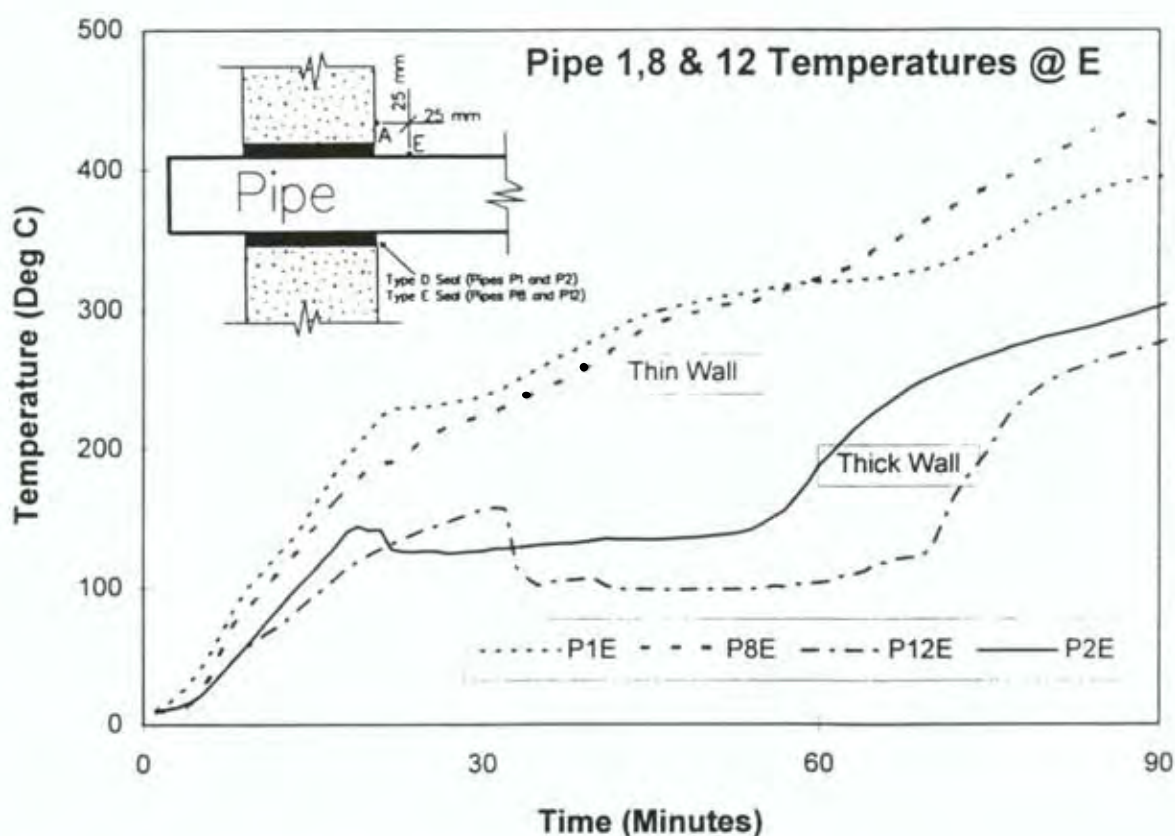


Figure 19. Temperature Development at "E" on Pipes 1,2,8 & 12

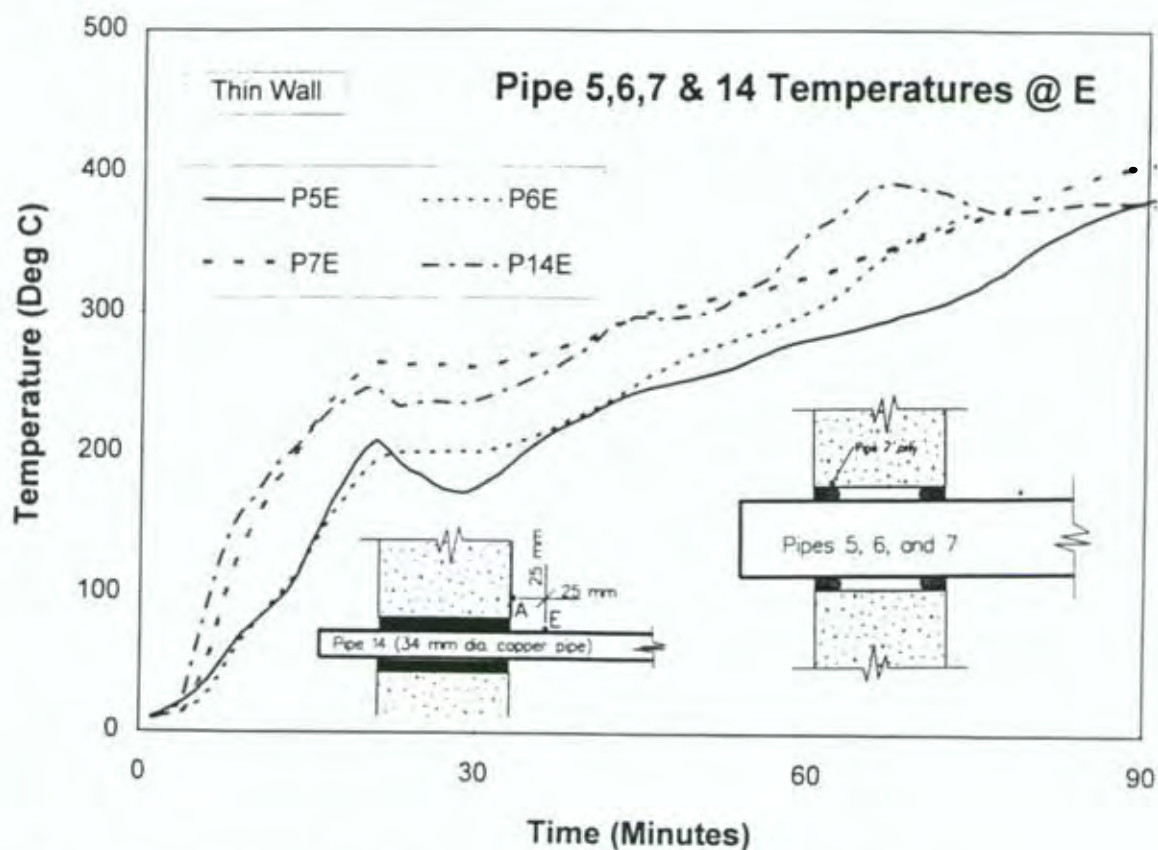


Figure 20. Temperature Development at "E" on Pipes 5,6,7 & 14

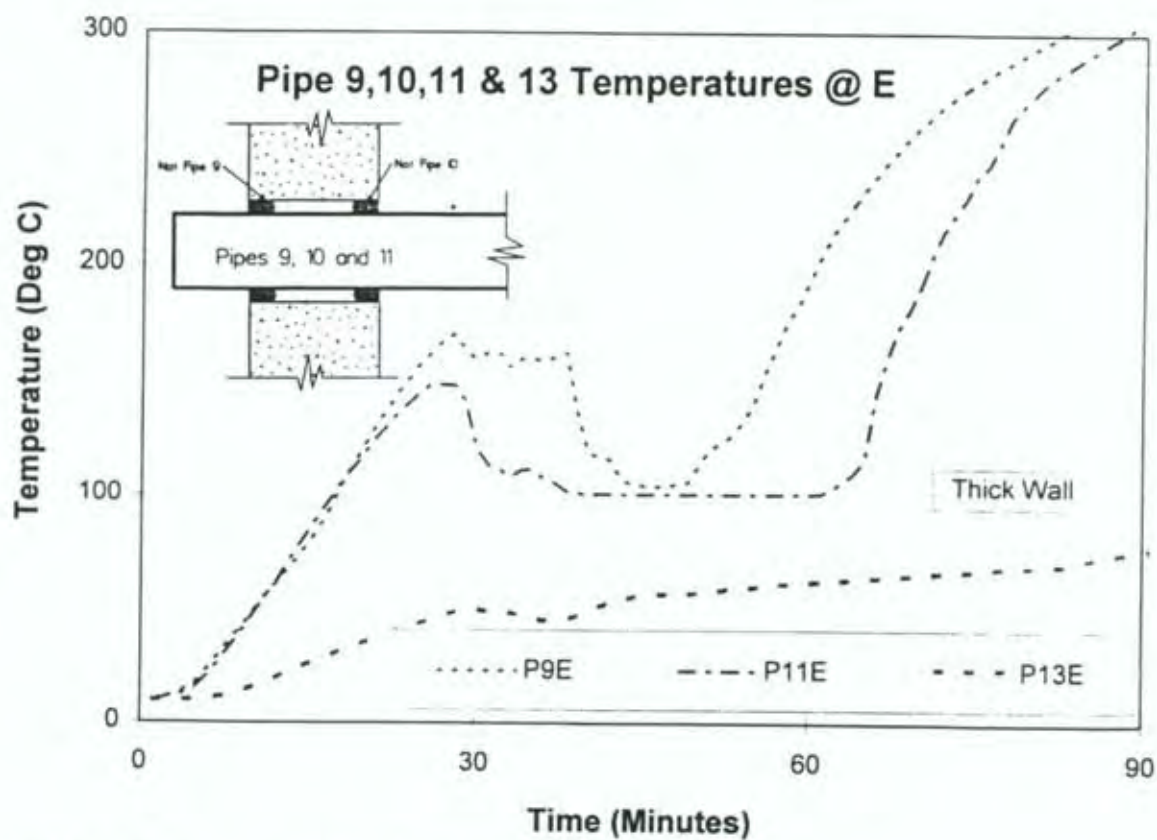


Figure 21. Temperature Development at "E" on Pipes 9,11 & 12

Table 8. Time to Reach 180° Temperature Rise

(Time in Minutes)					
Pipe Number	On Pipe, 25 mm from unexposed face		On concrete, 25 mm from hole edge		Slab Thickness (mm)
	Location E		Location A		
	Top	Side	Top	Side	
1	16	20	115	94	100
2	59	65	216	*	175
3	70	77	*	*	175
4	13	13	110	144	100
5	17	38	112	113	100
6	19	36	73	82	100
7	12	13	98	99	100
8	19	26	111	125	100
9	58	66	127	127	175
10	**	**	**	**	175
11	68	104	135	192	175
12	73	77	235	*	175
13	*	*	*	*	175
14	10	10	137	145	100

Legend

- A temperature of 180 °C was not reached at this location during the 4 hour test.
- ** Failure of seal occurred at this location at 14 minutes.

3.4.3 Thermocouples at "A"

Figure 14 plots temperature time histories at thermocouples where the seal is of lightweight cement composition (i.e. type E). Temperatures at A rise significantly faster in the 100 mm thick wall than the 175 mm thick wall. These temperature rises were largely independent of pipe type.

Figure 15 plots temperatures at thermocouples where the seal is a gypsum based filler (Type D). For comparison, plots for Pipe 1 and 2 have also been included. Higher temperatures were obtained with the Type D seal than the Type E for the 100 mm thick concrete between 30-90 minutes, but this was not so for the 175 mm thick concrete. A comparison is difficult because the seal was less than half the thickness with the Type D product and thus its insulating effect for conduction from the pipe to the thermocouple at "A" will be less.

Temperature rises at A for the remaining pipes are plotted in Figure 16 for the 100 mm thick wall and Figure 17 for the 175 mm thick wall. These pipes all had plug-type seals except for Pipes 13 and 14 (as shown in the sketches included with the plots). Where the seal has not failed, temperature rises at location "A" are similar to those plotted in Figures 14-15 for Type D and E seals respectively (gap between pipe and concrete completely filled). This indicates that the air gaps for Type A, B and C seals are equally as effective as Type D and E seals in protecting concrete temperature at location "A".

Slightly lower temperatures were recorded at "A" with the smaller diameter pipes (Pipes 13 and 14).

3.4.4 Thermocouples at "E"

From Table 8, temperatures recorded by thermocouples at "E" were always significantly higher than thermocouple temperatures at location "A", showing that this is the critical location with regard to satisfying the Standard (AS 1530.4 [SA 1990]).

The temperatures at location "E" for the 100 mm thick wall were significantly higher than for the 175 mm thick wall (Figure 18). Average times to reach 180 °C temperature rise was 16 minutes for the 100 mm thick wall and 68 minutes for the 175 mm thick wall. A comparison of the plots for Pipes 1 and 4 shows that the temperature rises were largely independent of pipe material (i.e. copper or steel). Note that the temperatures at the concrete exposed (hot) face were also similar for the two pipes (see Figure 12). Thus, as copper has approximately 8 times the thermal conductivity of steel, the result suggests that a large proportion of the heat transfer took place within the pipe (e.g. by convection and radiation). However, temperature rises at "E" were lower with the thicker Pipe 3 than with the otherwise identical Pipe 2.

Temperatures at location "E" were similar for seal types D and E (Figure 19). The pipe temperatures for the 175 mm thick wall show a cooling between 20-60 minutes in both Figure 18 and 19, probably due to water running down the unexposed face of the wall cooling the pipes.

Where Type A, B or C seals did not fail, measured temperature rises at location "E" are similar to those where Type D and E seals, (i.e. complete fill seals) were used. This may be because heat conduction/convection within the pipe was the most dominant heat transfer mechanism. The exception is for Pipe 13, which stayed far cooler at location "E". This steel pipe was only 25 mm diameter, and heat movement within it may have been far less than for the larger diameter pipes. However, the 34 mm diameter copper pipe (Pipe 14) had similar results to the 105 mm diameter copper pipe (Pipe 3). Thus the influence of pipe diameter on rate of temperature rise at "E" may not be a simple relationship.

3.4.5 Temperature profiles

Measured temperature profiles along the pipes (starting from mid-wall thickness) are presented in Appendix D for times 30, 90 and 210 minutes. The temperatures at 30 minutes near the unexposed face have been influenced by water flowing down the wall as observed at this time.

Generally, the temperatures for the 100 mm diameter pipes for corresponding wall thicknesses, locations and times were similar for all pipe types (including the copper pipe) except that the temperatures for the thicker steel pipe (8 mm thick Pipe 3) were considerably lower.

The temperatures on the 34 mm diameter copper pipe (Pipe 14) were close to those of the 100 mm diameter pipes near the unexposed face but cooled far more rapidly. The small diameter steel pipe temperatures (Pipe 13, diameter 25 mm) were significantly lower than for the 100 mm diameter pipes over the full pipe length.

3.4.6 Radiation guard temperatures

A radiation guard is sometimes used around pipes penetrating fire walls to protect against excessive pipe temperature rises. To check that the guards themselves do not become excessively hot from pipe radiation, guards (with thermocouples) were used in some tests. The temperature rises recorded on these guards (see Table A.1) were low, indicating that there was no problem in this regard. The length of guard must be selected to cover the length of pipe where the temperature rise on the pipe surface is likely to be excessive. The temperature profiles along the pipes given in this report give some guidance in this regard. More discussion on radiation guards (including effect of separation distance) is provided by Brown and Burn (1980). Pipe lagging is also commonly used to protect against excessive pipe temperature rises but has not been considered within the scope of this project.

4. FINITE ELEMENT (NISA) ANALYSIS

4.1 Program

This report makes use of a finite element program called NISA III (EMRC, 1993) for modelling the temperatures within concrete walls penetrated by metal pipes exposed to fire. The computer program used is a commercial general-purpose finite element package capable of handling non-linearity and temperature-dependent material properties for problems of transient heat transfer. The program is called NISA II and is supplied and supported by the Engineering Mechanics Research Corporation. In addition to the main module for heat transfer analysis (HEAT) there are pre- and post- processing modules for ease of model construction, finite element meshing and analysis of results.

Details of the NISA computer model, including finite element mesh, processing procedure and sample listings are provided in Appendix C.

With respect to problems concerning heat transfer at fire temperatures, NISA II is capable of taking the following factors into account:

- time-dependent fire/furnace gas temperatures
- material properties which are time and/or temperature-dependent
- 2 or 3 dimensional analysis
- emissivity and convective heat transfer coefficients which may vary with temperature
- phase changes (e.g. evaporation of moisture)
- automatic finite element meshing routines

Wade (1993) found a good agreement between temperatures measured in full-scale tests and those predicted from NISA modelling of corresponding tests. Many of the assumptions

used by Wade, such as the concrete thermal properties, were adopted for this study. Wade presented the basic equations which govern heat flow in a fire wall.

The assumed material properties used in the NISA analysis are discussed for each material in turn below. Where properties in the analysis varied from this, the actual values used are noted.

4.2 Assumed Concrete Properties

The thermal properties of dry concrete used in the NISA analysis are given in Table 9 and were taken from Wade (1993).

The effect of moisture in the concrete can be significant because the energy required to evaporate the water is not available to increase the temperature of the concrete. Typically, therefore, a plateau will be apparent in the time-temperature curve at about 100 °C.

The effect of moisture is taken into account by specifying the volumetric enthalpy versus temperature curve for moist concrete as explained in detail by Wade (1993). This assumes that the moisture evaporates between the temperatures of 100 °C and 115 °C. The heat of vaporisation of water was taken as 2257 kJ/kg. The enthalpy of concrete was added separately. Wade presented equations for calculating the enthalpy of moist concrete which can be readily solved by spreadsheet analysis. An example of this (for the 100 mm thick slab) is given in Table 9.

Enthalpy is defined as the summation of the product of specific heat and temperature starting from room temperature. It is used to avoid the sharp peaks that occur in the specific heat of some materials at near 100 °C, due to the evaporation of moisture. Using an input with large discontinuities in the slope can lead to numerical instabilities in a finite element model.

The finite element model assumes that once the moisture has been evaporated it is removed from the system. In reality it is not so straightforward, because of mass transport of moisture which can be driven through a slab, evaporating and condensing at various depths. Imagine a single point within the thickness of a concrete slab. Not only is energy required to drive off moisture associated with that element volume, but moisture associated with other elements closer to the fire-exposed face may have been driven through the slab to condense at the element in question. So, to that element, in terms of the energy requirement to remove moisture, it may appear to have a higher "effective" moisture content than its original measured moisture content. For the same reason the "effective" thermal conductivity may also appear to be higher. This effect is likely to become more dominant the greater the distance from the fire-exposed face.

The measured concrete moisture content as given in Table 4 was used to calculate enthalpy for verification of the computer model developed as part of this study. However, for predictions of real wall performance, the expected equilibrium moisture content of the concrete should be used.

Table 9. Volumetric Enthalpy as a Function of Temperature

Latent Heat of evaporation = 2257 kJ/kg
 Concrete moisture content = 5.04%
 Concrete density = 2374 kg/m³

Temperature		k	c	$\Delta e(\text{conc})$	c(water)	Δe_w	$\Delta e(\text{total})$	Enthalpy
C	K	W/mK	J/kgK	J/kg	J/kgK	J/kg	J/kg	MJ/m ³
0	273	2.57	765					
25	298	2.57	765	19125	4184	5271.84	24397	58
50	323	2.49	809	19675	4184	5271.84	24947	117
75	348	2.42	852	20763	4184	5271.84	26034	179
100	373	2.36	883	21688	4184	5271.84	26959	243
115	388	2.34	935	13635	150467	113753	127388	545
125	398	2.31	987	9610	0	0	9610	568
150	423	2.25	1061	25600	0	0	25600	629
175	448	2.19	1096	26963	0	0	26963	693
200	473	2.14	1113	27613	0	0	27613	759
225	498	2.09	1126	27988	0	0	27988	825
250	523	2.05	1139	28313	0	0	28313	892
275	548	2.02	1148	28588	0	0	28588	960
300	573	1.99	1157	28813	0	0	28813	1028
325	598	1.96	1165	29025	0	0	29025	1097
350	623	1.93	1174	29238	0	0	29238	1167
375	648	1.9	1183	29463	0	0	29463	1237
400	673	1.86	1196	29738	0	0	29738	1307
425	698	1.81	1274	30875	0	0	30875	1381
450	723	1.76	1478	34400	0	0	34400	1462
475	748	1.7	1683	39513	0	0	39513	1556
500	773	1.64	1796	43488	0	0	43488	1659
525	798	1.57	1683	43488	0	0	43488	1763
550	823	1.52	1509	39900	0	0	39900	1857
575	848	1.49	1400	36363	0	0	36363	1944
600	873	1.45	1287	33588	0	0	33588	2023
625	898	1.43	1191	30975	0	0	30975	2097
650	923	1.41	1178	29613	0	0	29613	2167
675	948	1.38	1174	29400	0	0	29400	2237
700	973	1.36	1183	29463	0	0	29463	2307
750	1023	1.31	1171	58850	0	0	58850	2447
800	1073	1.28	1135	57650	0	0	57650	2583
850	1123	1.28	1117	56300	0	0	56300	2717
900	1173	1.28	1122	55975	0	0	55975	2850
1000	1273	1.28	1139	113050	0	0	113050	3118
1100	1373	1.31	1148	114350	0	0	114350	3390
1200	1473	1.34	1161	115450	0	0	115450	3664
1275	1548	1.36	1170	87413	0	0	87413	3871

Legend

k concrete conductivity
 c (conc) concrete specific heat
 $\Delta e(\text{conc})$ change in concrete enthalpy = integral of specific heat times temp. change
 c(water) water specific heat
 Δe_w change in water enthalpy = integral of specific heat times temp. change
 $\Delta e(\text{total})$ $\Delta e(\text{conc}) + \Delta e_w$
 Enthalpy Integral of $\Delta e(\text{total})$

4.3 Assumed Steel Properties

4.3.1 Thermal conductivity

The thermal conductivity of steel as a function of temperature is given in Table 10 from Wainman et al. (1990).

4.3.2 Specific heat

The specific heat of steel as a function of temperature is also given in Table 10 from Wainman et al. (1990). At around 730 °C, steel undergoes a phase change to adopt a denser internal structure. This is characterised by an increment in the specific heat at that temperature as shown in Table 10.

4.3.3 Density

The density of steel is approximately 7850 kg/m³. Table 10 also tabulates mass density as a function of temperature, again from Wainman et al. (1990).

Table 10. Assumed Steel and Copper Thermal Properties

Temperature (°C)	Steel			Copper	
	Thermal Conductivity (W/m.°K)	Specific Heat (J/kg.°K)	Density (kg/m ³)	Thermal Conductivity (W/m.°K)	Specific Heat (J/kg.°K)
20	52.0	440	7850	409	377
100	51.0	480	7827	393	385
200	48.8	530	7797		
300	46.0	565	7765	379	397
400	42.7	610	7731		
500	39.2	675	7695	366	433
600	35.5	760	7655		
700	32.0	1010	7616	352	451
725	31.0	1600	7608		
735	30.0	5000	7612		
750	28.5	1300	7618		
775	26.5	1010	7622		
800	26.0	810	7626		
825	25.8	730	7627		
900	26.5	650	7599	339	480
1000	27.5	650	7549		
1100	28.5	650	7500		
1200	29.5	655	7453	339	480

4.4 Assumed Copper Properties

The thermal properties of copper were obtained from Kaye and Laby (1985) and are given in Table 10. The density was taken as 8933 kg/m^3 and the melting point as 1356°C .

4.5 Assumed Lightweight Concrete Properties

Trethowen (1994) estimated the following properties for lightweight concrete:

Density kg/m^3	Thermal Conductivity $\text{W/m}\cdot^\circ\text{K}$
1200	0.4
900	0.15
500	0.1

The measured density of this lightweight concrete product E (see Table 2) was 764 kg/m^3 . After drying in the oven the density reduced to 426 kg/m^3 . Based on these densities, the conductivity of the product was estimated to be: $K = 0.1 \text{ W/m}\cdot^\circ\text{K}$

The specific heat of the lightweight concrete was taken to be the same as for concrete. The energy required to drive water from the lightweight concrete was ignored.

4.6 Assumed Gypsum Filler Fire-Stop Properties

The thermal properties of this product D (see Table 2) were estimated to be the same as for gypsum plasterboard. Gypsum ($\text{CaSO}_4 \cdot 2\text{H}_2\text{O}$) will lose two water molecules at temperatures between 100 and 160°C , depending on the rate of heating (Harmathy, 1988).

The following thermal properties for the gypsum filler were taken from Thomas et al., 1994. The conductivity was taken as $0.2 \text{ W/m}\cdot^\circ\text{K}$ between 0 - 800°C , and then increasing linearly to $0.75 \text{ W/m}\cdot^\circ\text{K}$ at 1500°C . The enthalpy was assumed to increase at $0.95 \text{ kJ/kg}\cdot^\circ\text{K}$ except for an additional increase of 500 kJ/kg which occurs linearly between 100 - 150°C and is the energy required to evaporate water from the gypsum. The specific heat was assumed to be independent of temperature, with a value of $1000 \text{ J/kg}\cdot^\circ\text{K}$.

4.7 Assumed Air Properties

For some analyses an attempt was made to model the convection and radiation heat flow within the pipe by providing an artificially high value of air conductivity. Air thermal properties assumed were based on data from West (1987). The specific heat was assumed to be independent of temperature, with a value of $1010 \text{ J/kg}\cdot\text{K}$, while the air density was taken as:

$$\text{Density} = 1.29 \times \frac{273}{T} \frac{\text{kg}}{\text{m}^3} \quad \text{where } T = \text{air temperature in } ^\circ\text{K}$$

4.8 Assumed Boundary Conditions

4.8.1 Standard fire resistance test

This study is concerned with comparing the measured temperatures from standard fire resistance tests, on and within building components, with the results of analytical studies based on finite element modelling techniques. It is necessary to establish confidence in the model's prediction of standard fire test results before modelling alternative design fires. In standard fire resistance testing, the furnace temperature is driven to follow a prescribed time-temperature curve. For example, ISO 834 (ISO, 1975) and BS 476 Part 8 (BSI, 1972) specify the following:

$$\begin{array}{ll} T_{fire} &= 345 \log_{10} (8t + 1) + T_o \\ \text{where: } T_{fire} &= \text{furnace gas temperature (}^\circ\text{C)} \\ T_o &= \text{initial temperature (}^\circ\text{C)} \\ t &= \text{time interval (min)} \end{array}$$

The time-temperature curve specified in BS 476 Part 20 (BSI, 1987) is identical except that $T_o = 20^\circ\text{C}$. The fire temperatures used for the testing described in this report followed the ISO 834 curve. In making practical use of the finite element model, the prescribed standard time-temperature curve or any time-temperature curve which is appropriate to the fire, and which may depend on ventilation, fire load, rate of burning, etc. would be specified. Predictions of wall performance made in this report use the ISO 834 fire curve.

4.8.2 Radiation

The boundary conditions to be specified for radiation are the emissivity at the concrete surface and the ambient temperature. For fire-exposed surfaces, the ambient temperature is time-dependent and was specified as the ISO 834 standard time-temperature curve given above. For non-exposed surfaces, e.g. on the unexposed side of a wall or floor slab, the ambient temperature was assumed to be constant.

The term resultant emissivity is commonly used to represent emissivity modified by surface properties and geometric configuration, although this approach has been disputed by Mooney (1992). The resultant emissivity of building materials exposed to fire is typically in the range 0.6 to 1.0 (Sterner and Wickström, 1990) and will vary with temperature and the characteristics of the test furnace.

A concrete emissivity of 0.9 was used in all modelling described in this report.

In this study radiation exchange between the different surfaces (e.g. between pipe and wall) has not been taken into account. This effect is assumed to be insignificant.

4.8.3 Convection

Convection is generally not as important as radiation on the fire-exposed surfaces, but can be significant on the unexposed surfaces. Sterner and Wickström (1990) state that a value of approximately $25 \text{ W/m}^2 \cdot ^\circ\text{K}$ for the radiant heat transfer coefficient is commonly found in fire literature. CEB (1987) propose a value of $25 \text{ W/m}^2 \cdot ^\circ\text{K}$ for fire-exposed concrete surfaces and $15 \text{ W/m}^2 \cdot ^\circ\text{K}$ for unexposed surfaces. Values of $5 \text{ W/m}^2 \cdot ^\circ\text{K}$ and $10 \text{ W/m}^2 \cdot ^\circ\text{K}$ have been used in this study for the unexposed and exposed surfaces respectively, based on work by Wade (1993). Convection and radiation heat flow within the pipes was assumed to be zero in most analyses performed for this report because initially it was thought to be insignificant and because it could not be modelled by NISA. This assumption turned out to be wrong, and critical, and several trial runs were made using a variation of the computer model which allowed heat flow within the pipe. Details are provided in the next section. Convection and radiation heat flow within the void between pipe and concrete where the seal does not effectively fill this cavity was also assumed to be zero for the same reasons that it was ignored within the pipes.

5. COMPARISON OF EXPERIMENTAL RESULTS WITH NISA PREDICTIONS

5.1 Ignoring Heat Flow Within the Pipes

These analyses assumed zero convective and radiative heat flows within the pipes.

The first NISA runs were performed using a heat transfer coefficient of $7 \text{ W/m}^2 \cdot ^\circ\text{K}$ (rather than $5 \text{ W/m}^2 \cdot ^\circ\text{K}$ noted in Section 4.8.3) for the unexposed surfaces, and using the following properties for the lightweight concrete (see Appendix B):

Density	= 1860	kg/m^3
Conductivity	= 0.72	$\text{W/m} \cdot ^\circ\text{K}$
Specific Heat	= 780	$\text{J/kg} \cdot ^\circ\text{K}$

A comparison of the temperatures predicted by NISA using these assumptions and those measured for Pipe 1 is given in Figure 22 for points P1A and P1E (see Figure 7) and for temperature profiles along the pipe in Figure 23. The NISA model predicted lower temperatures on the pipe at the unexposed concrete wall face than measured, and the predicted temperatures cooled more rapidly along the pipe than measured. In an attempt to simulate these experimental data the heat transfer coefficient was changed from 7 to $5 \text{ W/m}^2 \cdot ^\circ\text{K}$ and the lightweight concrete assumed to have more insulating characteristics (as per details in Section 4.5). The re-run produced the graphs in Figures 24 and 25. Agreement with experimental results was again poor. The lower heat transfer coefficient had little effect on the cooling rate along the pipe, and the greater insulation of the lightweight concrete only had significant influence on the predicted temperatures at the unexposed wall face during the first 25 minutes of the fire loading.

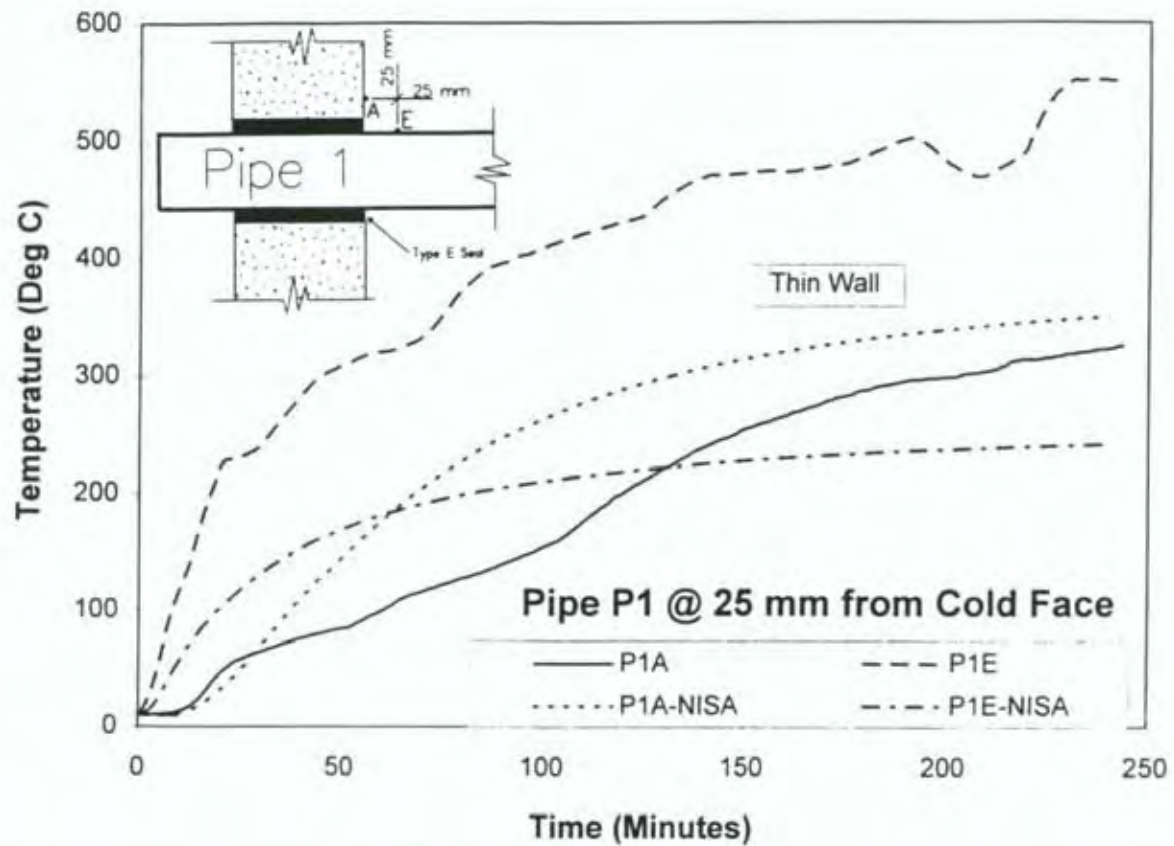


Figure 22. Comparison of Predicted and Measured Temperatures at P1A and P1E (First Material Assumptions)

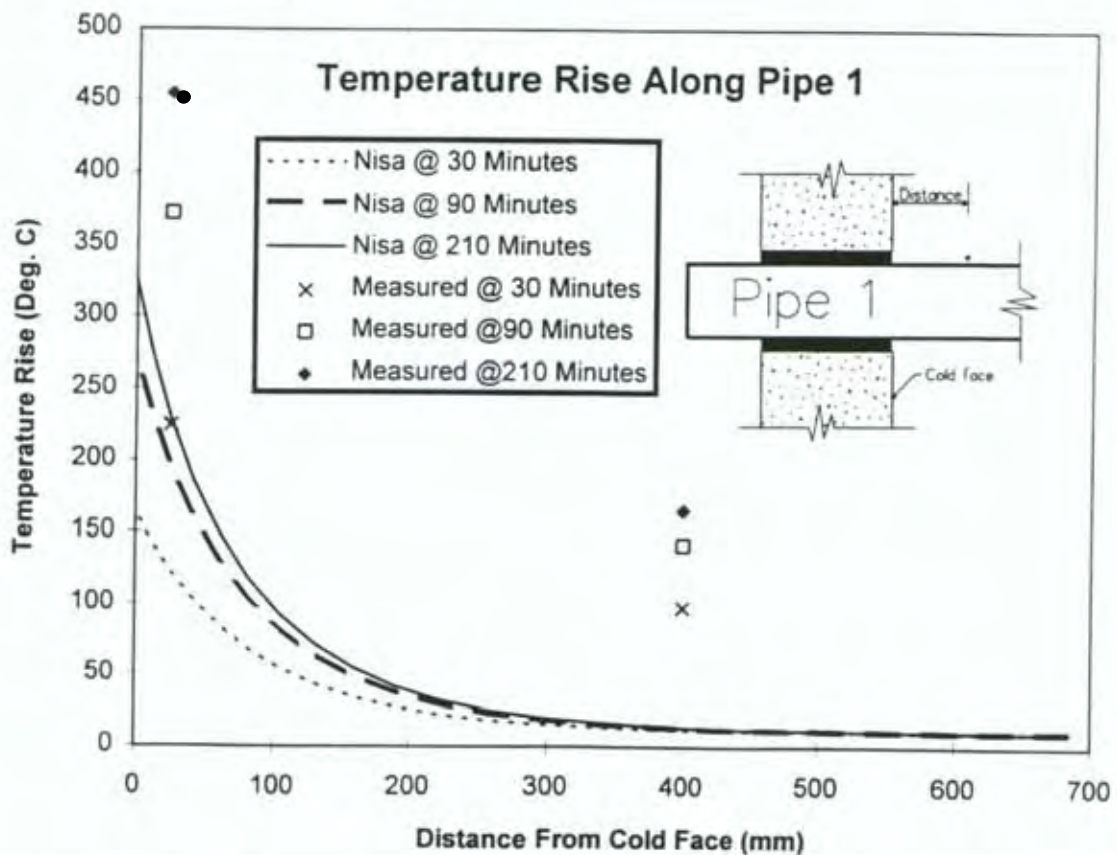


Figure 23. Comparison of Predicted and Measured Temperature Profiles Along Pipe 1 (First Material Assumptions)

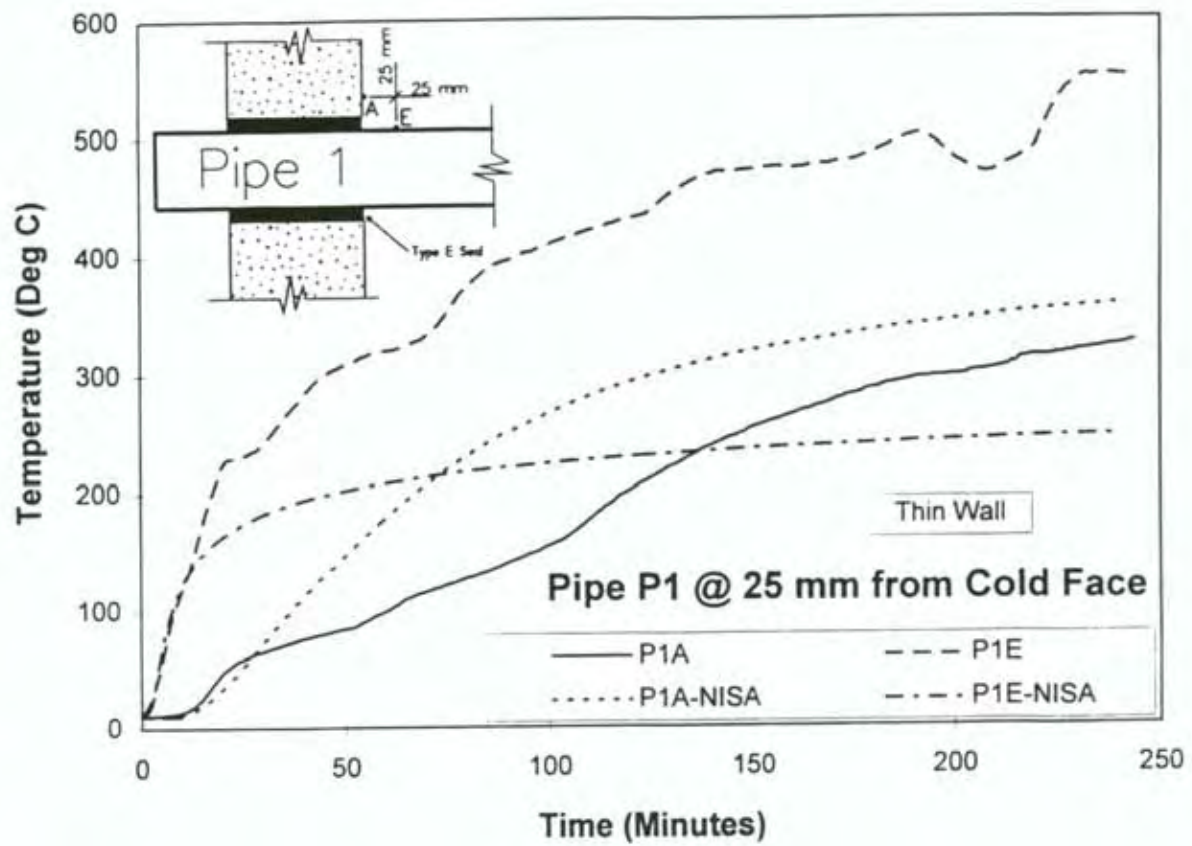


Figure 24. Comparison of Predicted and Measured Temperature at P1A and P1E (Second Material Assumptions)

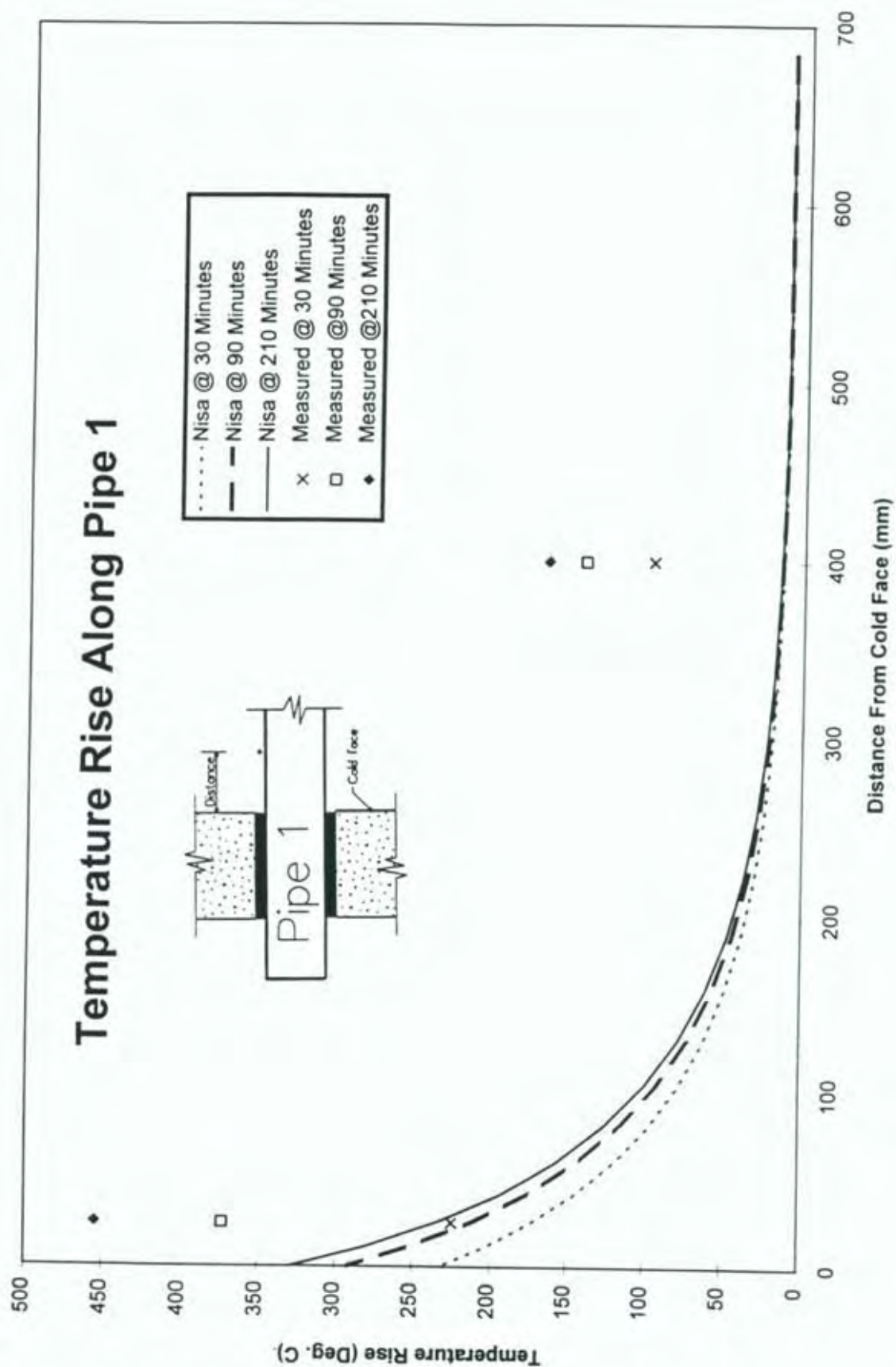


Figure 25. Comparison of Predicted and Measured Temperature Profiles Along Pipe 1 (Second Material Assumptions)

Figure 26 compares the predicted and measured temperature time history for concrete midway between pipes (the radiant heat transfer coefficient was again assumed to be $7 \text{ W/m}^2 \cdot ^\circ\text{K}$ on the unexposed surfaces). Agreement is excellent on the exposed face but gets progressively worse with distance towards the unexposed concrete face, with the NISA predictions indicating higher temperatures than measured. This may have been due to the concrete moisture being driven from the hot (exposed) side of the wall to the colder unexposed side. Note that the experimental data exhibits a plateau at about 100°C , consistent with energy being required to drive off water at this temperature. This plateau only occurred in the NISA predictions on the cold (unexposed) face.

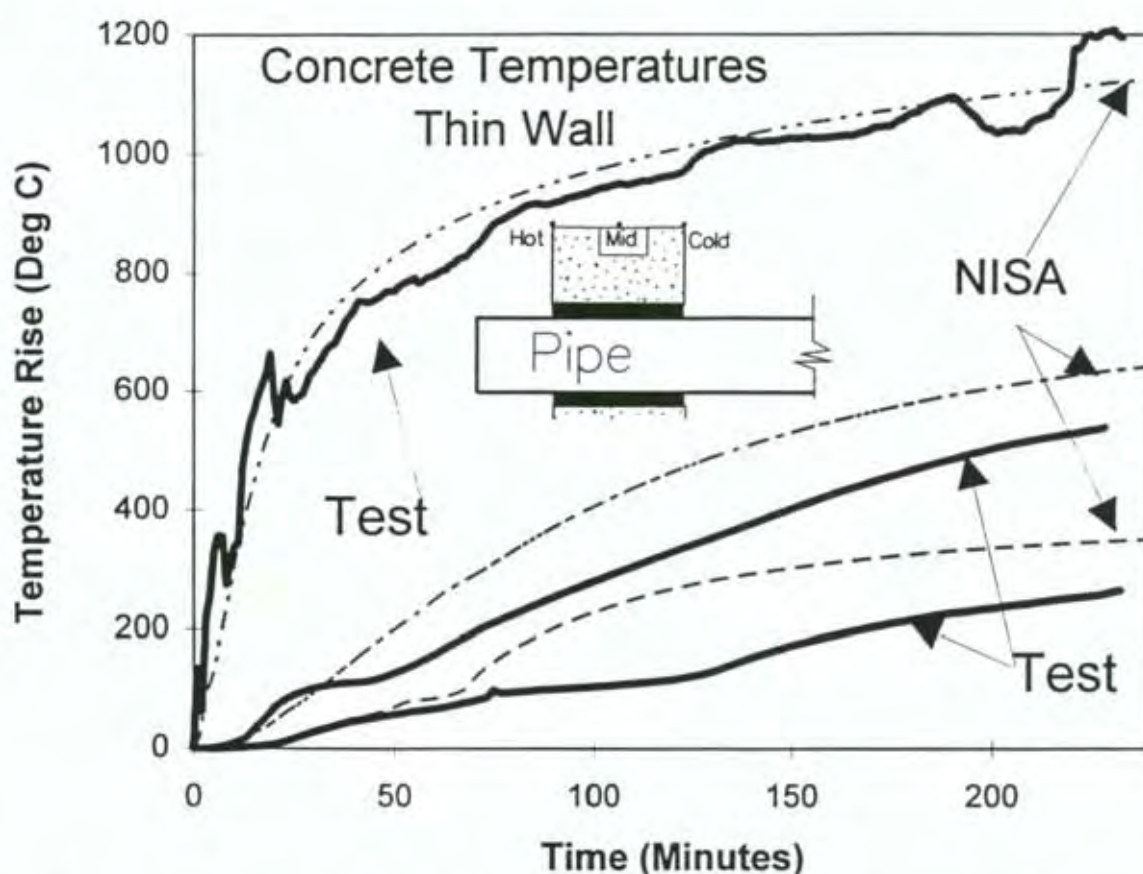


Figure 26. Comparison of Predicted and Measured Concrete Temperatures

One reason for the pipe temperatures being higher in the test than in the NISA model is that heat was being transferred inside the pipe by convection and radiation. This heat transfer mechanism has been modelled in Section 5.2.

A comparison of temperatures from test and NISA prediction is also provided for Pipe 4 (a copper pipe) in Figures 27 and 28. (All properties were as noted in Section 4.) Agreement for temperatures along the pipe are still poor, although somewhat better than for the steel Pipe 1. The better agreement may be because the conductivity of the copper pipe is greater than for the steel pipe, and thus heat transfer along the pipe is less dominated by radiation and convection within the pipe.

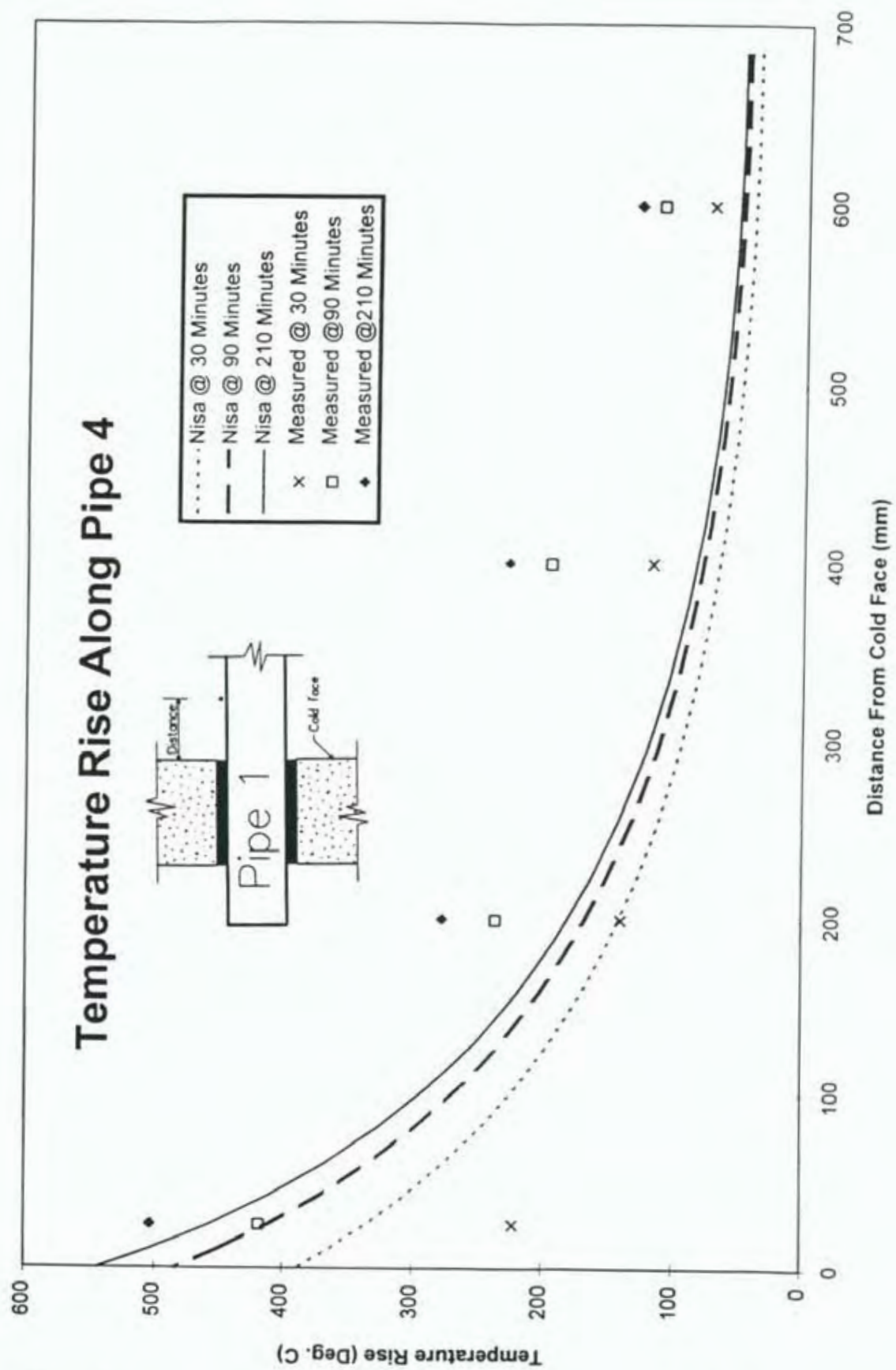


Figure 28. Comparison of Predicted and Measured Temperature Profiles Along Pipe 4

Figure 29 compares temperatures on the pipe and concrete surface at mid-wall depth. Apart from the plateau on the experimental curve for concrete temperatures (see discussion above) agreement is reasonable.

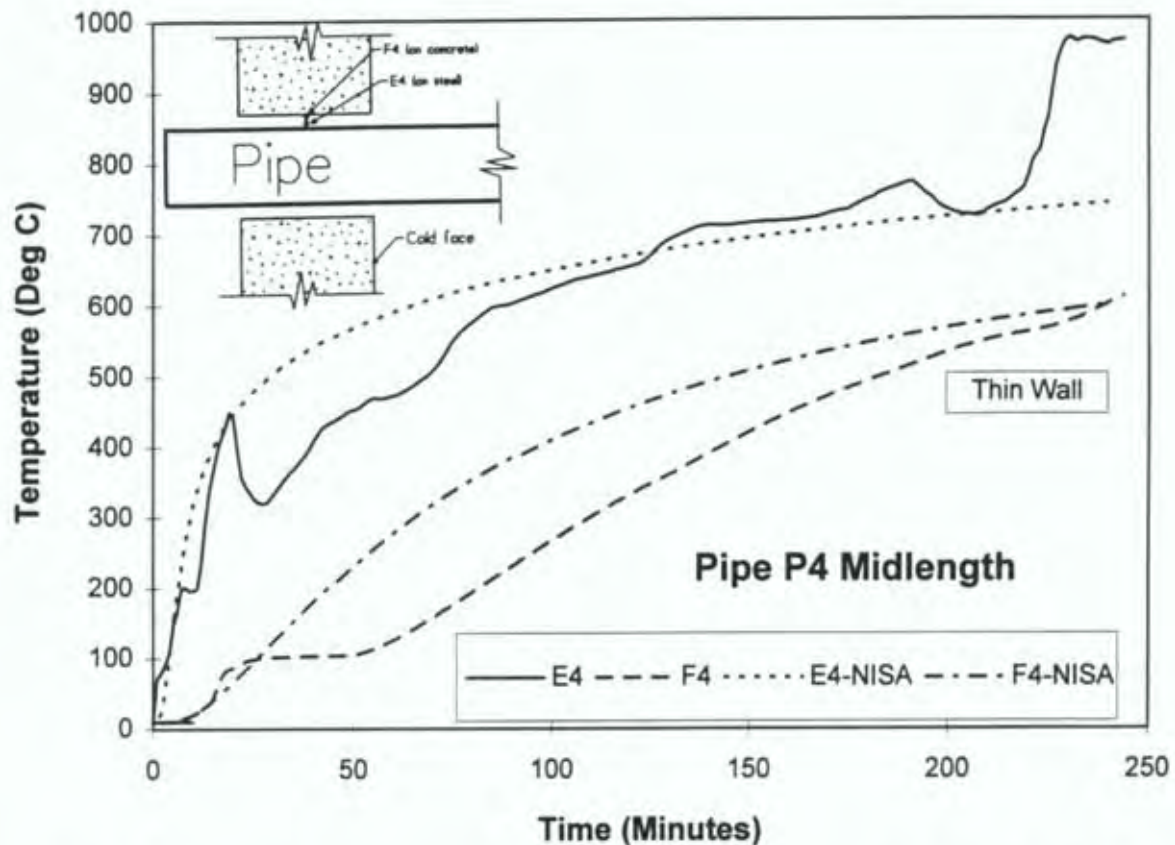


Figure 29. Comparison of Predicted and Measured Temperature at Pipe 4 at Mid Wall Thickness

5.2 Modelling Heat Flow Within the Pipes

An attempt was made to model convection and radiation heat flow within the pipes by using the thermal properties of air given in Section 4.7 with the artificially high values of air thermal conductivity given below. These values were chosen purely in an empirical attempt to get agreement with experimental data and have no correspondence with actual air thermal conductivity properties.

- a) $K = 40 \text{ W/m.}^\circ\text{K}$ (independent of temperature)
- b) $K = 4 \text{ W/m.}^\circ\text{K}$ (independent of temperature)
- c) $K = 100 \left(\frac{273}{T} \right)^2$ where $T = ^\circ\text{K}$ $\text{W/m.}^\circ\text{K}$ (i.e. a function of temperature).

The equation shown for assumption (c) provides an extreme reduction of air conductivity with temperature in an attempt to reduce the predicted pipe temperature at the unexposed face while still providing high temperatures further along the pipe.

A comparison of measured and predicted temperatures along Pipe 4 is given in Figure 30 for the three assumptions described above. At time 30 minutes the NISA predictions using assumptions (a) and (b) are too high at the "cold" (i.e. unexposed) face and predicted cooling along the pipe is too rapid (although better than predicted in Figure 28). Assumption (c) gives better agreement except at the unexposed face. On the other hand assumption (a) gives excellent agreement with experimental results at 180 minutes. Note that pipe temperatures at the unexposed face were significantly cooled from water running down this face during the first hour of the test (water thermally driven from the concrete [see Table 6]). It is concluded that (for Pipe 4) assumption (a) gives best agreement for initially dry concrete.

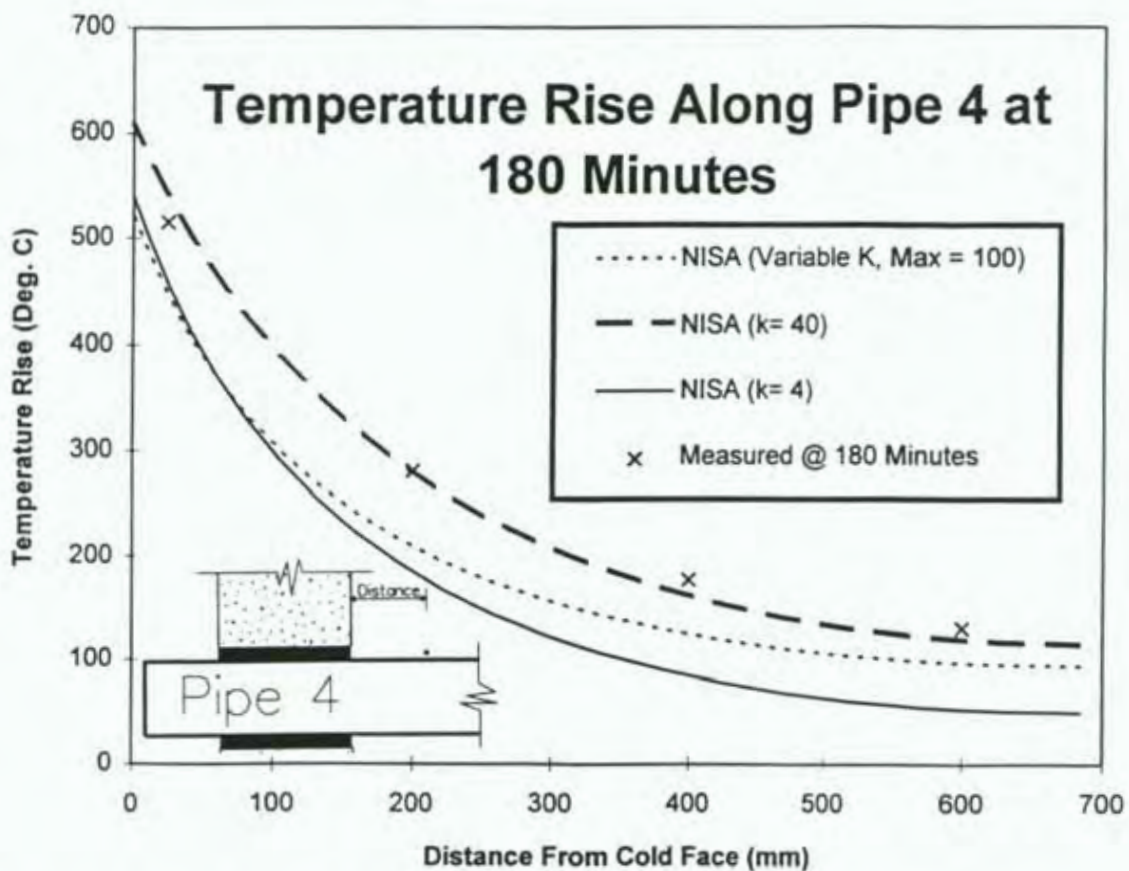
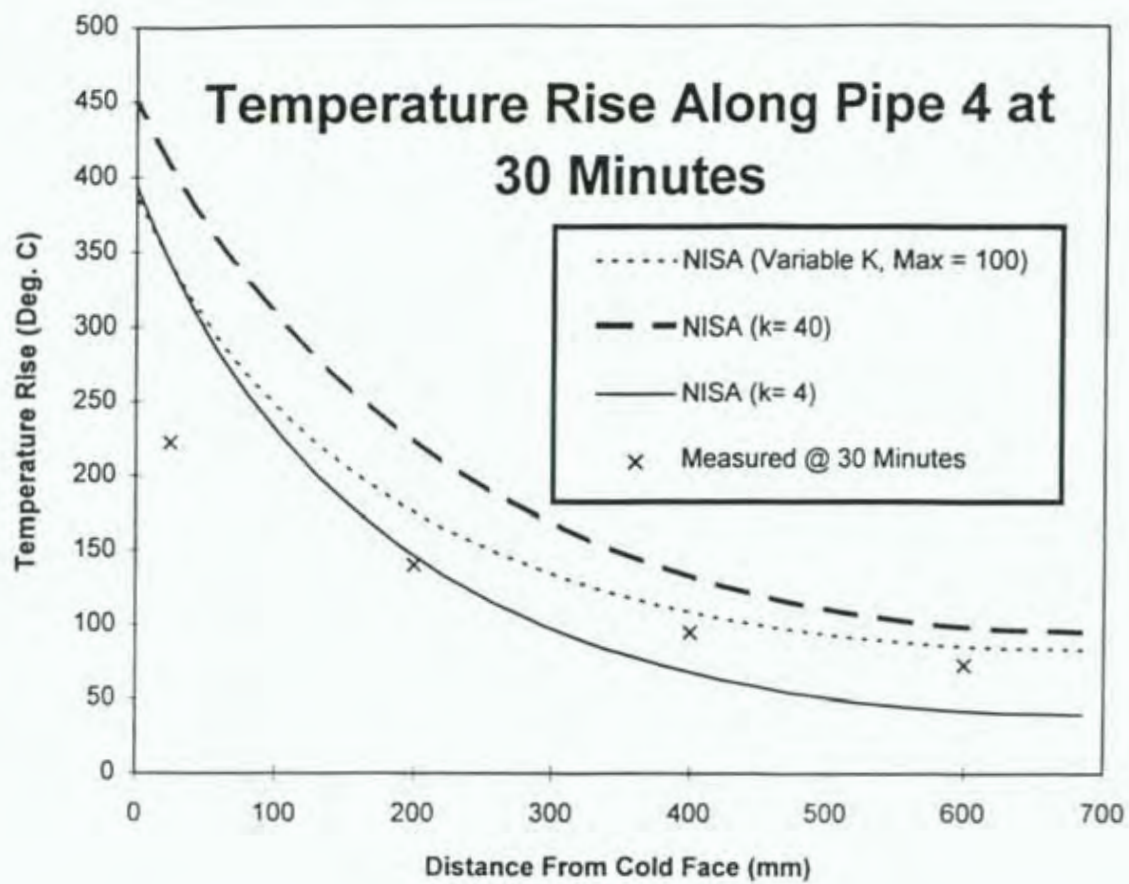


Figure 30. Comparison of Measured and Predicted Temperatures Along Pipe 4

6. CONCLUSIONS

The conclusions given below assume the pipes contain still air. Different conclusions may apply to pipes filled with a liquid.

At the inception of this project it was assumed that heat flow within pipes was not important. The results within this report show that the converse is true. As NISA was unable to model this heat transfer from principles of radiation and convection, the major objective of this project of using NISA to extrapolate test results was unable to be accomplished. However, the experimental results have been presented in detail, which will enable predictions from a more sophisticated model to be compared with experimental data.

6.1 From Research

There is considerable doubt as to whether the 180 °C insulation temperature rise requirement of AS 1530.4 (SA, 1990) is applicable to pipe penetrations of walls. It is unlikely that ignition of nearby combustibles will occur at this temperature, and a somewhat higher temperature may be applicable.

6.2 From Experimental Comparisons

- Temperature rises were largely independent of the pipe material (i.e. copper or steel). As copper has approximately 8 times the conductivity of steel this result suggests that a large proportion of the heat transfer took place within the air in the pipe.
- Pipe temperature rises were largely independent of the type of seal used (where this seal did not fail).
- The Standard (AS 1530.4 [SA, 1990]) provides two potentially critical temperature locations (one on the pipe and one on the concrete). As expected the pipe temperature was always the more critical of the two in the tests performed.
- The temperatures at the critical pipe location (location "E", see Figure 7) were significantly higher for the 100 mm thick wall than for the 175 mm thick wall. Average time to reach 180 °C temperature rise was 16 minutes for the 100 mm thick wall and 68 minutes for the 175 mm thick wall.
- In otherwise identical pipes, pipe temperature rises were lower with pipes of greater wall thickness. Generally, pipe temperature rises were lower with smaller diameter pipes, except that one small diameter copper pipe had similar temperature rises to a larger diameter copper pipe near the unexposed face, although it cooled down faster than the larger diameter pipe with distance from this face.
- The pipe temperatures for the 175 mm thick wall show a cooling between 20-60 minutes, caused by water running down the unexposed face of the wall cooling the pipes.

- A steel mesh radiation guard is sometimes used around pipes penetrating fire walls to keep combustible material away from hot pipes. The temperature rises recorded on the guards used in the tests were low, indicating that there was no problem of the guards themselves (on the unexposed side of the wall) becoming excessively hot during a fire. The length of guard must be selected to cover the length of pipe where the temperature rise on the pipe surface is excessive. The temperature profiles along the pipes given in this report give some guidance in this regard.

6.3 From Comparisons of Predicted and Measured Temperatures

The heat flow within pipes is important and ignoring this flow leads to grossly non-conservative results. This heat flow can be modelled by using an artificially high conductivity for the air in the pipes, to simulate the conduction and radiation heat that is actually transmitted within the pipe. Good agreement between experimental and predicted results was obtained using a conductivity, K (independent of temperature) = $40 \text{ W/m.}^\circ\text{K}$ for air when modelling a 100 mm diameter copper pipe. In practice, cooling of the pipe may occur within the first hour of the fire due to water running down the unexposed face (from water thermally driven out of the concrete) and this will not be predicted by the model.

7. RECOMMENDATIONS

More investigation is needed into suitable values for the artificially high conductivity required for the air in the pipes to simulate the conduction and radiation heat that is actually transmitted along the pipe. This is likely to be a function of pipe diameter.

8. REFERENCES

- Australian Uniform Building Regulations Co-ordinating Council (AUBRCC). 1990. Building Code of Australia. Canberra.
- ASFPCM. Undated. Fire stopping and penetration seals for the construction industry. Association of Specialist Fire Protection Contractors and Manufacturers. United Kingdom.
- British Standards Institution. 1972. BS 476. Fire tests on building materials and structures. Part 8. London.
- British Standards Institution. 1987 BS 476. Fire tests on building materials and structures. Part 20. Method for Determination of the Fire Resistance of Elements of Construction (general principles). London.
- Brown, S.K. and Burn, L.S. 1980. Model fire resistance tests of metal pipes penetrating concrete slabs. CSIRO - Division of Building Research. Sydney.

Carey, W.B. 1977. 'The Problems of penetrations in fire-resistive construction.' Building Standards 41 (1).

Engineering Mechanics Research Corporation. 1993. Users manual for NISA III, Version 93.0. Michigan, USA.

Incropera, F.P. de Witt, D.P. 1990. Fundamentals of heat transfer. 3rd edition. John Wiley and Sons. New York.

Kaye and Laby. 1985. Table of Physical and Chemical Constants. Longman. London.

Keough J.J., Rogleff, S. and Cunin, D. 1976. PVC pipes penetrating fire-resisting concrete floors. Experimental Building Station, Technical Record 44/153/392. Sydney.

Harmathy, T.W. 1988. Properties of building materials. In SFPE Handbook of Fire Protection Engineering (378-391). Linville, J.L. (Ed). National Fire Protection Association. Winey, MA, USA.

Hunter, L. W. and Farin, S. 1981. Fire resistance of penetrated walls. Fire Technology Volume 17(4). November 1981. The National Fire Protection Association. USA.

International Standards Organisation (ISO). 1975. ISO 834. Fire resistance tests - elements of construction. Switzerland.

Martin, C. 1983. The penetration of fire resistance construction by services. Design and construction recommendations based on a literature survey. Experimental Building Station. Australia. Technical Record 500.

Parker, W.J., Paabo, M., Scott, J.T., Gross D., and Benjamin, I.A. 1975. Fire endurance of gypsum board walls and chases containing plastic and metallic SWV plumbing systems. Building Science Series No. 72. National Bureau of Standards. USA.

BIA, 1992. New Zealand Building Code Approved Document for Fire, C3/AS1. Building Industry Authority. Wellington. 1992.

Standards Australia, 1992. AS 4072-1. Components for the protection of openings in fire-resistant separating elements. Part 1: Service penetrations and control joints. Sydney.

Standards Australia, 1990. AS 1530.4. Methods for fire tests on building materials, components and structures. Part 4: Fire resistance tests of elements of building construction. Sydney.

Thomas, G.C., Buchanan, A.H., Fleischman, C., and Moss, P.I. 1994. Light framed timber walls exposed to compartment fires, FTEC Timber Engineering Conference, 531-538. Gold Coast. Australia.

Trethowen, H.A. 1994. Personal Communications.

Building Regulations 1992. First Schedule. New Zealand Government. Wellington. 1992.

Wainman, D.E., Kirby, B.R., Tomlinson, L.N., Kay, T.R., Preston, R.P. 1990. The behaviour of unprotected steel floor beams in the standard fire resistance test - compendium of predicted temperature profiles. British Steel. Swinden Laboratories. Rotherham.

Wade, C.A. 1993. Summary report on a finite element program for modelling the thermal response of building components exposed to fire. Building Research Association of New Zealand. BRANZ Study Report SR 51. Judgeford, New Zealand.

Weast, R.C. 1987. CRC Handbook of Chemistry and Physics. CRC Press Inc. Boca Raton, Florida.

Appendix A Time History Temperature Plots

A.1 Introduction

This appendix contains plots of the measured temperature time histories of all thermocouples used in the two fire tests. The labelling system used is described in Section 2.5.

Table A.1 Recorded Temperatures on Thermocouples						
(Associated With Particular Pipes)						
Gauge	Temperatures (°C) at Times Shown)					
	30	60	90	120	180	240
P1A	64.7	98.5	139.2	200.9	287.4	323.7
P1B	98.3	102.3	158.3	222.2	271.9	307.2
P1C	77.8	96.9	124.1	209.1	266.2	315.1
P1D	48.6	85.8	175.0	251.3	321.9	362.0
P1E	241.3	320.5	396.2	430.9	486.7	550.6
P1F	208.0	279.9	348.6	387.9	452.4	522.3
P1-400T	104.5	132.6	151.1	160.4	177.5	203.3
P1-400S	90.1	116.0	131.9	140.0	154.6	181.5
P1-G25T	52.3	72.3	89.5	108.9	141.9	167.7
P1-G25S	36.1	40.0	46.0	58.0	88.6	114.2
P1-G400T	20.8	26.4	29.2	32.3	39.5	49.5
P1-G400S	14.2	17.5	19.3	22.1	30.8	44.0
P2A	24.1	65.4	74.0	99.7	140.2	214.0
P2B	46.8	70.0	77.2	101.4	186.2	235.4
P2C	43.2	51.1	65.5	91.8	126.9	192.7
P2D	12.3	49.4	70.1	90.5	119.2	179.8
P2E	128.8	196.3	305.5	345.6	429.4	434.0
P2F	107.7	170.7	244.9	274.7	350.2	364.4
P2-400T	103.4	128.1	149.8	155.6	182.2	182.5
P2-400S	83.0	104.6	121.4	126.5	147.3	148.0
P2-G25T	20.3	37.7	41.0	62.1	80.6	98.6
P2-G25S	13.6	33.8	35.0	33.0	40.7	54.7
P2-G400T	15.8	20.7	20.8	24.1	24.2	26.9
P2-G400S	11.6	15.0	15.6	17.6	19.1	22.5
P3A	16.5	57.7	65.5	77.1	108.5	153.2
P3B	23.4	70.6	70.6	86.2	140.7	200.0
P3C	27.6	64.7	76.8	88.6	101.2	149.0
P3D	12.3	40.4	61.7	65.9	90.8	103.5
P3E	89.5	153.4	229.9	276.8	331.6	366.7
P3F	73.3	143.4	212.4	259.2	301.1	342.5
P3-200T	45.4	87.8	120.0	141.9	160.1	173.6
P3-400T	28.8	57.4	76.6	90.5	102.7	112.3
P3-400S	22.0	46.3	66.0	77.9	89.8	91.7
P3-600T	20.4	39.5	52.2	60.9	69.6	76.1
P3-G25T	24.0	45.6	55.5	75.9	86.4	107.3
P3-G25S	16.0	30.3	38.3	38.6	48.5	74.8
P3-G400T	15.5	18.9	24.0	27.7	30.5	34.7
P3-G400S	13.6	16.6	19.5	22.4	26.1	30.4
A3	183.9	272.7	339.1	386.6	464.5	511.8
E3	204.7	336.2	441.0	535.3	637.9	688.8
F3	37.2	106.4	129.2	209.2	367.4	483.2
HF3	644.0	797.3	910.9	970.5	1060.1	1047.2

Gauge	Temperatures (°C) at Times Shown)					
	30	60	90	120	180	240
P4A	59.3	77.7	128.9	213.5	295.2	365.7
P4B	73.1	97.8	167.5	249.6	304.0	444.8
P4C	49.2	90.1	109.8	167.7	246.3	369.6
P4D	38.3	72.1	106.7	136.6	243.8	309.8
P4E	226.4	341.6	431.1	466.7	530.5	268.9
P4F	218.0	317.9	405.7	438.5	500.3	315.8
P4-200T	140.1	194.1	237.1	252.9	280.8	558.0
P4-400T	95.5	126.1	153.7	162.6	179.3	480.9
P4-400S	93.2	123.3	150.4	158.8	175.0	486.0
P4-600T	72.6	92.6	111.9	118.8	130.5	452.2
P4-G25T	43.6	69.0	86.8	108.9	141.4	217.6
P4-G25S	29.2	45.7	58.9	79.5	112.0	182.6
P4-G400T	16.2	20.7	24.1	27.4	37.5	73.5
P4-G400S	22.8	29.3	33.1	34.8	42.4	87.0
A4	301.2	449.4	596.0	647.5	753.3	1040.4
E4	332.7	471.8	601.4	653.7	748.5	964.0
F4	100.9	124.5	229.6	331.3	492.2	600.2
P5A	51.4	89.2	145.8	207.3	305.2	363.3
P5B	77.1	135.5	169.2	199.2	247.0	256.6
P5C	69.9	149.4	207.4	258.2	311.1	365.2
P5D	43.3	90.0	141.5	205.7	300.7	342.9
P5E	180.0	283.5	383.4	431.1	496.8	566.1
P5F	135.5	246.2	325.4	381.2	462.0	549.1
P5-400T	92.5	133.6	159.9	172.6	195.8	229.5
A5	307.1	445.6	579.0	650.3	786.4	866.0
E5	257.3	404.5	550.7	635.6	763.9	889.2
F5	99.1	301.7	499.8	622.9	796.7	941.4
P6A	49.6	107.0	Ignition at 74 minutes			
P6B	104.4	167.1				
P6C	62.9	147.5				
P6D	51.7	86.2				
P6E	202.1	306.4				
P6F	170.7	268.8				
P6-200T	61.1	82.6				
P6-400T	96.9	139.3				
P6-400S	80.3	114.8				
P6-600T	72.5	104.7				
A6	338.4	532.8				
E6	306.3	515.0				
F6	99.4	254.4				
P7A	262.2	328.6	407.0	437.0	483.1	544.7
P7B	234.7	292.2	360.0	388.9	434.3	491.8
P7C	114.3	143.4	165.2	172.9	188.3	212.8
P7D	97.7	122.7	143.2	150.1	165.8	188.9
P7E	25.2	31.6	35.7	38.4	47.4	240.5
P7F	52.1	84.9	111.3	152.7	251.4	305.1
P7-400T	99.5	101.3	134.5	183.1	248.9	360.4
P7-400S	92.2	101.0	99.8	176.4	253.7	392.4

Gauge	Temperatures (°C) at Times Shown)					
	30	60	90	120	180	240
P8A	72.9	115.6	137.0	208.2	284.1	321.7
P8B	123.3	190.6	299.6	340.4	389.5	451.5
P8C	83.1	124.2	238.7	298.4	364.1	420.6
P8D	47.9	77.6	110.6	175.3	271.7	309.0
P8E	227.1	326.6	430.4	445.6	483.8	563.8
P8F	200.5	287.1	390.6	415.6	455.3	537.5
P8-200T	160.5	215.2	247.8	253.4	269.0	311.1
P8-400T	112.9	159.3	182.3	185.4	195.6	223.5
P8-400S	84.1	120.1	135.5	137.6	143.4	164.8
P8-600T	81.1	119.9	137.7	140.9	148.5	167.8
P9A	22.1	51.7	73.6	120.8	Ignition at 137 min.	
P9B	59.7	73.2	128.5	270.3		
P9C	53.5	73.3	140.6	221.0		
P9D	15.9	43.2	69.9	107.5		
P9E	161.9	204.4	321.3	411.2		
P9F	117.1	116.4	265.1	335.7		
P9-400T	61.3	88.0	104.0	128.7		
P9-400S	70.6	101.7	123.8	142.0		
A9	345.5	446.8	588.6	720.8		
E9	316.0	412.2	570.9	718.7		
F9	81.8	99.9	222.2	448.4		
Note Pipe 10 had ignition at 14 minutes - thus no data provided here						
P11A	25.2	53.7	81.0	131.4	277.9	364.1
P11B	58.1	83.9	89.6	268.7	469.3	503.3
P11C	68.1	63.5	102.4	193.7	299.0	366.1
P11D	15.9	40.1	60.9	94.2	170.3	243.8
P11E	113.3	100.9	310.5	428.0	471.7	515.1
P11F	78.0	87.9	161.1	236.4	303.8	353.0
P11-200T	116.1	155.2	195.9	242.3	257.7	276.2
P11-400T	82.5	123.3	147.6	179.4	188.6	201.9
P11-400S	63.1	97.1	114.9	140.4	146.4	156.1
P11-600T	62.1	93.1	112.7	137.2	144.2	154.0
A11	301.8	401.8	496.9	659.3	747.0	813.5
E11	231.4	318.5	427.1	622.5	738.5	816.2
F11	63.2	97.7	215.6	457.1	670.1	786.8
HF11	617.2	797.8	892.8	1043.2	1040.9	1077.1
P12A	30.6	67.1	69.3	99.2	135.9	192.1
P12B	78.9	86.2	93.4	211.7	270.2	311.6
P12C	46.1	83.6	93.3	123.2	199.1	244.2
P12D	17.7	67.7	74.3	75.8	96.7	132.8
P12E	158.0	104.5	279.3	405.8	402.4	429.6
P12F	120.1	120.8	217.3	312.5	325.1	359.2
P12-200T	123.5	168.1	203.8	247.7	242.2	256.6
P12-400T	88.6	127.8	150.7	183.9	177.8	187.3
P12-400S	67.9	101.1	118.1	143.1	136.8	144.5
P12-600T	65.6	95.0	113.1	137.1	134.5	141.6

Gauge	Temperatures (°C) at Times Shown)					
	30	60	90	120	180	240
P13A	13.3	39.2	54.1	65.3	86.9	97.7
P13B	18.6	66.8	69.9	75.9	92.5	95.2
P13C	21.7	41.0	51.3	63.2	81.2	89.4
P13D	10.7	44.2	54.3	59.5	92.5	98.0
P13E	49.1	62.3	77.3	99.8	139.7	169.0
P13F	49.4	64.1	77.7	100.6	138.1	167.0
P13-200T	19.4	25.7	31.4	38.4	47.8	57.5
P13-400S	13.4	17.3	21.4	24.4	29.3	34.9
P13-600T	12.1	14.9	18.3	20.6	24.5	28.4
HF13	596.1	715.0	779.4	888.7	819.9	843.4
P14A	52.1	84.9	111.3	152.7	251.4	
P14B	99.5	101.3	134.5	183.1	248.9	
P14C	92.2	101.0	99.8	176.4	253.7	
P14D	43.5	86.7	104.2	131.5	241.8	
P14E	240.0	363.2	377.9	385.6	425.1	
P14F	242.6	349.3	373.3	391.4	427.3	
P14-200T	97.3	124.4	143.8	150.8	166.7	
P14-400T	43.2	54.2	62.9	67.0	78.2	
P14-400S	42.4	38.4	42.6	46.5	56.6	
P14-600T	25.2	31.6	35.7	38.4	47.4	

Table A.2 Recorded Temperatures on Thermocouples						
(General Thermocouples)						
Gauge	Temperatures (°C) at Times Shown)					
	30	60	90	120	180	240
100 mm Thick Wall						
FA1	830.1	858.4	975.7	1002.9	1113.6	1224.1
FA2	861.3	857.2	955.0	1004.4	1122.9	1231.3
FA3	777.3	951.8	1012.2	1034.5	1091.4	1208.3
FA4	828.1	977.1	1042.8	1060.4	1112.2	1228.2
AAIR	10.7	11.6	11.4	12.0	13.0	13.1
C1	36.0	74.6	110.1	127.4	226.1	276.9
C2	32.5	71.9	109.8	123.6	225.6	292.3
C3	46.4	84.4				
F1	722.6	821.4	951.1	993.2	1105.8	1211.4
F2	689.8	787.3	905.4	970.1	1096.3	1209.1
F3	557.0	742.5	879.2	930.3	1041.7	1180.3
F4	505.8	736.9				
F5	748.9	933.0	1016.3	1040.1	1099.7	1221.7
M1	122.9	183.7	274.7	349.6	486.9	581.8
M2	105.5	140.8	239.6	316.3	457.0	552.0
M3	107.3	177.5				568.2
175 mm Thick Wall						
FA1	883.9	930.3	1021.3	1037.5	1162.3	1105.3
FA2	0.0	934.3	1030.0	1041.4	1136.8	1099.3
FA3	789.7	931.3	973.0	1173.4	1079.1	1153.5
FA4	821.9	959.5	1018.7	1161.6	1083.4	1131.5
AAIR	10.1	10.4	10.6	11.0	12.3	13.0
C1	13.5	37.4	49.8	64.3	90.4	139.7
C2	12.0	34.1	59.4	63.3	52.4	86.8
C3	11.3	38.4	77.2	93.3	39.0	75.9
F1	837.2	923.6	1026.3	1035.6	1155.0	1113.2
F2	0.0	0.0	0.0	0.0	0.0	0.0
F3	553.0	834.0	923.8	1049.1	1066.0	1071.9
F4	673.4	890.0	971.0	1158.3	1081.4	1154.2
F5	864.2	991.7	1041.4	1186.5	1112.2	1140.6
M1	37.1	154.5	262.9	346.9	465.1	561.8
M2	29.6	131.8	242.3	345.2	487.7	595.1
M3	32.6	271.6	435.8	563.8	672.5	772.1

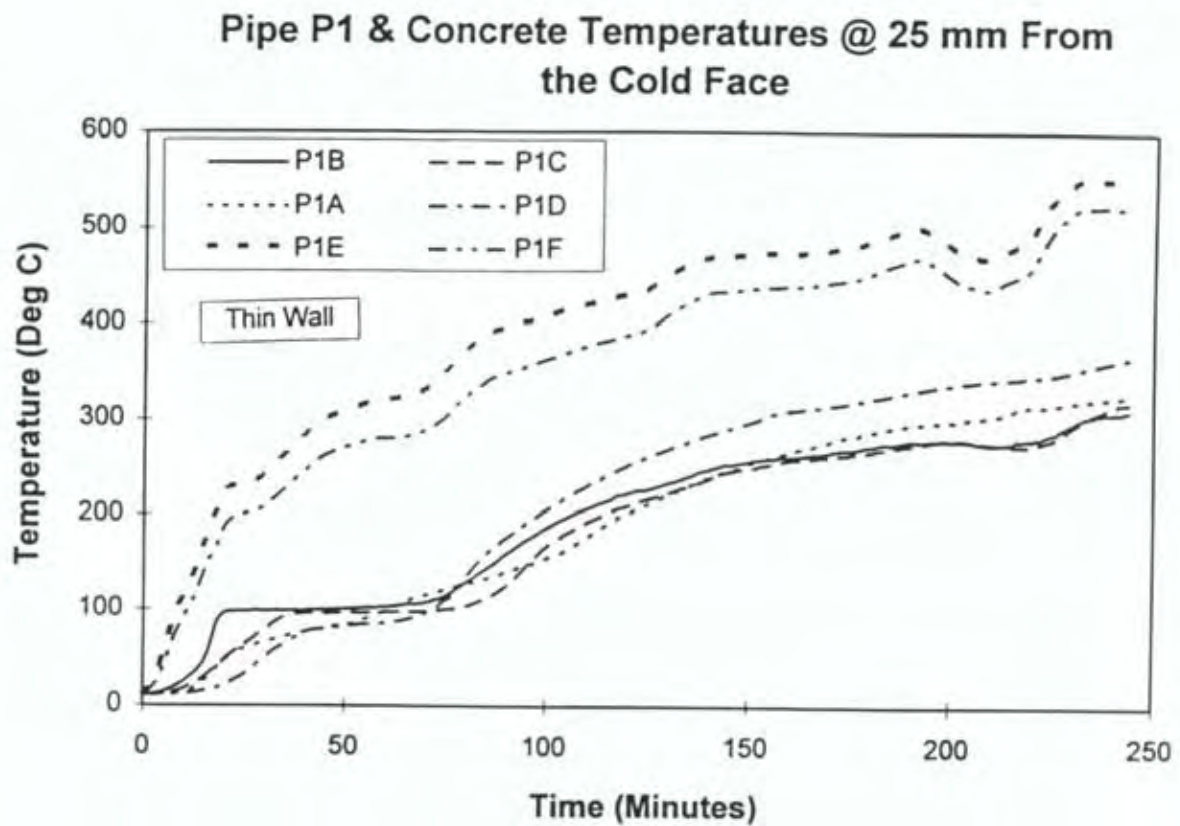


Figure A.1 Thermocouples P1A, P1B, P1C, P1D, P1E, P1F, 100 mm Thick Wall

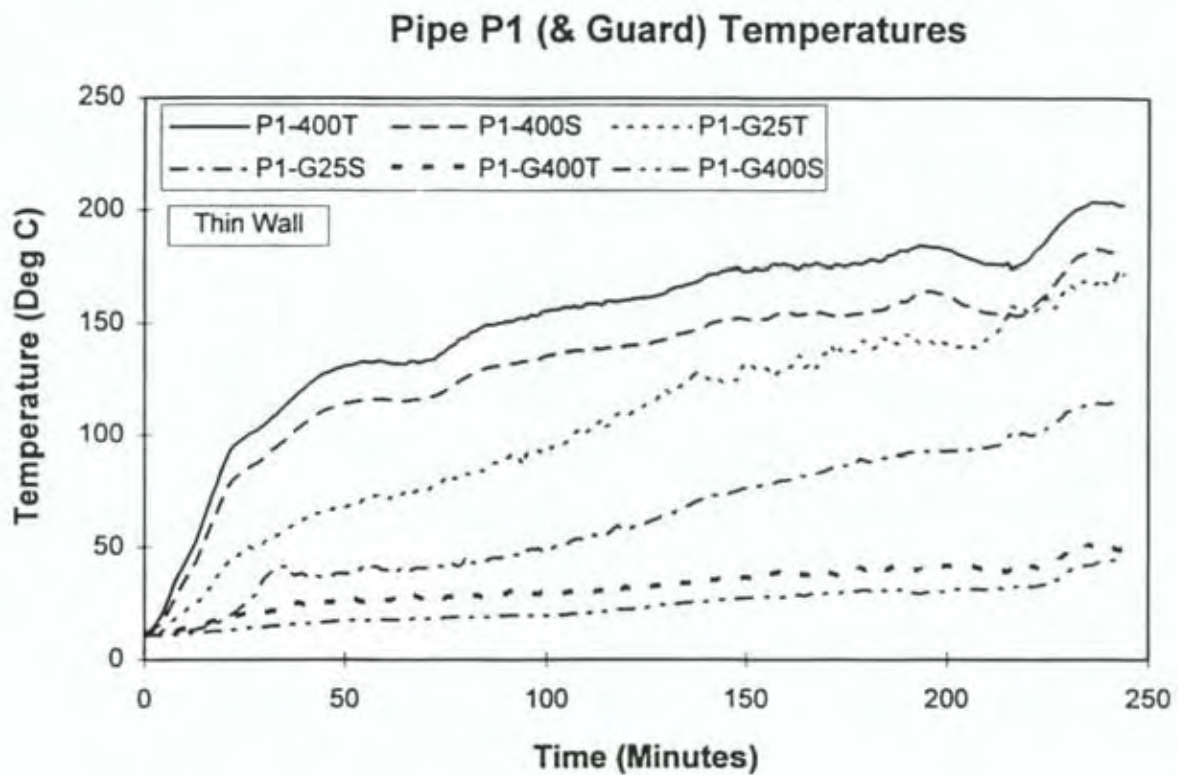


Figure A.2 Thermocouples P1-400T, P1-400S, P1-G25T, P1-G25S, P1-G400T, P1-G400S, 100 mm Thick Wall

Pipe P2 & Concrete Temperatures @ 25 mm From the Cold Face

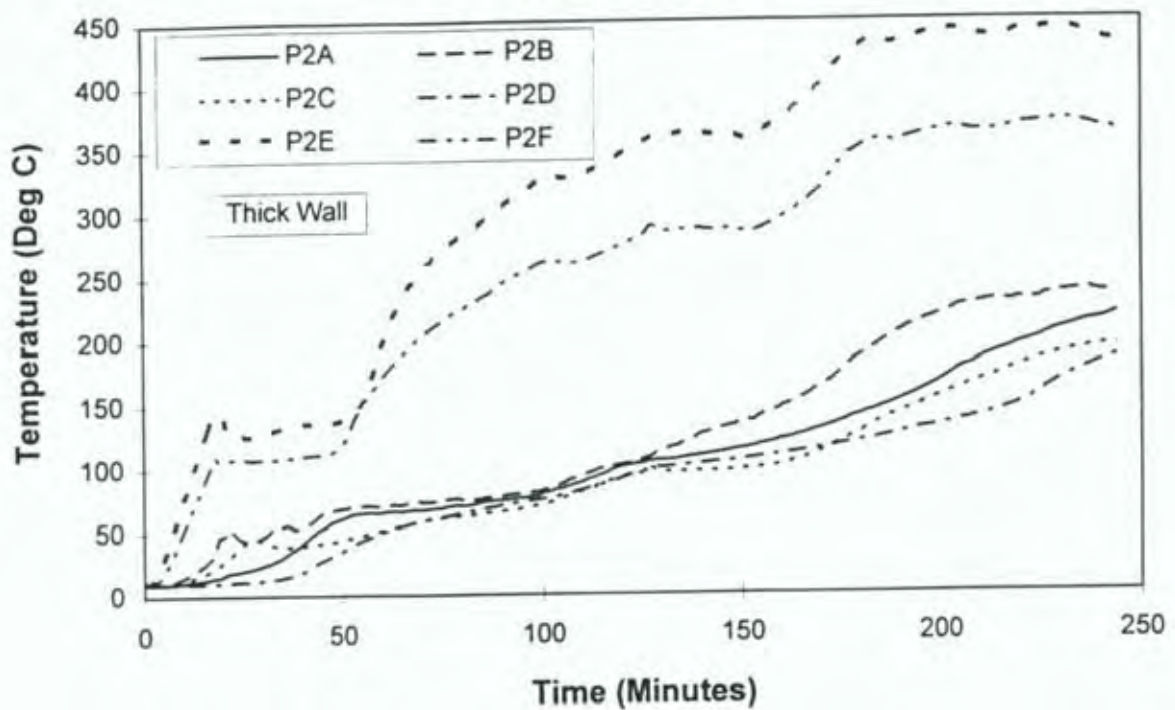


Figure A.3 Thermocouples P2A, P2B, P2C, P2D, P2E, P2F, 175 mm Thick Wall

Pipe P2 (& Guard) Temperatures

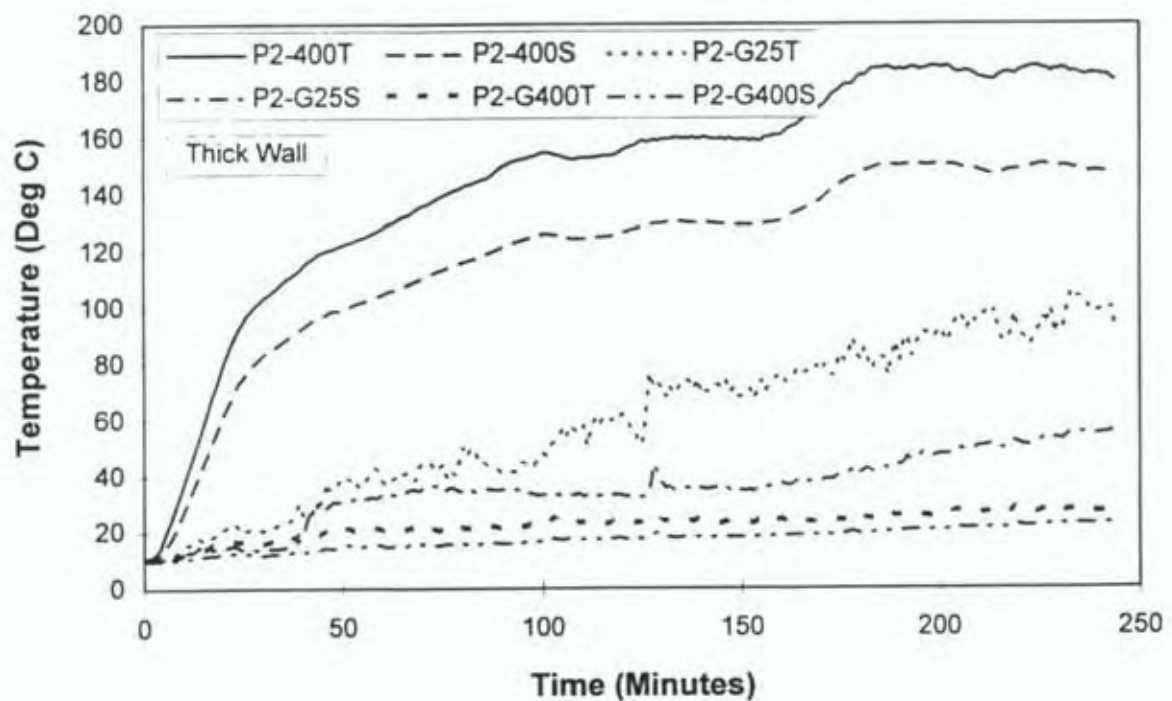


Figure A.4 Thermocouples P2-400T, P2-400S, P2-G25T, P2-G25S, P2-G400T, P2-G400S, 175 mm Thick Wall

Pipe P3 & Concrete Temperatures @ 25 mm From the Cold Face

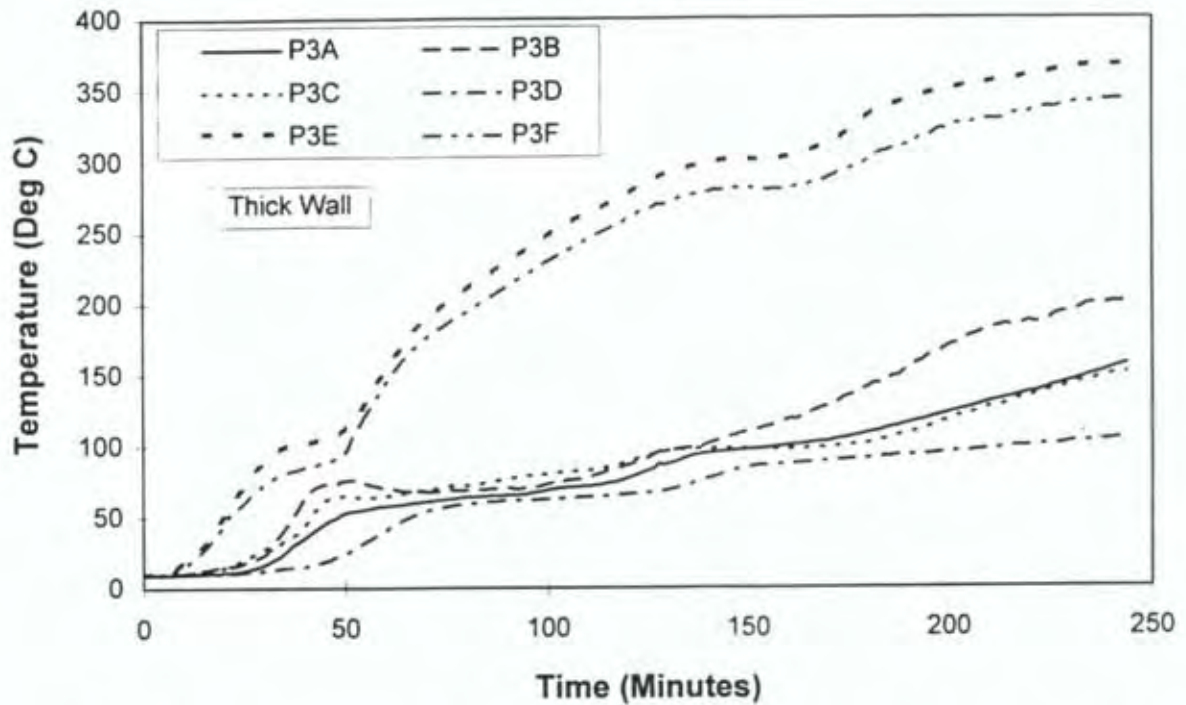


Figure A.5 Thermocouples P3A, P3B, P3C, P3D, P3E, P3F, 175 mm Thick Wall

Pipe P3 (& Guard) Temperatures

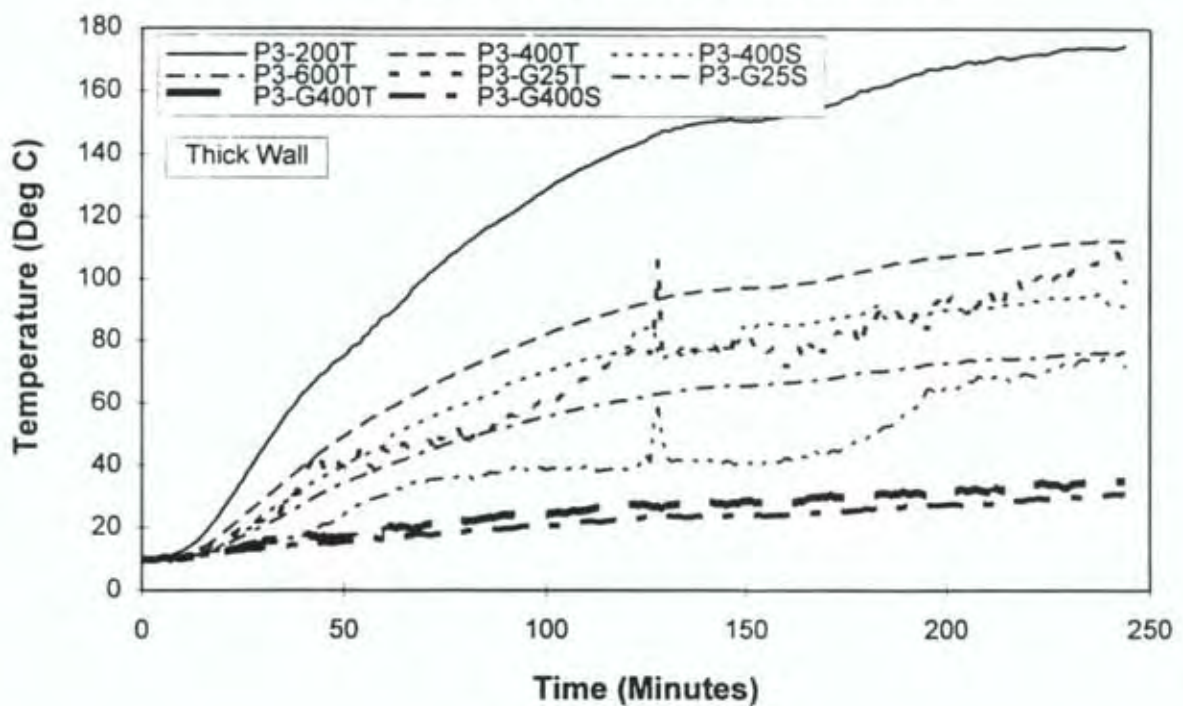


Figure A.6 Thermocouples P3-200T, P3-400T, P3-400S, P3-600T, P3-G25T, P3-G25S, P3-G400T, P3-G400S, 175 mm Thick Wall

Pipe P3 Temperatures Mid Pipe Length & Hot Face

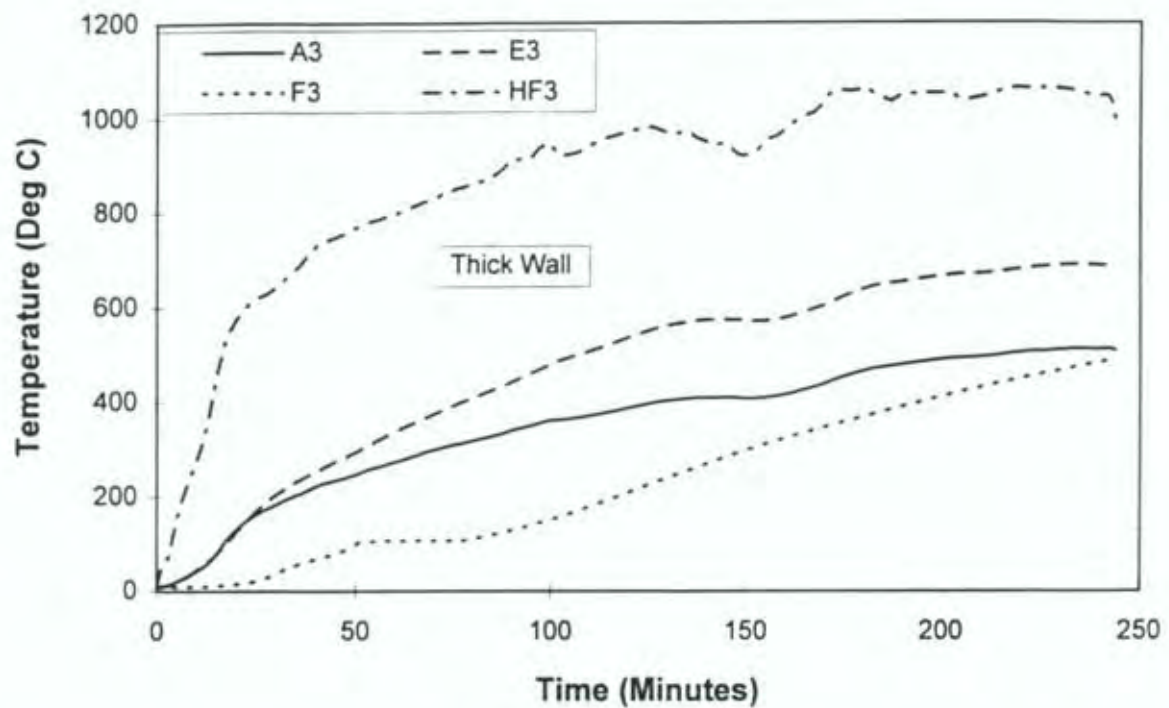


Figure A.7 Thermocouples at Mid Wall Thickness and Hot Face, A3, E3, F3, HF3, 175 mm Thick Wall

Pipe P4 & Concrete Temperatures @ 25 mm From the Cold Face

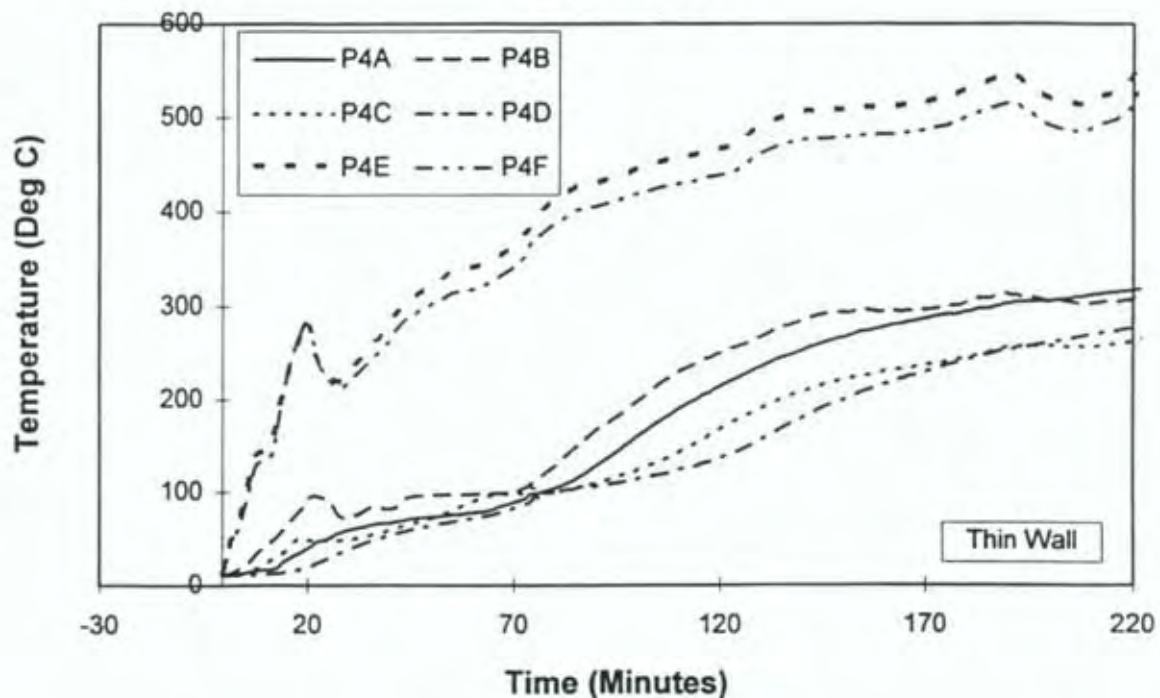


Figure A.8 Thermocouples P4A, P4B, P4C, P4D, P4E, P4F, 100 mm Thick Wall

Pipe P4 (& Guard) Temperatures

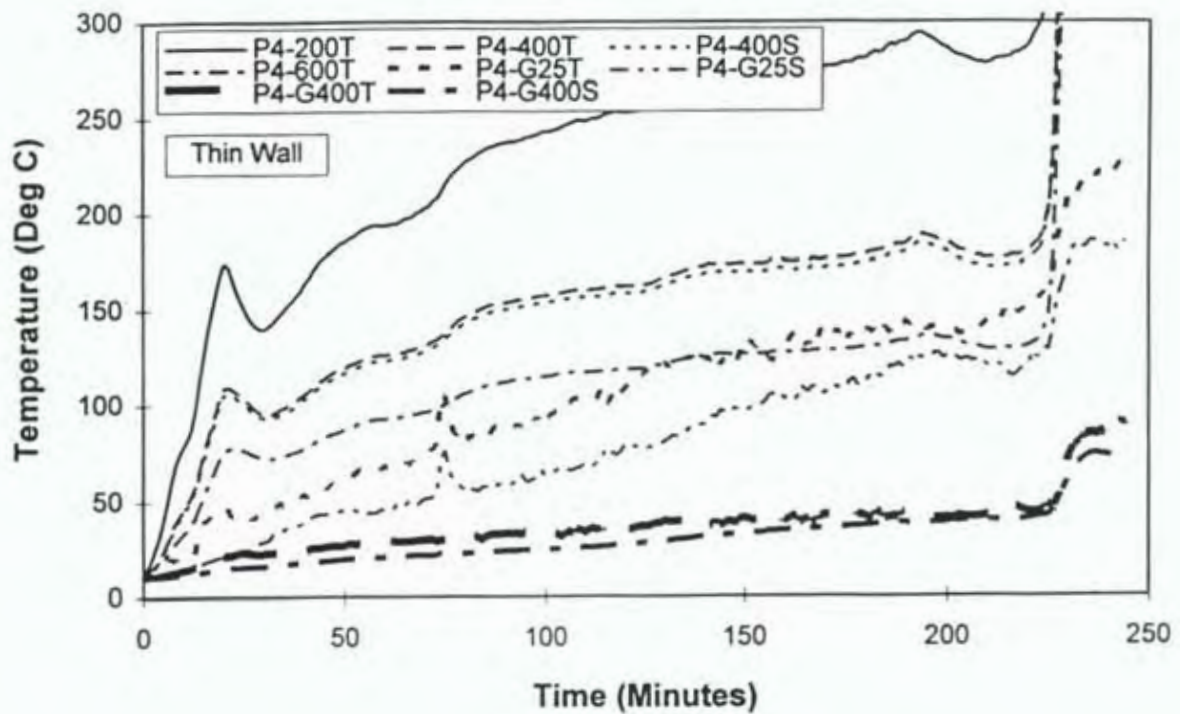


Figure A.9 Thermocouples P4-200T, P4-400T, P4-400S, P4-600T, P4-G25T, P4-G25S, P4-G400T, P4-G400S, 100 mm Thick Wall

Pipe P4 Temperatures Mid Pipe Length

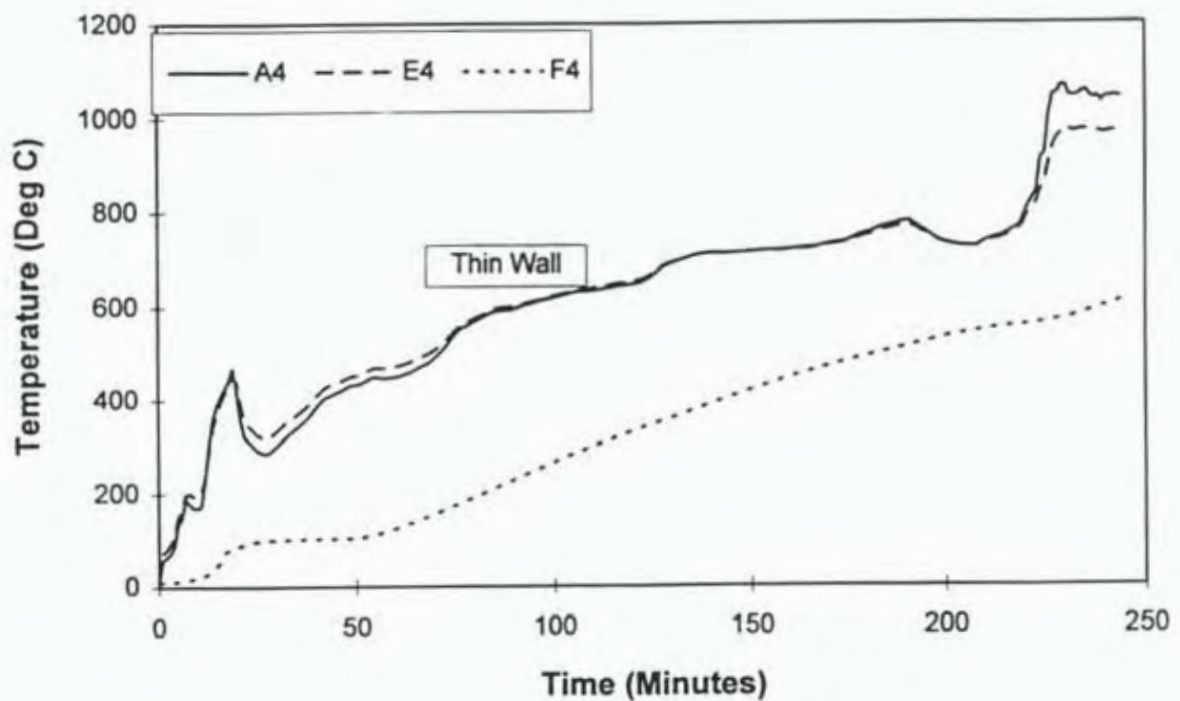


Figure A.10 Thermocouples at Mid Wall Thickness, A4, E4, F4, 100 mm Thick Wall

Pipe P5 & Concrete Temperatures

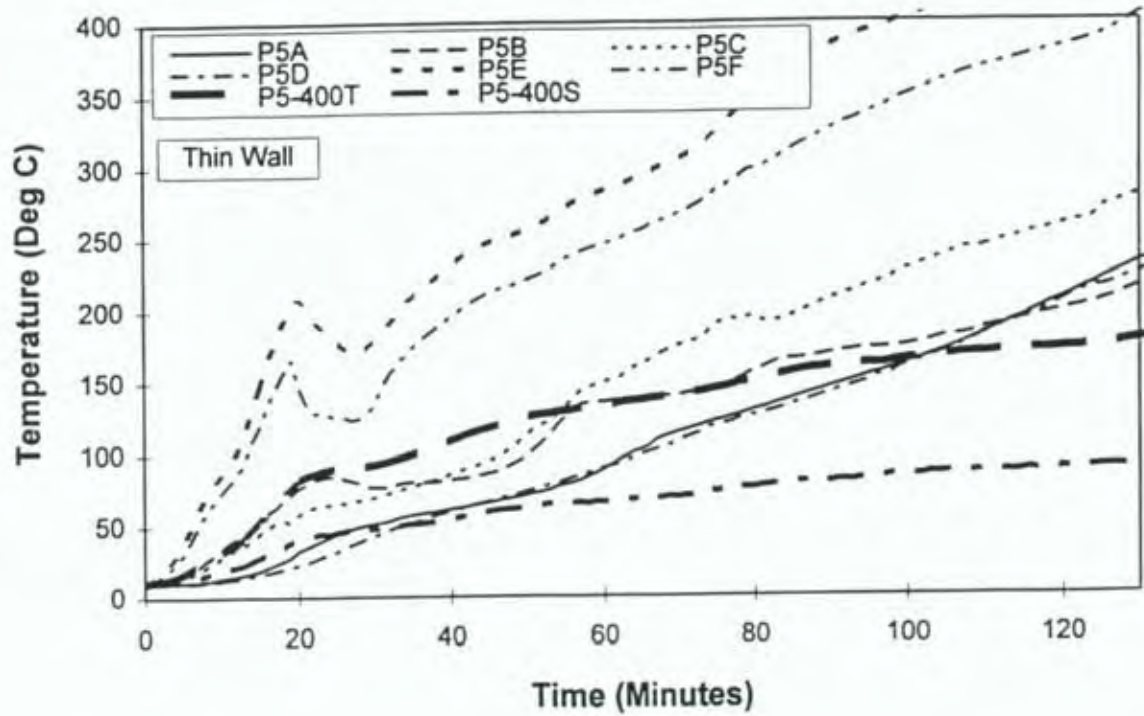


Figure A.11 Thermocouples P5A, P5B, P5C, P5D, P5E, P5F, P5-400T, P5-400S, 100 mm Thick Wall

Pipe P5 Temperatures Mid Pipe Length

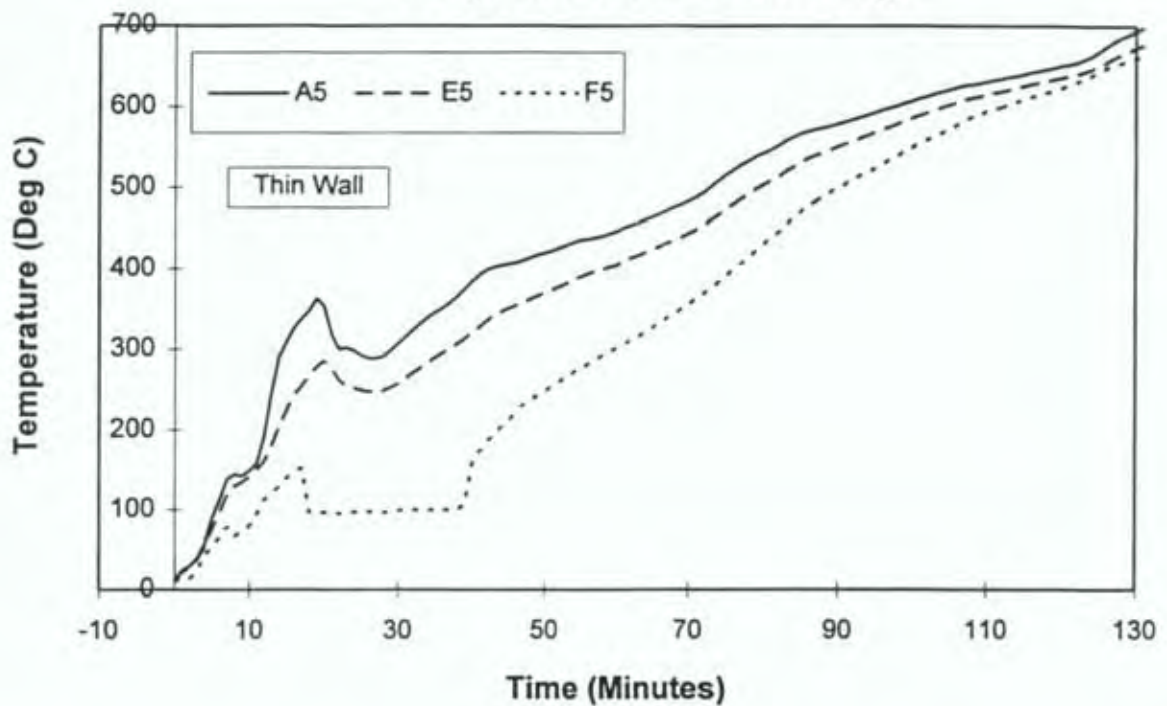


Figure A.12 Thermocouples at Mid Wall Thickness, A5, E5, F5 100 mm Thick Wall

Pipe P6 & Concrete Temperatures @ 25 mm From the Cold Face

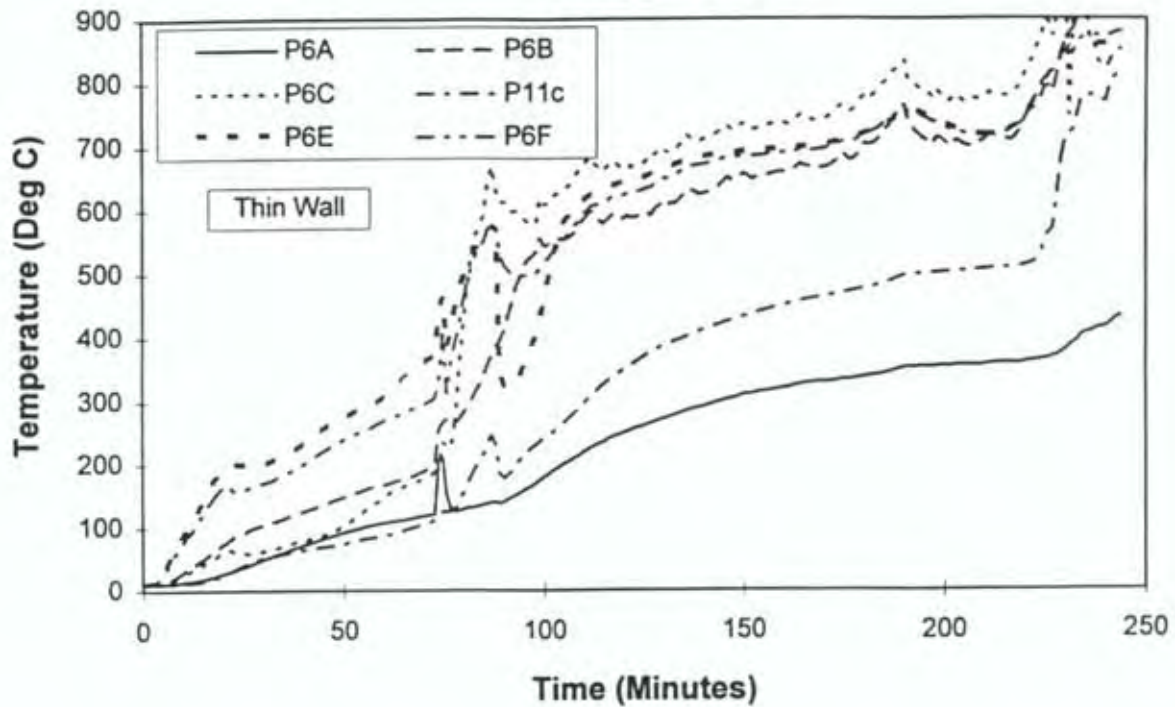


Figure A.13 Thermocouples P6A, P6B, P6C, P6D, P6E, P6F, 100 mm Thick Wall

Pipe P6 Temperatures

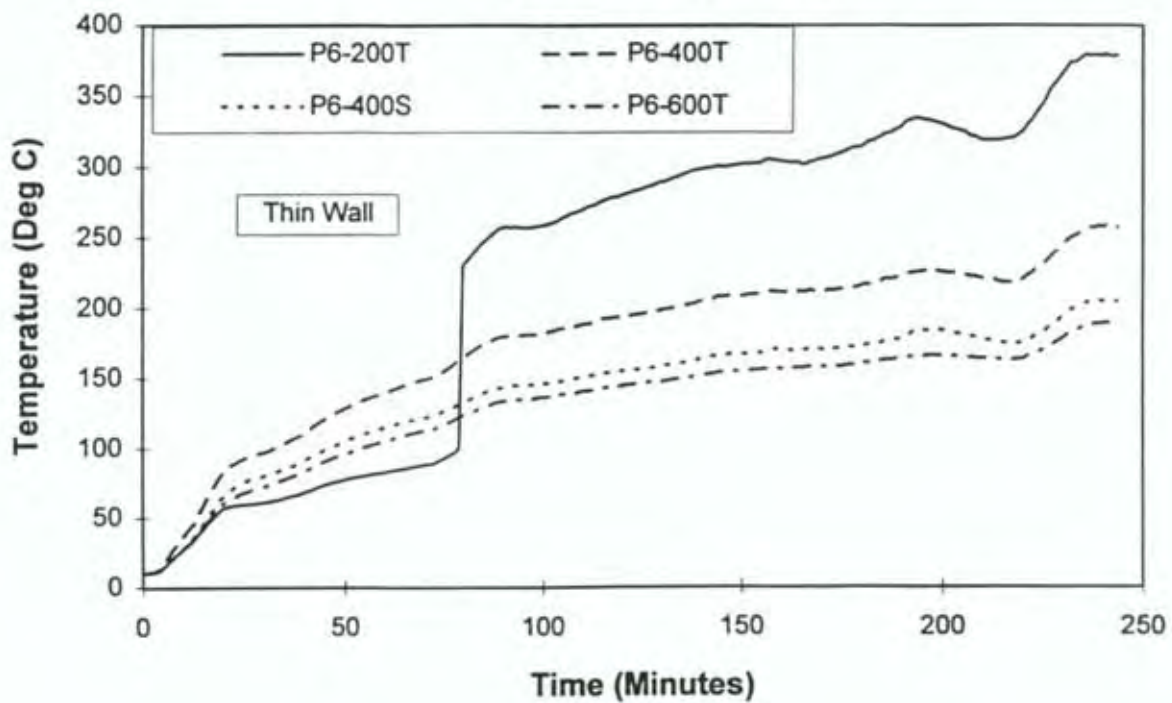


Figure A.14 Thermocouples P6-200T, P6-400T, P6-400S, P6-600T, 100 mm Thick Wall

Pipe P6 Temperatures Mid Pipe Length

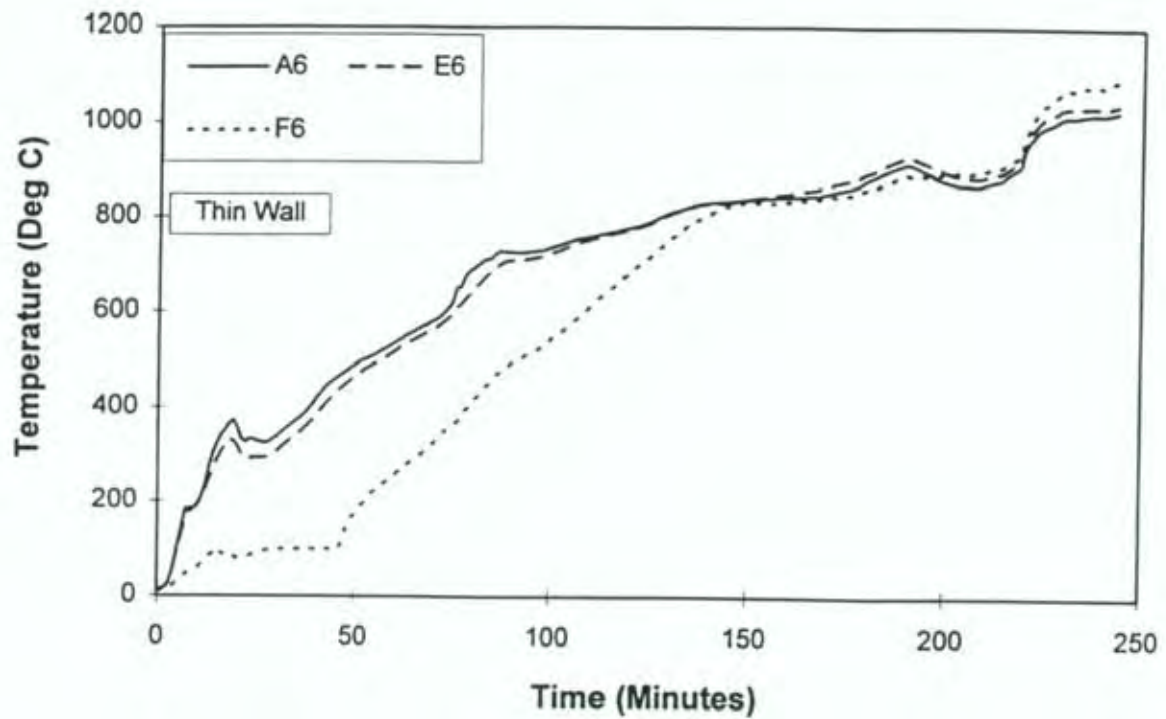


Figure A.15 Thermocouples at Mid Wall Thickness, A6, E6, F6 100 mm Thick Wall

Pipe P7 & Concrete Temperatures

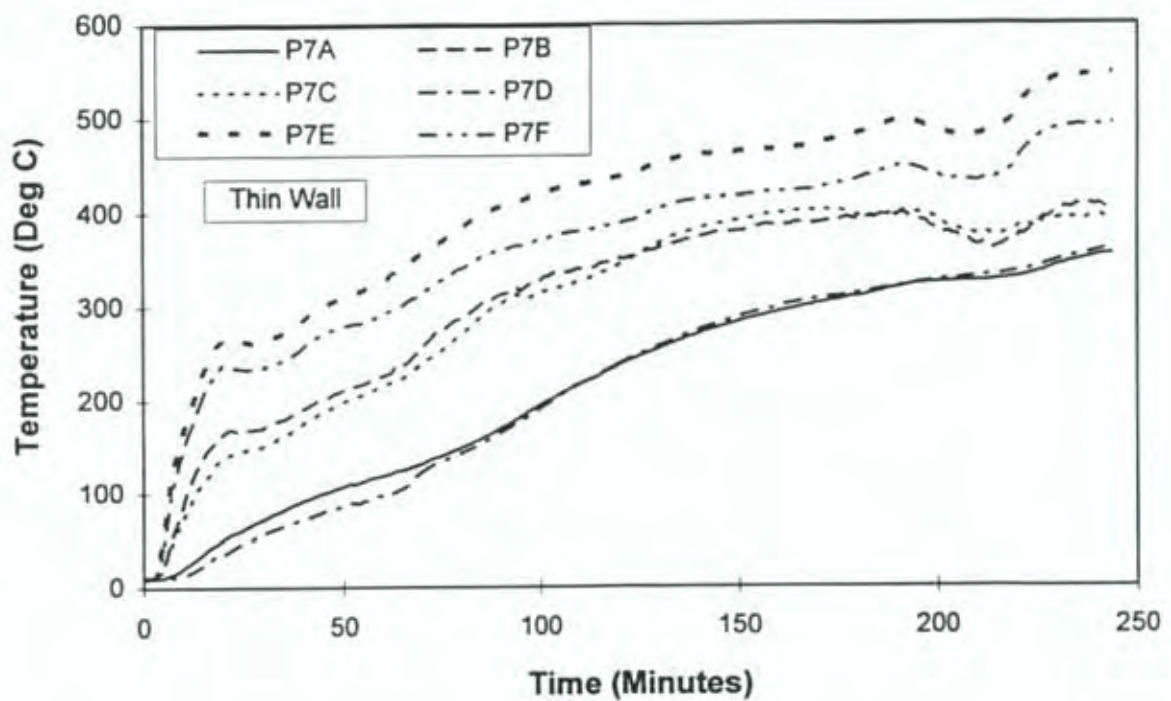


Figure A.16 Thermocouples P7A, P7B, P7C, P7D, P7E, P7F, P7-400T, P7-400S
100 mm Thick Wall

Pipe P8 & Concrete Temperatures @ 25 mm From the Cold Face

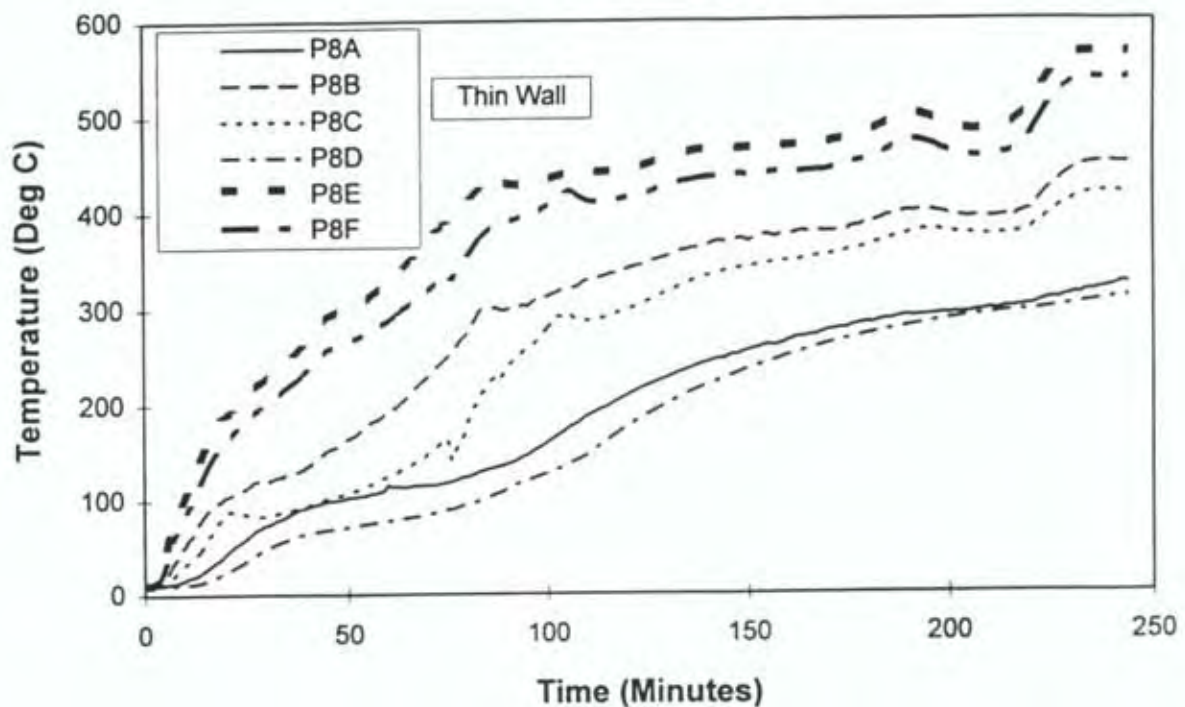


Figure A.17 Thermocouples P8A, P8B, P8C, P8D, P8E, P8F, 100 mm Thick Wall

Pipe P8 Temperatures

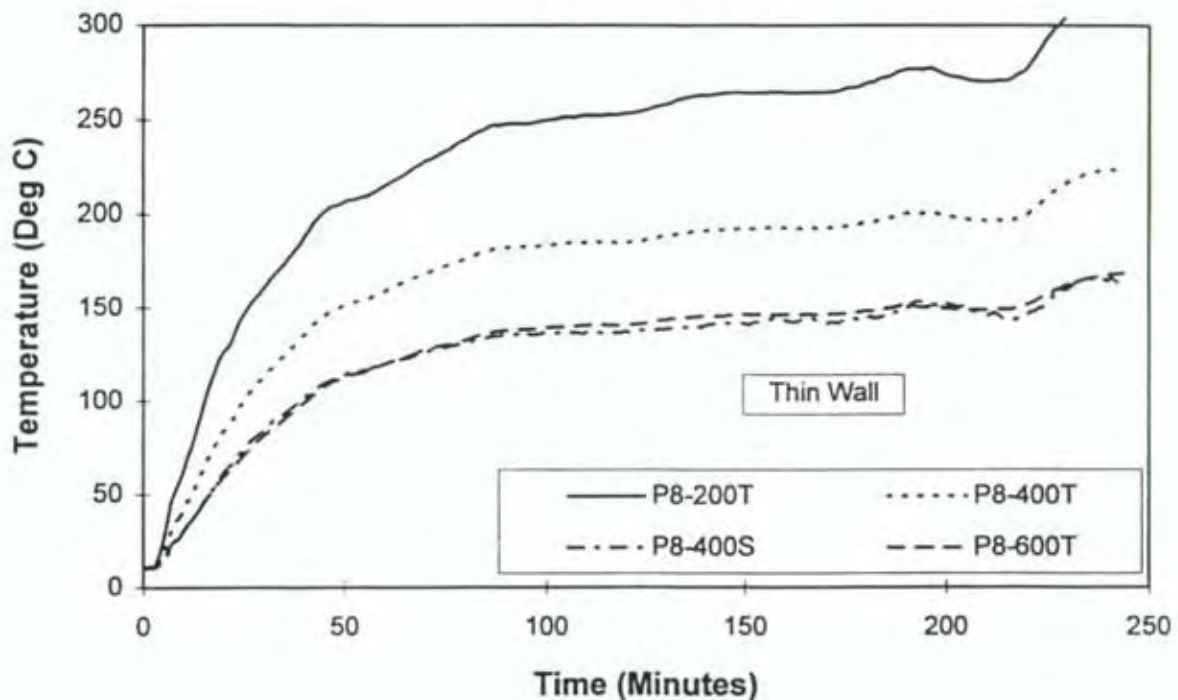


Figure A.18 Thermocouples P8-200T, P8-400T, P8-400S, P8-600T, 100 mm Thick Wall

Pipe P9 & Concrete Temperatures

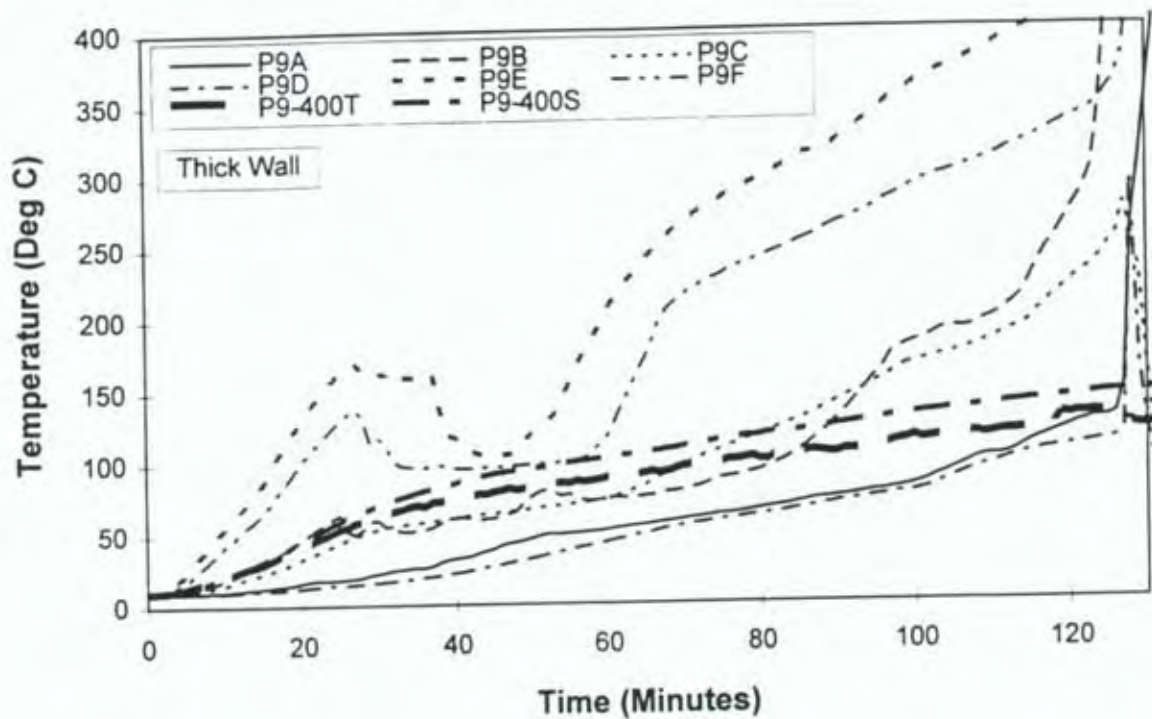


Figure A.19 Thermocouples P9A, P9B, P9C, P9D, P9E, P9F, P9-400T, P9-400S 175 mm Thick Wall

Pipe P9 Temperatures Mid Pipe Length

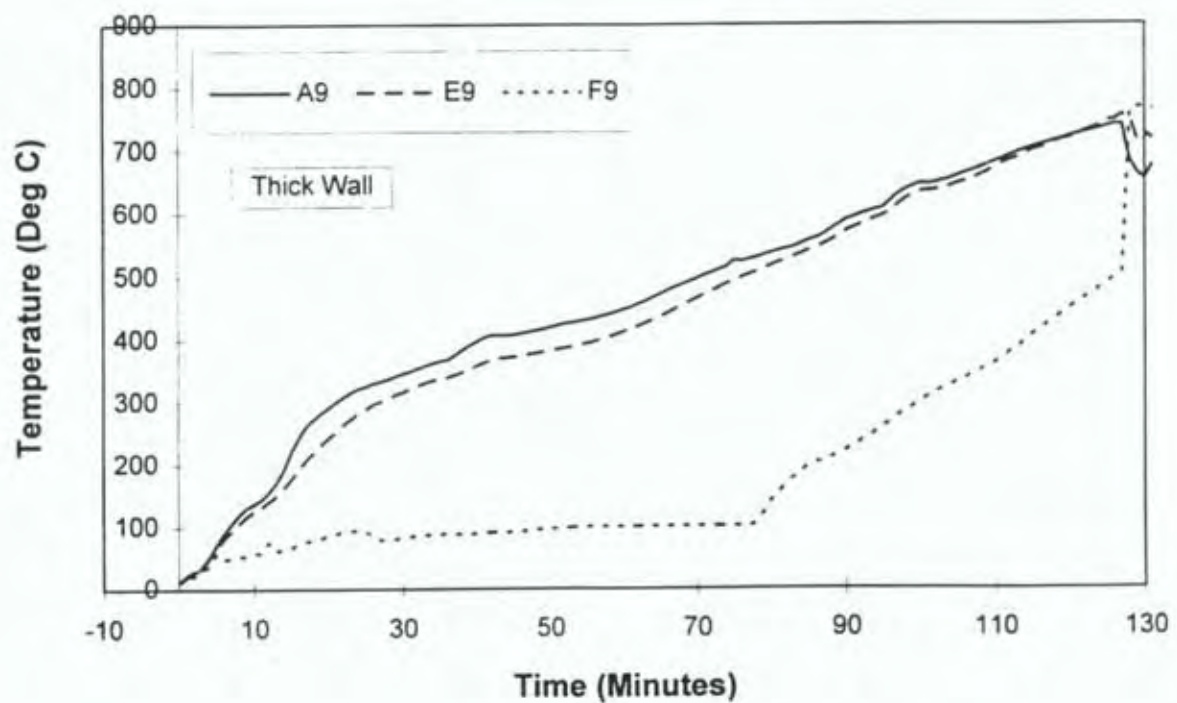


Figure A.20 Thermocouples at Mid Wall Thickness, A9, E9, F9 175 mm Thick Wall

Pipe P10 & Concrete Temperatures

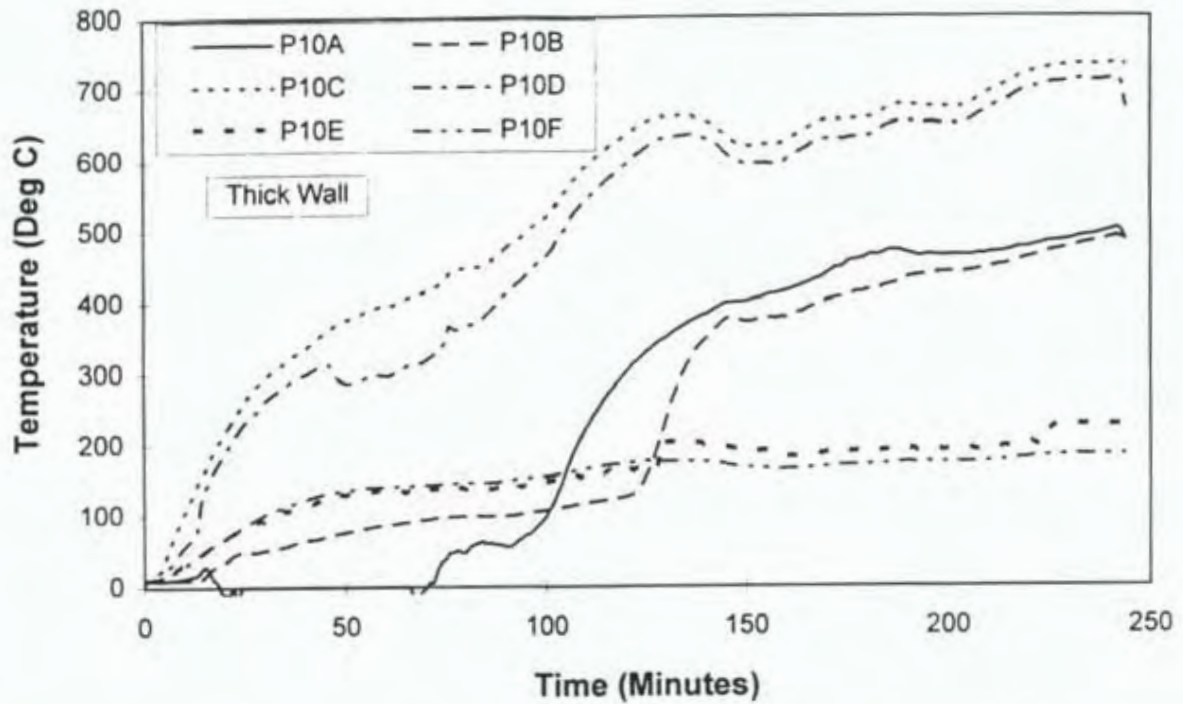


Figure A.21 Thermocouples P10A, P10B, P10C, P10D, P10E, P10F, 175 mm Thick Wall

Pipe P11 & Concrete Temperatures @ 25 mm From the Cold Face

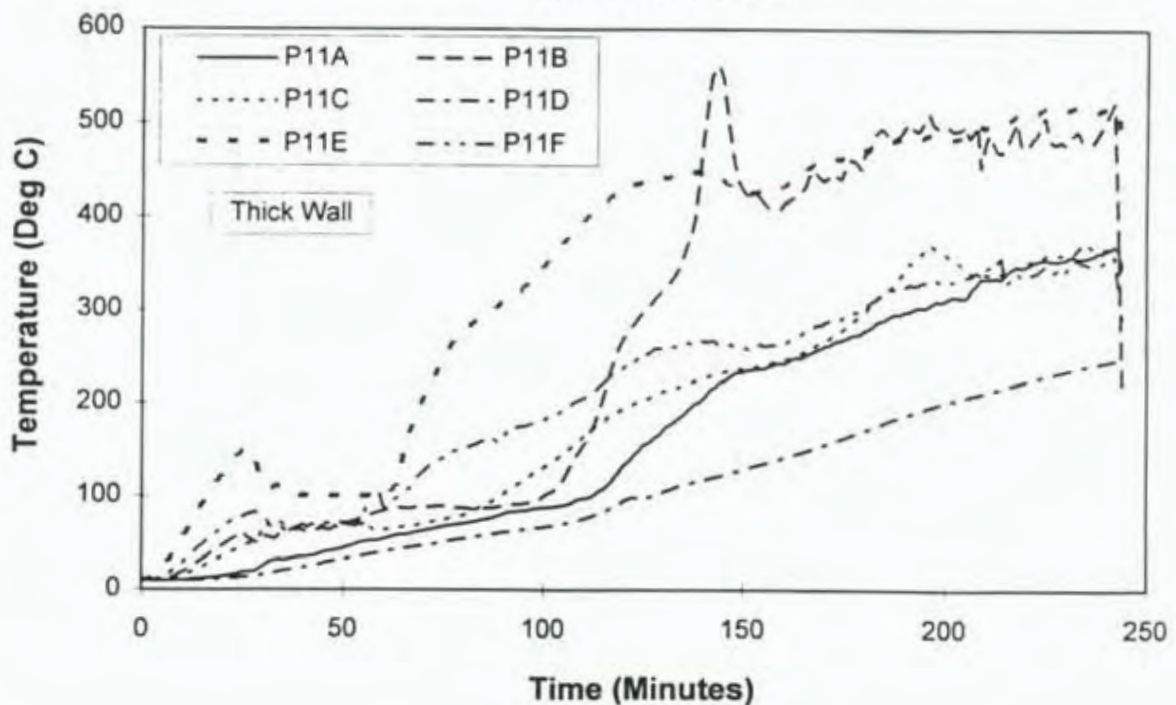


Figure A.22 Thermocouples P11A, P11B, P11C, P11D, P11E, P11F, 175 mm Thick Wall

Pipe P11 Temperatures Mid Pipe Length & Hot Face

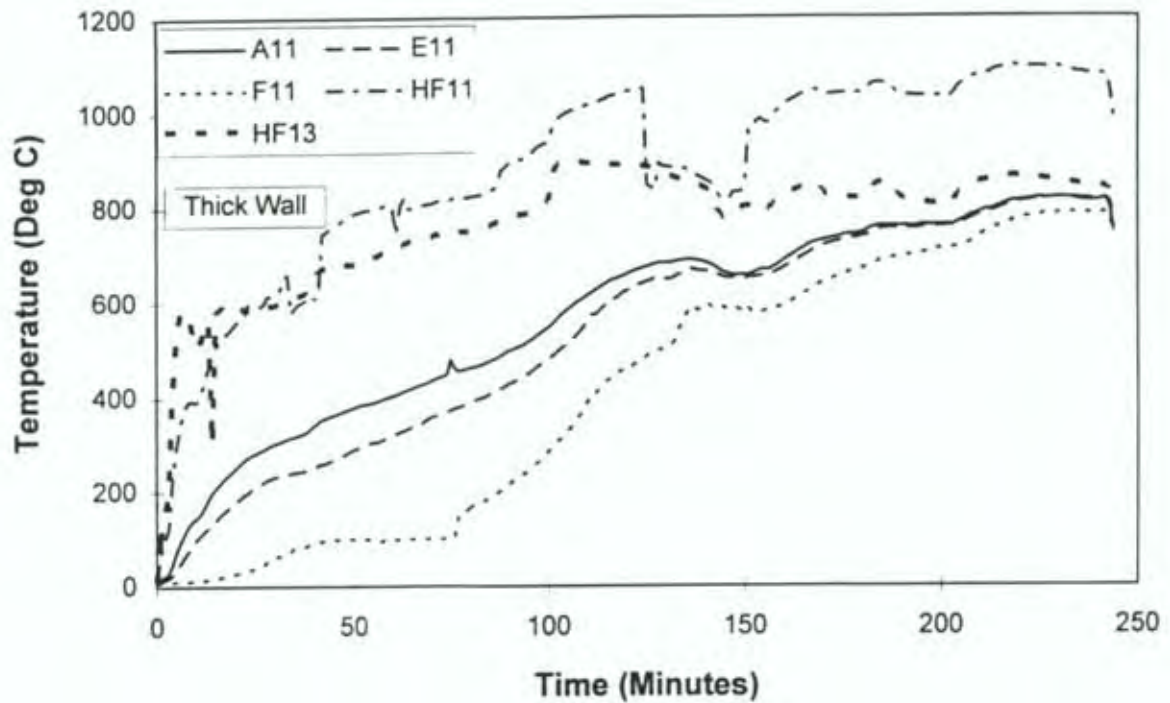


Figure A.24 Thermocouples at Mid Wall Thickness and Hot Face, A11, E11, F11, HF11, HF13 175 mm Thick Wall

Pipe P11 Temperatures

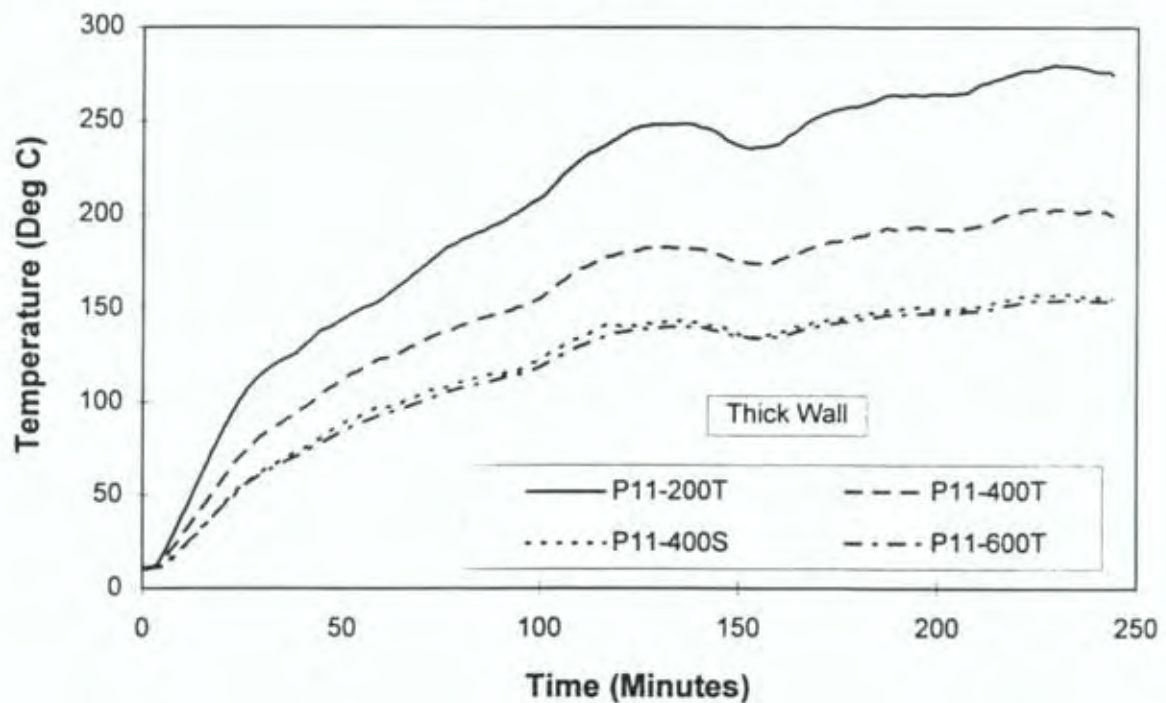


Figure A.23 Thermocouples P11-200T, P11-400T, P11-400S, P11-600T, 175 mm Thick Wall

Pipe P12 & Concrete Temperatures @ 25 mm From the Cold Face

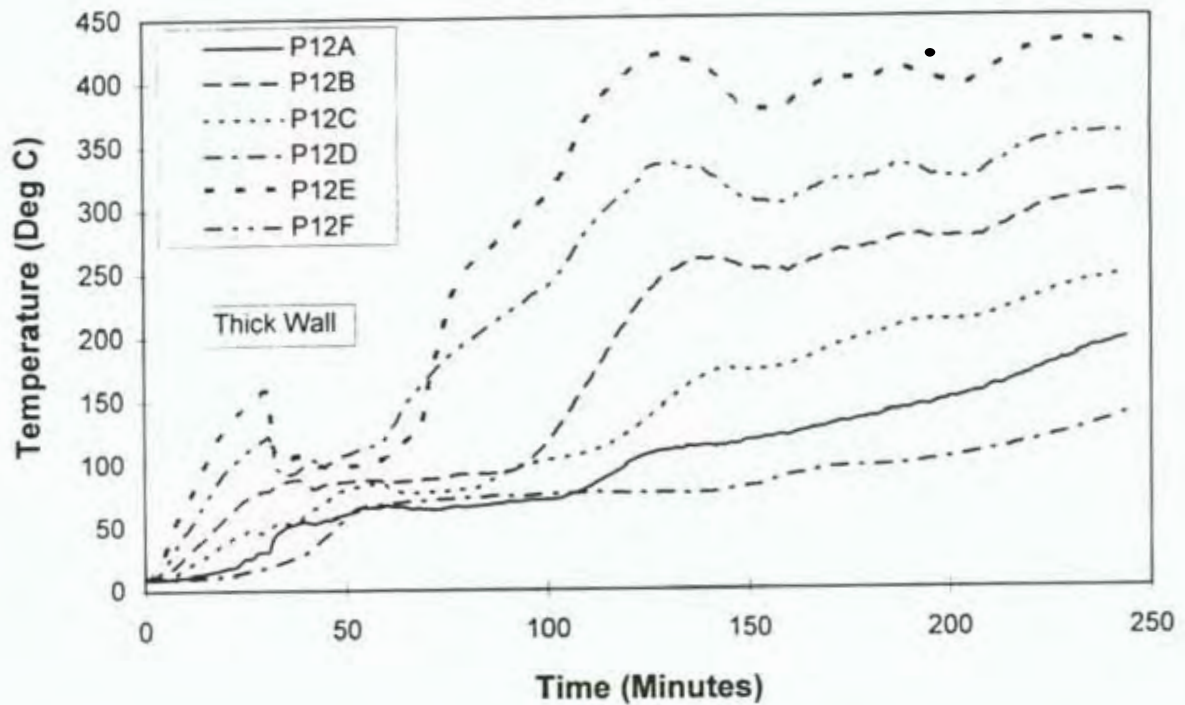


Figure A.25 Thermocouples P12A, P12B, P12C, P12D, P12E, P12F, 175 mm Thick Wall

Pipe P12 Temperatures

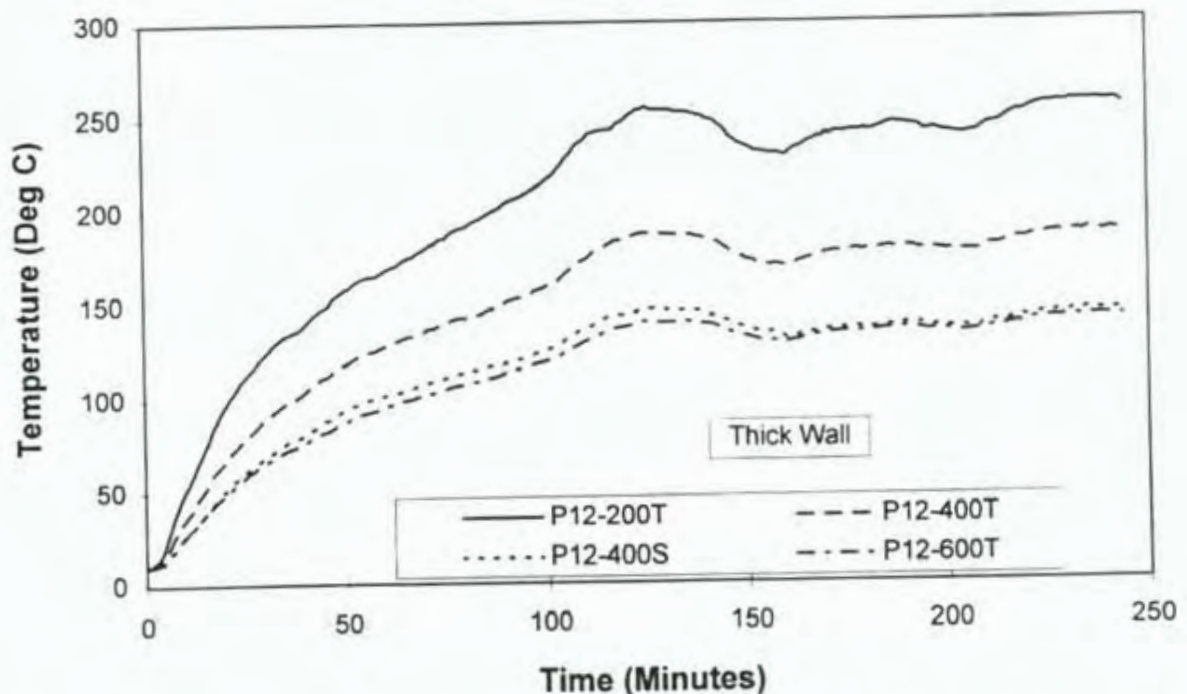


Figure A.26 Thermocouples P12-200T, P12-400T, P12-400S, P12-600T, 175 mm Thick Wall

Pipe P13 & Concrete Temperatures @ 25 mm From the Cold Face

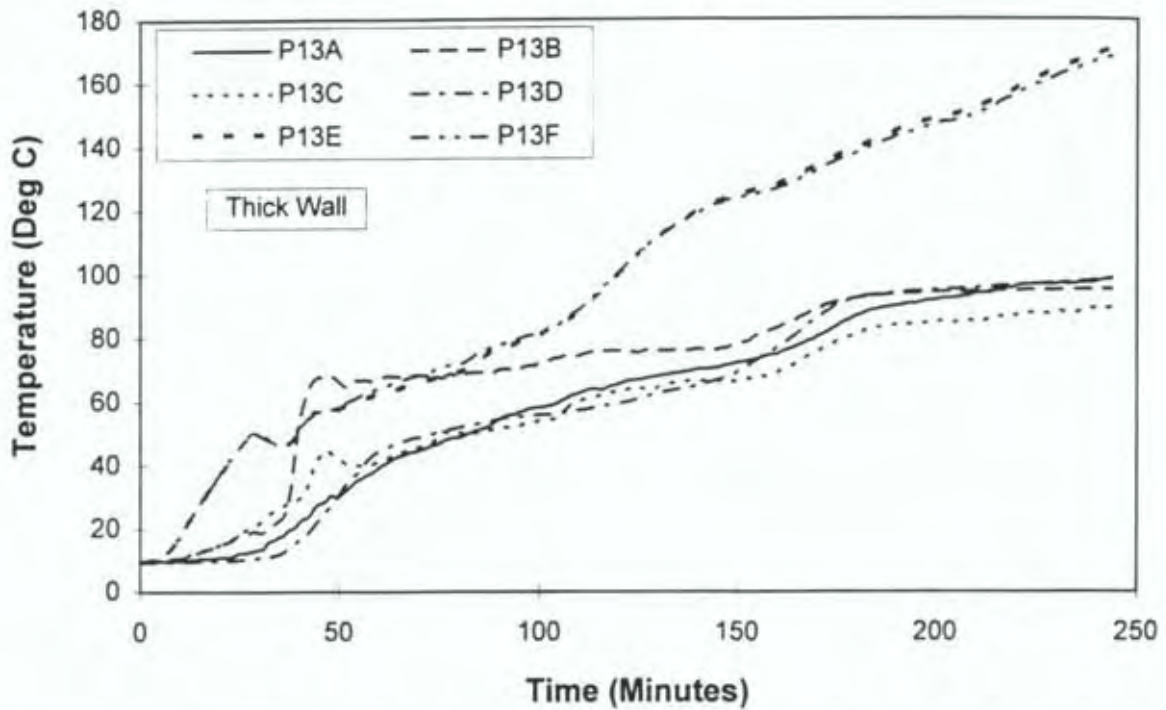


Figure A.27 Thermocouples P13A, P13B, P13C, P13D, P13E, P13F, 175 mm Thick Wall

Pipe P13 Temperatures

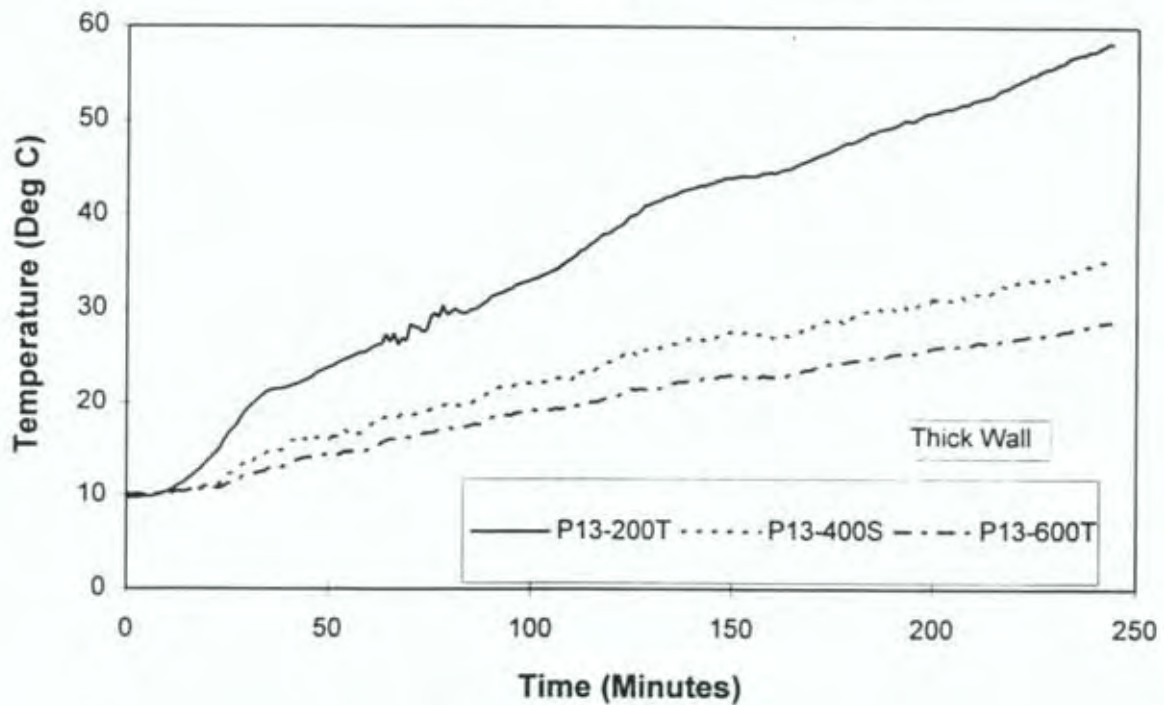


Figure A.28 Thermocouples P13-200T, P13-400S, P13-600T, 175 mm Thick Wall

Pipe P14 & Concrete Temperatures @ 25 mm From the Cold Face

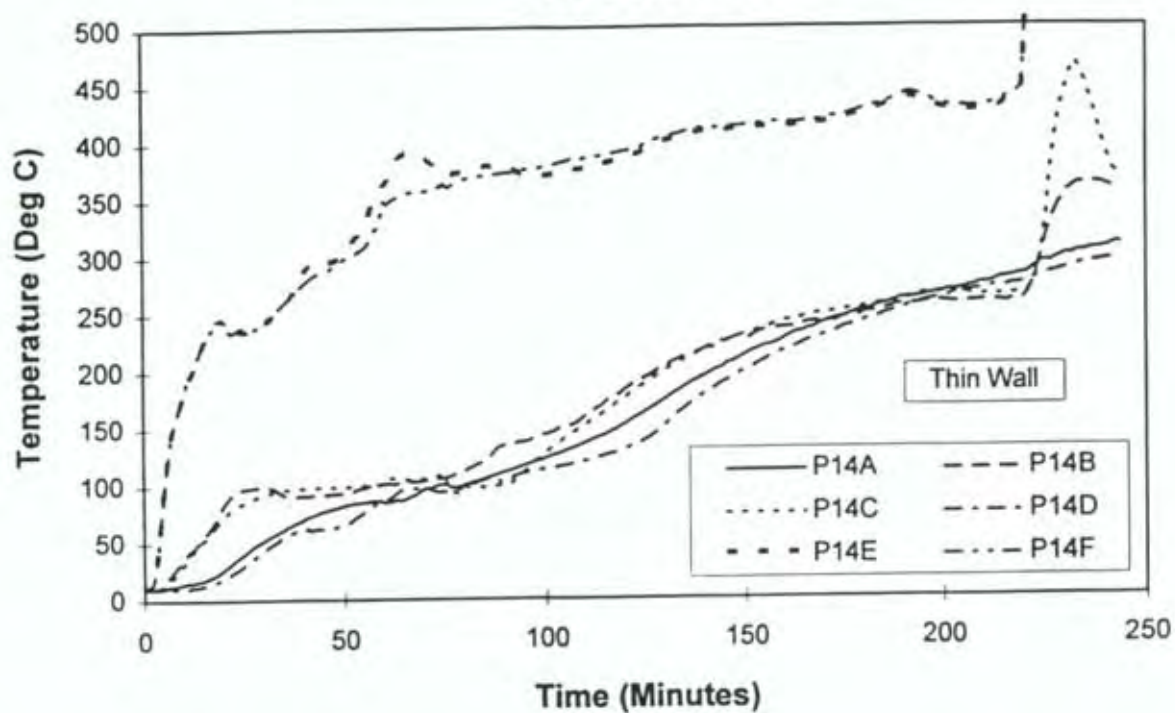


Figure A.29 Thermocouples P14A, P14B, P14C, P14D, P14E, P14F, 100 mm Thick Wall

Pipe P14 Temperatures

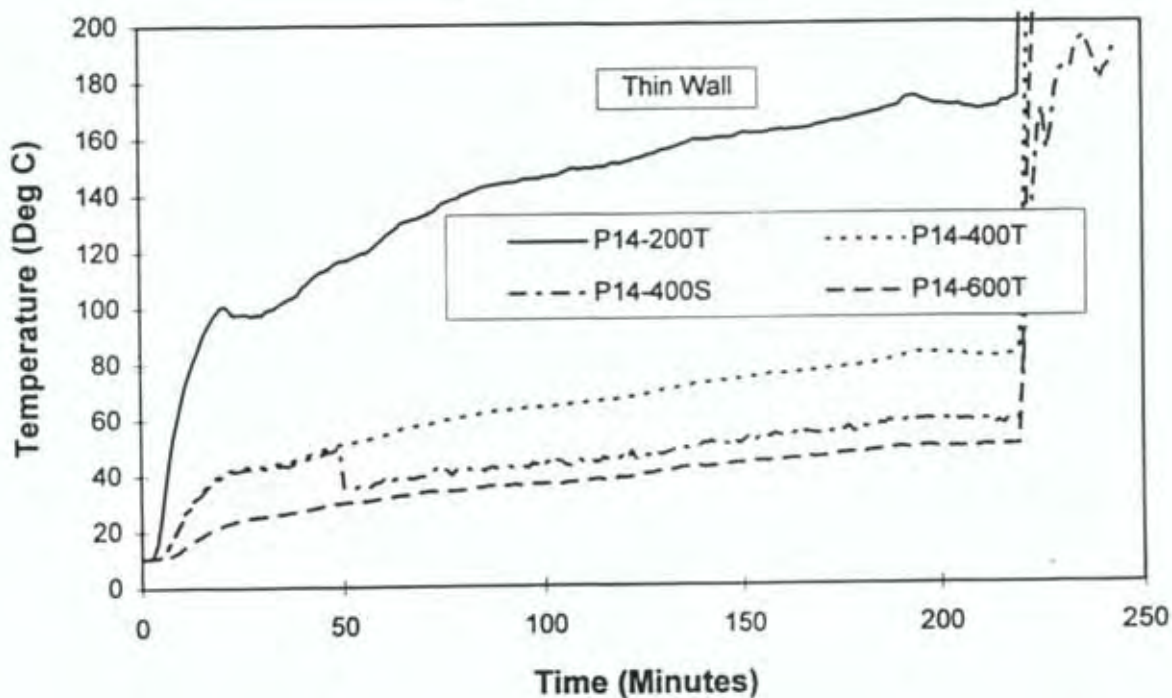


Figure A.30 Thermocouples P14-200T, P14-400T, P14-400S, P14-600T, 100 mm Thick Wall

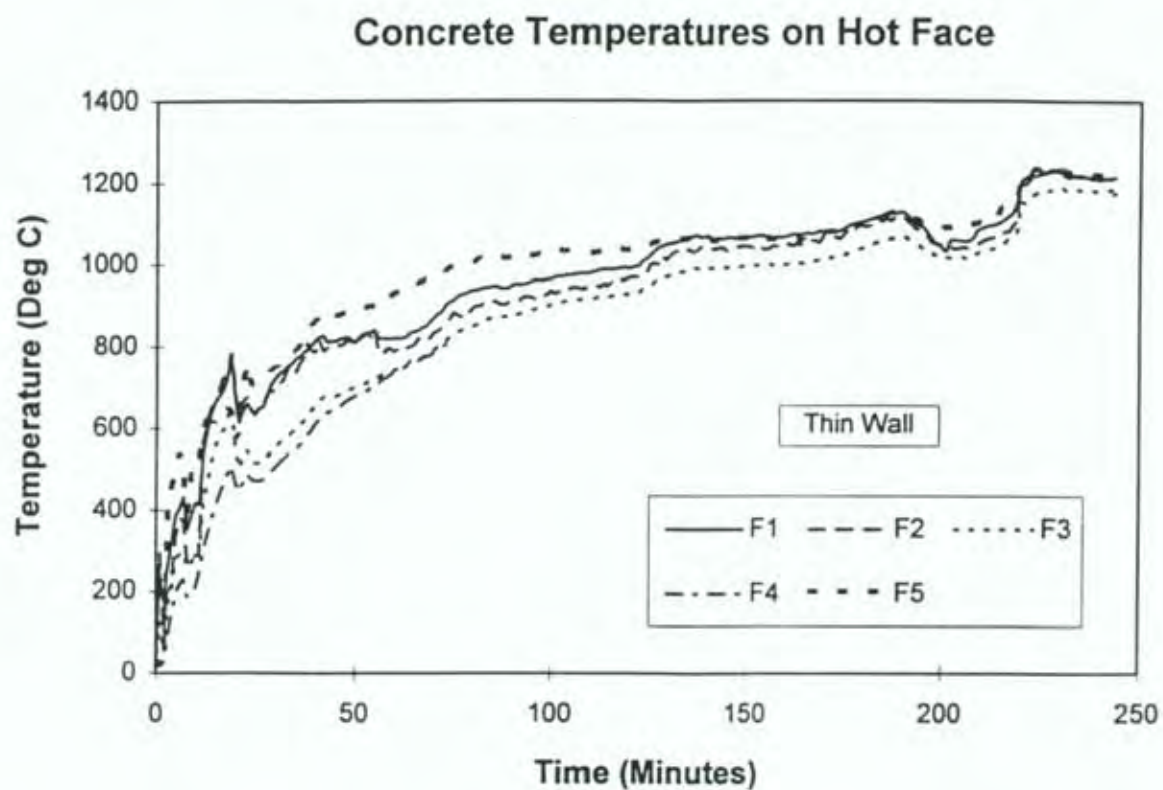


Figure A.31 Concrete Temperatures on the Exposed Face (Thermocouples F1, F2, F3, F4, F5), 100 mm Thick Wall

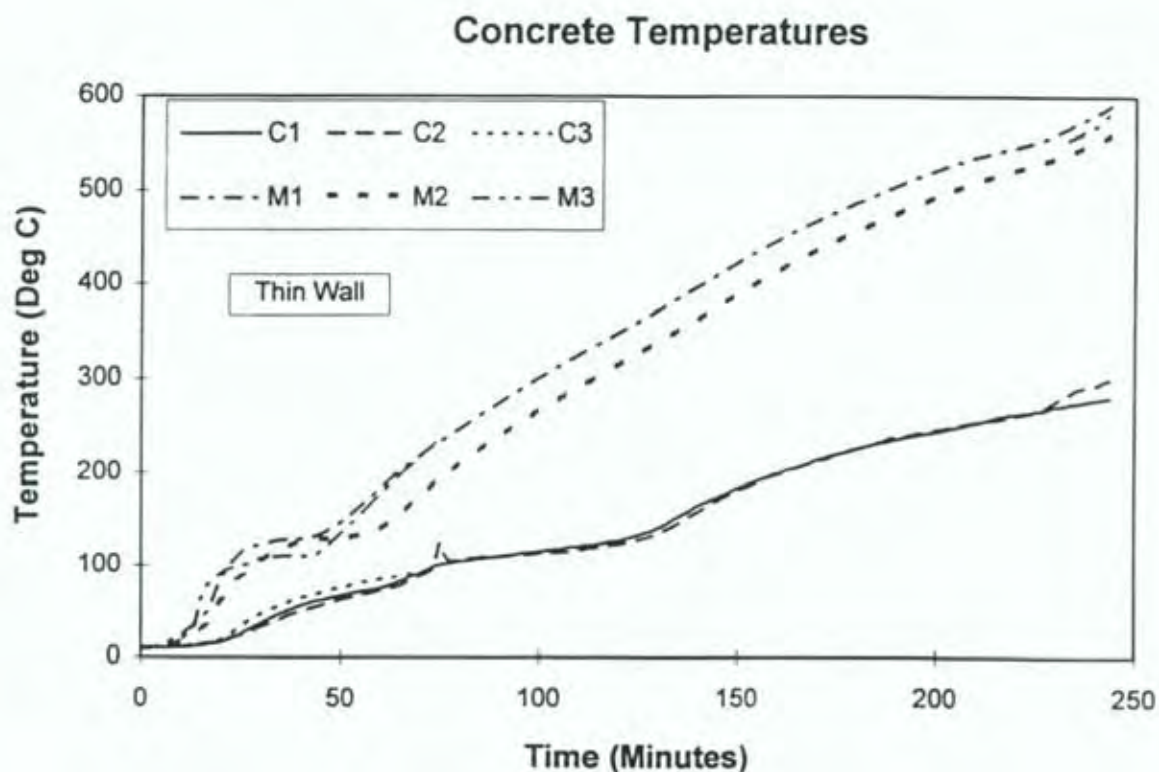


Figure A.32 Concrete Temperatures at Mid-depth and on the Unexposed Face (Thermocouples M1, M2, M3, C1, C2, C3), 100 mm Thick Wall

Concrete Temperatures on Hot Face

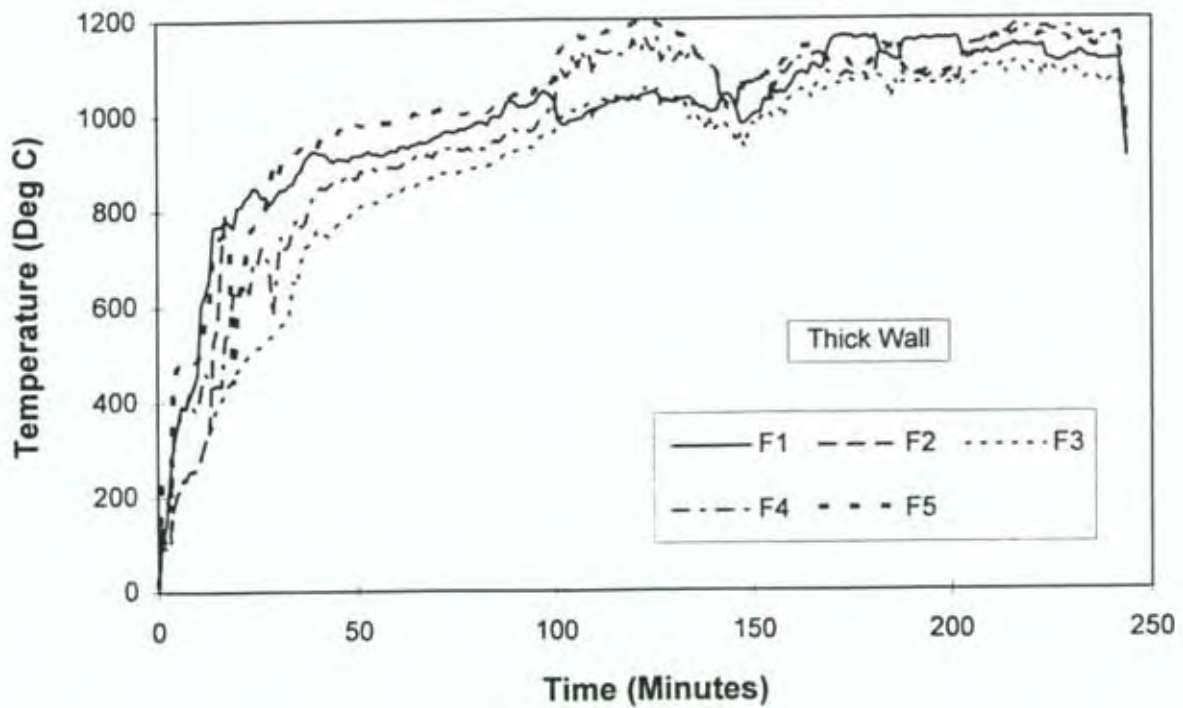


Figure A.33 Concrete Temperatures on the Exposed Face (Thermocouples F1, F2, F3, F4, F5), 175 mm Thick Wall

Concrete Temperatures

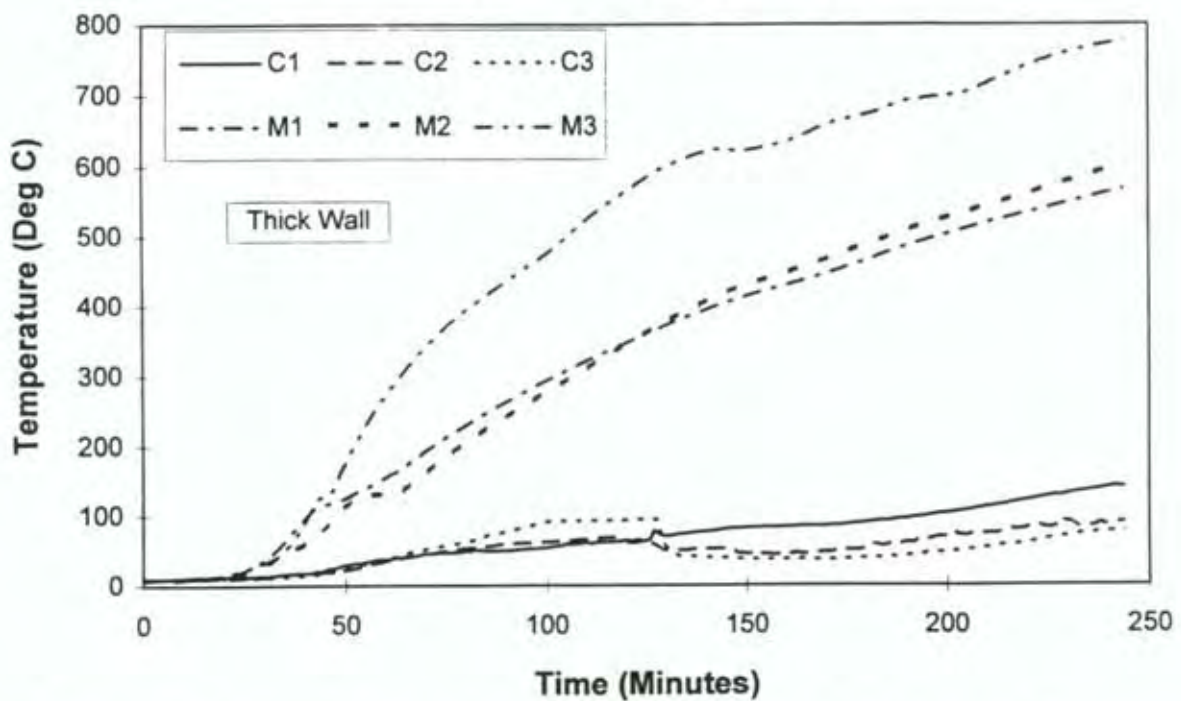


Figure A.34 Concrete Temperatures at Mid-depth and on the Unexposed Face (Thermocouples M1, M2, M3, C1, C2, C3), 175 mm Thick Wall

Appendix B Proprietary Products Used

Six proprietary products were used in the experimental program described in this report and are referred to as Type A, B, C, D, E or F. These products are described in generic terms in Table 2 and are further identified below:

Seal Type	Manufacturer	Brand Name	Generic Type**
A	Pyropanel Technologies	Intumex MW	Intumescent sealant
B*	Pyropanel Technologies	Pyropanel 201 SFR	Non-intumescent polyurethane sealant
C	Fosroc Ltd	Flamex One	Acrylic sealant
D	Firepro Safety Ltd	Firepro GPC Fire Stop Sealing Compound	Gypsum filler
E	Firepro Safety Ltd	Firepro Fyre-Mortar	Lightweight concrete
F	Fosroc Expandite Ltd	Flamex MS	Intumescent sealant

- Note: The manufacturer of seal Type B advised BRANZ that the seal used in this test came from old stock that had gone well past the expiry date, and therefore that good performance could not be expected.

** See Table 2 in the main text.

Note: Results obtained in this study relate only to the samples tested, and not to any other item of the same or similar description. BRANZ does not necessarily test all brands or types available within the class of items tested and exclusion of any brand or type is not to be taken as any reflection on it.

This work was carried out for specific research purposes, and BRANZ may not have assessed all aspects of the products named which would be relevant in any specific use. For this reason, BRANZ disclaims all liability for any loss or other deficit, following use of the named products, which is claimed to be reliance on the results published here.

Further, the listing of any trade or brand names above does not represent endorsement of any named product nor imply that it is better or worse than any other available product of its type. A laboratory test may not be exactly representative of the performance of the item in general use.

Appendix C Methodology for Performing Nisa Analysis

C.1 NISA Software Package

NISA consists of several modules. Only two, DISPLAY III and HEAT ANALYSIS, were used in this project.

DISPLAY III can be used interactively to generate the geometry, finite element mesh and convective and radiation boundary properties. As the interactive menu-driven commands are entered into the program, NISA generates several files. One is a Session file which is effectively a list of input commands. This file may be used to recreate a NISA job rather than manually re-entering the NISA interactive commands. Another file created is a NISA input file which may also be used to recreate a NISA job. Both are in ASCII format. The NISA input file must be used to run the HEAT module, but is difficult to alter if the finite element geometry is changed.

C.2 Processing Procedure

The procedure used in this study was to generate the first session file interactively, to define the basic finite element mesh. The pipe size, thickness or wall thickness definition cards within the session file were then altered using a text processor for each different geometry problem to be analysed. A separate session file was thus developed for each geometry to be analysed. Each session file was then used to generate a separate NISA input file for each geometry.

Member properties for the first problem were defined interactively on NISA. These were cut from the resulting NISA file and merged onto the other NISA file generated using the various session files. These amalgamated NISA files were used for the HEAT analysis module of NISA.

The output from the heat analysis is read back into DISPLAY III which will plot or print out temperature profiles or node time histories.

C.3 Input Data

A typical session file and NISA input file is provided at the back of this appendix. Within the session file the geometry of the problem can simply be altered by changing the co-ordinates of the beginning and end points defined in the "LIN" command. To facilitate alteration of the geometry, Figure C.1 shows the line and patch numbers used to generate the mesh in the session file.

The material properties can be altered in the NISA file. In particular, the enthalpy needs altering for the particular concrete moisture content. The calculation for enthalpy is achieved by the EXCEL spreadsheet shown in Table 8. This EXCEL data was pasted into WORD 6.0, put in the correct format by using the table facilities within this program, and then cut and pasted into the NISA file.

C.4 Output Data

Nodes for which temperature time histories are required are selected in the NISA file. The post processor facilities of DISPLAY III of NISA allow an ASCII file of node temperatures-histories to be generated. These can simply be plotted in a spreadsheet program.

The .OUT NISA file can be used to plot temperature profiles at a selected instant in time. The output time increment must be set in NISA to ensure the selected time coincides with the .OUT printout times. The data (temperatures at all nodes) at the selected time is cut from the .OUT file and pasted into a spreadsheet programme. Node co-ordinates are cut from the NISA file and pasted into the same spreadsheet. After match-up of nodes is achieved the profiles can be plotted.

C.5 Finite Element Mesh

A typical finite element mesh is shown in Figure C.2. The elements are axi-symmetric and the axis of rotation is shown in Figure C.1. In the model the pipe extends 150 mm into the furnace and 700 mm from the unexposed (cold face). The mesh is finer in zones of high temperature gradient and coarser in less critical areas.

In the example shown the seal is 24 mm thick. Normally this seal would be thinner and thus the mesh finer. The origin and mesh have been carefully selected to ensure two nodes (nodes 68 and 167) exactly coincide with the code-specified 25 mm critical points (see Section 1.3.2), irrespective of pipe or seal thickness.

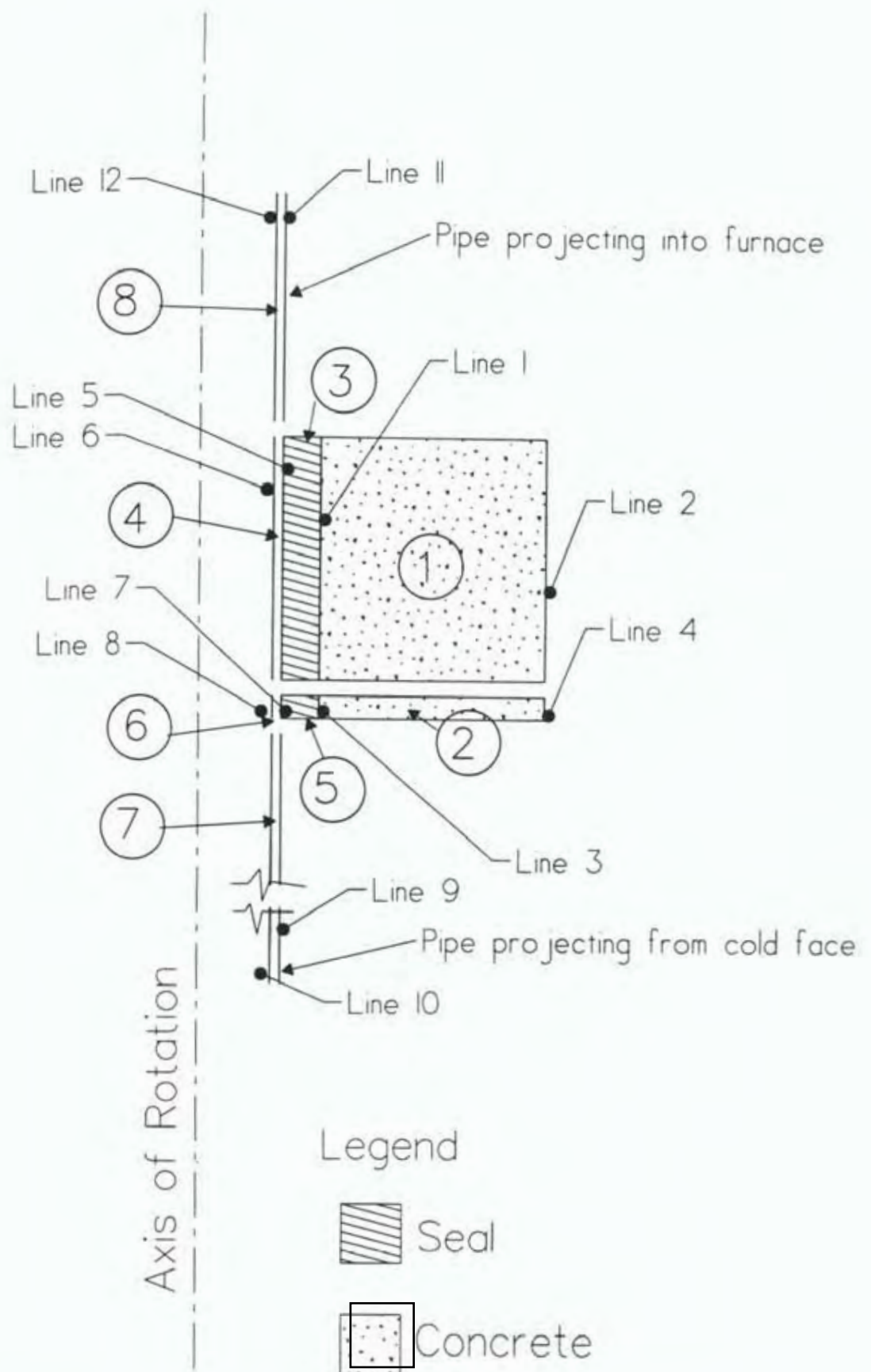


Figure C.1 Line and Patch Numbers Used in Mesh Generation

Session File For Pipe 4

```

SET,ANAL,THEAT
** 200 DIAMETER HOLE IN THE CONCRETE
** CONCRETE 100 MM THICK
** mortar SEAL 47.6 mm THICK
** PIPE 1.6 MM THICK copper pipe
** outside diameter 104.8 mm
** Define Patch 1 (Lines 1 and 2). Material 1 (Concrete)
WPL,PLO,1,
** line 1
LIN,2WP,1,,0.1/0///0.1/0.085///
** line 2
LIN,2WP,1,,0.25/0///0.25/0.085///
PAT,2LN,1,2,
FAM,QUA,1,,,6/7/6/7/,103/1/1/1,0.2/3.0/0.2/3.0
** Define Patch 2 (Lines 3 and 4) Material 1 (Concrete)
**line 3
LIN,2WP,1,,0.1/-0.015///0.1/0.00///
** line 4
LIN,2WP,1,,0.25/-0.015///0.25/0.00///
PAT,2LN,3,4,
FAM,QUA,2,,,1/7/1/7/,103/1/1/1,1.0/3.0/1.0/3.0
** Define Patch 3 & 4 (lines 5 & 1 and 6 and 5 respectively).
** Patch 3 is seal (material 2) while patch 4 is pipe (material 3)
** line 5
LIN,2WP,1,,0.0524/0///0.0524/0.085///
** line 6
LIN,2WP,1,,0.0508/0///0.0508/0.085///
PAT,2LN,5,1,
FAM,QUA,3,,,6/3/6/3/,103/1/2/2,0.2/1.0/0.2/1.0
PAT,2LN,6,5,
FAM,QUA,4,,,6/1/6/1/,103/1/3/3,0.2/1.0/0.2/1.0
** Define Patch 5 & 6 (Lines 7 & 3 and 8 & 7 respectively).
** Patch 5 is seal (material 2) while patch 6 is pipe (material 3)
** line 7
LIN,2WP,1,,0.0524/-0.015///0.0524/0.00///
** line 8
LIN,2WP,1,,0.0508/-0.015///0.0508/0.00///
PAT,2LN,7,3,
FAM,QUA,5,,,1/3/1/3/,103/1/2/2,1.0/1.0/1.0/1.0
PAT,2LN,8,7,
FAM,QUA,6,,,1/1/1/1/,103/1/3/3,1.0/1.0/1.0/1.0
** Define Patch 7 (Bottom pipe) Lines 9 & 10 material 3
** line 9
LIN,2WP,1,,0.0524/-0.7///0.0524/-0.015///
** line 10
LIN,2WP,1,,0.0508/-0.7///0.0508/-0.015///
PAT,2LN,10,9,
FAM,QUA,7,,,20/1/20/1/,103/1/3/3,0.2/1.0/0.2/1.0
** Define Patch 8 (Top pipe) Lines 11 & 12 material 3

```

```

** line 11
LIN,2WP,/1,,0.0524/0.085///0.0524/0.25///
** line 12
LIN,2WP,/1,,0.0508/0.085///0.0508/0.25///
PAT,2LN,12,11,
FAM,QUA,8,,,5/1/5/1/1,103/1/3/3,2.0/1.0/2.0/1.0
WPL,MXT,,-0.02/0.3/-0.20/0.3,0
VEW, TOP
NOD,MER,ALL,0.001
Y
CNV,ADD,6,1,3/10.0/1426.0, / /1
CNV,ADD,12,1,3/10.0/1426.0, / /1
CNV,ADD,18,1,3/10.0/1426.0, / /1
CNV,ADD,24,1,3/10.0/1426.0, / /1
CNV,ADD,30,1,3/10.0/1426.0, / /1
CNV,ADD,36,1,3/10.0/1426.0, / /1
CNV,ADD,42,1,3/10.0/1426.0, / /1
CNV,ADD,55,1,3/10.0/1426.0, / /1
CNV,ADD,61,1,3/10.0/1426.0, / /1
CNV,ADD,67,1,3/10.0/1426.0, / /1
CNV,ADD,98,1,2/10.0/1426.0, / /1
CNV,ADD,99,1,2/10.0/1426.0, / /1
CNV,ADD,100,1,2/10.0/1426.0, / /1
CNV,ADD,101,1,2/10.0/1426.0, / /1
CNV,ADD,102,1,2/10.0/1426.0, / /1
CNV,ADD,43,1,1/7.0/293.0, / /0
CNV,ADD,44,1,1/7.0/293.0, / /0
CNV,ADD,45,1,1/7.0/293.0, / /0
CNV,ADD,46,1,1/7.0/293.0, / /0
CNV,ADD,47,1,1/7.0/293.0, / /0
CNV,ADD,48,1,1/7.0/293.0, / /0
CNV,ADD,49,1,1/7.0/293.0, / /0
CNV,ADD,74,1,1/7.0/293.0, / /0
CNV,ADD,75,1,1/7.0/293.0, / /0
CNV,ADD,76,1,1/7.0/293.0, / /0
CNV,ADD,78,1,2/7.0/293.0, / /0
CNV,ADD,79,1,2/7.0/293.0, / /0
CNV,ADD,80,1,2/7.0/293.0, / /0
CNV,ADD,81,1,2/7.0/293.0, / /0
CNV,ADD,82,1,2/7.0/293.0, / /0
CNV,ADD,83,1,2/7.0/293.0, / /0
CNV,ADD,84,1,2/7.0/293.0, / /0
CNV,ADD,85,1,2/7.0/293.0, / /0
CNV,ADD,86,1,2/7.0/293.0, / /0
CNV,ADD,87,1,2/7.0/293.0, / /0
CNV,ADD,88,1,2/7.0/293.0, / /0
CNV,ADD,89,1,2/7.0/293.0, / /0
CNV,ADD,90,1,2/7.0/293.0, / /0
CNV,ADD,91,1,2/7.0/293.0, / /0
CNV,ADD,92,1,2/7.0/293.0, / /0
CNV,ADD,93,1,2/7.0/293.0, / /0
CNV,ADD,94,1,2/7.0/293.0, / /0
CNV,ADD,95,1,2/7.0/293.0, / /0

```


CNV,ADD,96,1,2/7.0/293.0, / /0
CNV,ADD,97,1,2/7.0/293.0, / /0
RAD,ADD,102,1,2/0.9/1426, / /1
RAD,ADD,101,1,2/0.9/1426, / /1
RAD,ADD,100,1,2/0.9/1426, / /1
RAD,ADD,99,1,2/0.9/1426, / /1
RAD,ADD,98,1,2/0.9/1426, / /1
RAD,ADD,6,1,3/0.9/1426, / /1
RAD,ADD,12,1,3/0.9/1426, / /1
RAD,ADD,18,1,3/0.9/1426, / /1
RAD,ADD,24,1,3/0.9/1426, / /1
RAD,ADD,30,1,3/0.9/1426, / /1
RAD,ADD,36,1,3/0.9/1426, / /1
RAD,ADD,42,1,3/0.9/1426, / /1
RAD,ADD,55,1,3/0.9/1426, / /1
RAD,ADD,61,1,3/0.9/1426, / /1
RAD,ADD,67,1,3/0.9/1426, / /1
RAD,ADD,78,1,2/0.9/293, / /0
RAD,ADD,79,1,2/0.9/293, / /0
RAD,ADD,80,1,2/0.9/293, / /0
RAD,ADD,81,1,2/0.9/293, / /0
RAD,ADD,82,1,2/0.9/293, / /0
RAD,ADD,83,1,2/0.9/293, / /0
RAD,ADD,84,1,2/0.9/293, / /0
RAD,ADD,85,1,2/0.9/293, / /0
RAD,ADD,86,1,2/0.9/293, / /0
RAD,ADD,87,1,2/0.9/293, / /0
RAD,ADD,88,1,2/0.9/293, / /0
RAD,ADD,89,1,2/0.9/293, / /0
RAD,ADD,90,1,2/0.9/293, / /0
RAD,ADD,91,1,2/0.9/293, / /0
RAD,ADD,92,1,2/0.9/293, / /0
RAD,ADD,93,1,2/0.9/293, / /0
RAD,ADD,94,1,2/0.9/293, / /0
RAD,ADD,95,1,2/0.9/293, / /0
RAD,ADD,96,1,2/0.9/293, / /0
RAD,ADD,97,1,2/0.9/293, / /0
RAD,ADD,43,1,1/0.9/293.0, / /0
RAD,ADD,44,1,1/0.9/293.0, / /0
RAD,ADD,45,1,1/0.9/293.0, / /0
RAD,ADD,46,1,1/0.9/293.0, / /0
RAD,ADD,47,1,1/0.9/293.0, / /0
RAD,ADD,48,1,1/0.9/293.0, / /0
RAD,ADD,49,1,1/0.9/293.0, / /0
RAD,ADD,74,1,1/0.9/293.0, / /0
RAD,ADD,75,1,1/0.9/293.0, / /0
RAD,ADD,76,1,1/0.9/293.0, / /0

NISA File For Pipe 4

**EXECUTIVE

ANALYSIS = THEAT

FILE=ITEM4

SAVE=26

INIT=283

*TITLE

FIRE EXPOSURE OF Copper PIPE THROUGH 100 MM CONCRETE WALL
(ITEM 4)

*ELTYPE

1, 103, 1

*NODES

1,, 1.00000E-01, 0.00000E+00, 0.00000E+00, 0

2,, 1.00000E-01, 8.50000E-02, 0.00000E+00, 0

3,, 2.50000E-01, 8.50000E-02, 0.00000E+00, 0

..... etc. for each node

178,, 5.24000E-02, 1.34500E-01, 0.00000E+00, 0

179,, 5.24000E-02, 1.67500E-01, 0.00000E+00, 0

180,, 5.24000E-02, 2.06000E-01, 0.00000E+00, 0

*ELEMENTS

1, 1, 1, 1, 0

26, 4, 16, 27,

2, 1, 1, 1, 0

27, 16, 17, 28,

..... etc. for each element

102, 3, 1, 3, 0

176, 180, 171, 170,

*MATHEAT

** Concrete subject to phase change

DENS, 1,0, 0.2300,0,0,0,1

KXX, 1,0, 1.2.59,0,0,0,1

KYY, 1,0, 1.2.59,0,0,0,1

KZZ, 1,0, 1.2.59,0,0,0,1

C, 1,0, 2.1796,0,0,0,1

** Cement Mortar seal constant properties

DENS, 2,0, 0.600,0,0,0,0

KXX, 2,0, 0.0.2,0,0,0,0

KYY, 2,0, 0.0.2,0,0,0,0

KZZ, 2,0, 0.0.2,0,0,0,0

C, 2,0, 0.1796,0,0,0,0

** Copper Pipe temperature dependent props

DENS, 3,0, 0.8933,0,0,0,0

KXX, 3,0, 5.413,0,0,0,0

KYY, 3,0, 5.413,0,0,0,0

KZZ, 3,0, 5.413,0,0,0,0

C, 3,0, 6.480,0,0,0,0

*PCHANGE1

** 5.04% moisture content by mass - alluvial quartz

273, 0.00E+00, 298, 58E+06, 323, 117E+06, 348, 179E+06

373, 243E+06, 388, 545E+06, 398, 568E+06, 423, 629E+06
 448, 693E+06, 473, 759E+06, 498, 825E+06, 523, 892E+06
 548, 960E+06, 573, 1028E+06, 598, 1097E+06, 623, 1167E+06
 648, 1237E+06, 673, 1307E+06, 698, 1381E+06, 723, 1462E+06
 748, 1556E+06, 773, 1659E+06, 798, 1763E+06, 823, 1857E+06
 848, 1944E+06, 873, 2023E+06, 898, 2097E+06, 923, 2167E+06
 948, 2237E+06, 973, 2307E+06, 1023, 2447E+06, 1073, 2583E+06
 1123, 2717E+06, 1173, 2850E+06, 1273, 3118E+06, 1373, 3390E+06
 1473, 3664E+06, 1548, 3871E+06

*TIMEAMP

**ISO 834 FIRE

**PEAK TEMP AT 14400 SEC = 1426 K

1,52,0

0,0.207,120,0.505,240,0.574,360,0.614

480,0.644,600,0.667,900,0.709,1200,0.739

1500,0.763,1800,0.782,2100,0.798,2400,0.812

2700,0.824,3000,0.835,3300,0.845,3600,0.854

3900,0.863,4200,0.871,4500,0.878,4800,0.885

5100,0.891,5400,0.897,5700,0.903,6000,0.908

6300,0.913,6600,0.918,6900,0.923,7200,0.927

7500,0.932,7800,0.936,8100,0.940,8400,0.943

8700,0.947,9000,0.951,9300,0.954,9600,0.957

9900,0.961,10200,0.964,10500,0.967,10800,0.970

11100,0.973,11400,0.975,11700,0.978,12000,0.981

12300,0.983,12600,0.986,12900,0.988,13200,0.991

13500,0.993,13800,0.996,14100,0.998,14400,1.000

*TEMPFN

**concrete thermal conductivity

1,37

273,1.000,298,1.000,323,0.969,348,0.942

373,0.918,398,0.899,423,0.875,448,0.852

473,0.833,498,0.813,523,0.798,548,0.786

573,0.774,598,0.763,623,0.751,648,0.739

673,0.724,698,0.704,723,0.685,748,0.661

773,0.638,798,0.611,823,0.591,848,0.580

873,0.564,898,0.556,923,0.549,948,0.537

973,0.529,1023,0.510,1073,0.498,1123,0.498

1173,0.498,1273,0.498,1373,0.510,1473,0.521

1548,0.529

**concrete specific heat

2,37

273,0.426,298,0.426,323,0.450,348,0.475

373,0.492,398,0.550,423,0.591,448,0.610

473,0.620,498,0.627,523,0.634,548,0.639

573,0.644,598,0.649,623,0.654,648,0.659

673,0.666,698,0.709,723,0.823,748,0.937

773,1.000,798,0.937,823,0.840,848,0.780

873,0.717,898,0.663,923,0.656,948,0.654

973,0.659,1023,0.651,1073,0.632,1123,0.622

1173,0.625,1273,0.634,1373,0.639,1473,0.646

1548,0.651

**steel thermal conductivity

3,14

```

273,1,373,0.98,473,0.94,573,0.88
673,0.82,773,0.75,873,0.68,973,0.62
1073,0.50,1173,0.51,12763,0.53,1373,0.55
1473,0.57,1573,0.57
**steel specific heat
4,17
273,0.088,373,0.096,473,0.106,573,0.113
673,0.122,773,0.135,873,0.152,973,0.202
998,0.320,1008,1.000,1023,0.260,1048,0.202
1073,0.162,1173,0.130,1273,0.130,1373,0.130
1473,0.131
**copper thermal conductivity
5,8
200,1,300,0.971,400,0.952,600,0.918
800,0.886,1000,0.852,1200,0.821,1500,0.821
**copper specific heat
6,8
200,0.742,300,0.802,400,0.827,600,0.869
800,0.902,1000,0.940,1200,1.000,1500,1.000
*HEATCNTL, ID= 1
15,15,5,0.001
*TIMEINTEG
0.5,60,14400,
*STEPSIZE
5,5,5,5,5,5,5,
5,5,5,5,5,5,5,
5,5,5,5,5,5,5,
5,5,10,10,10,10,10,10,
10,10,10,10,10,10,10,10,
15,15,15,15,15,15,20,20,
20,20,20,20,20,20,20,20,
20,20,20,20,20,20,20,20,
20,20,20,20,20,20,20,20,
20,20,20,20,20,20,20,20,
20,20,20,20,20,20,20,20,
25,25,25,25,25,25,30,30,
30,30,30,30,30,30,30,30,
30,30,30,30,30,30,30,30,
30,30,30,30,30,30,30,30,
30,30,30,30,30,30,30,30,
30,30,30,30,30,30,30,30,
30,30,30,60,60,60,60,60,
60,60,60,60,60,60,60,60,
60,60,60,60,60,60,60,60,
60,60,60,60,60,60,60,60,
60,60,60,60,60,60,60,60,
60,60,60,60,60,60,60,60,
120
*CONVBC
** CONVBC SET = 1
6,,,3,-1, , , 1
0.100E+02,0.143E+04
etc. for each element face for which convection is set.

```



```

102,,,2,-1, , , 1
0.100E+02,0.143E+04
*RADBC,SIGMA=5.667E-08
** RADBC SET = 1
6,,,3,-1, , , 1
0.900E+00,0.143E+04
etc. for each element face for which radiation is set.
102,,,2,-1, , , 1
0.900E+00,0.143E+04
*TEMPHISTORY
10,68,60,16,17,3,5,6,167,77,78
*TEMPOUT
0,14400,1800
*PRINTCNTL
TEMP,0
*ENDDATA

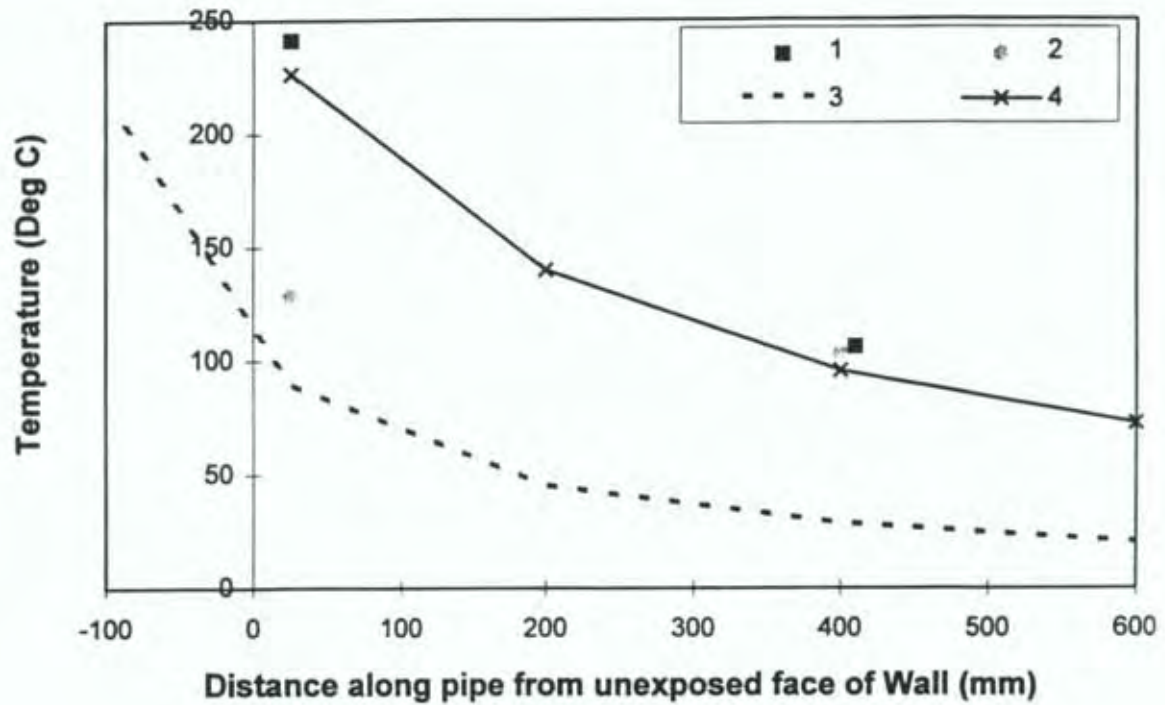
```

Appendix D Measured Temperature Profiles Along Pipes

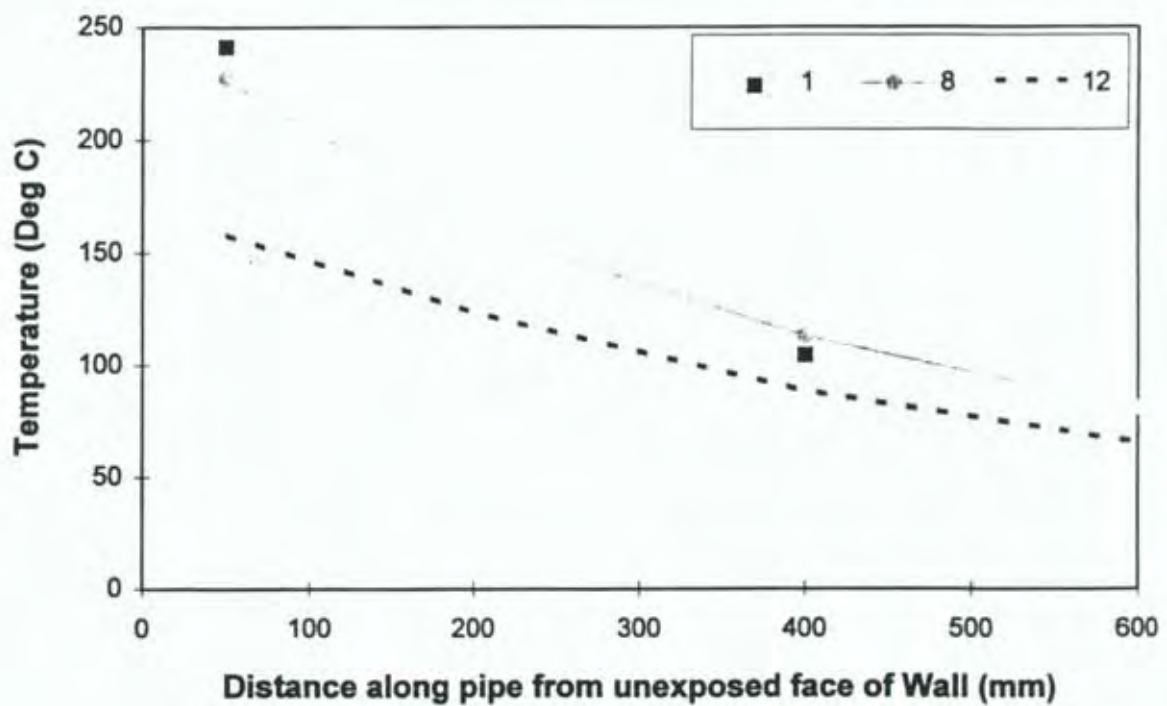
Measured temperature profiles along the pipes are presented in this Appendix for times 30, 90 and 210 minutes. Zero distance corresponds to a point in the unexposed face of the wall with positive values indicating greater distance from the furnace. Hence, where a thermocouple was used at mid-wall thickness, this is plotted as a negative distance.

The temperatures at 30 minutes near the unexposed face have been influenced by water flowing down the wall, as observed at this time.

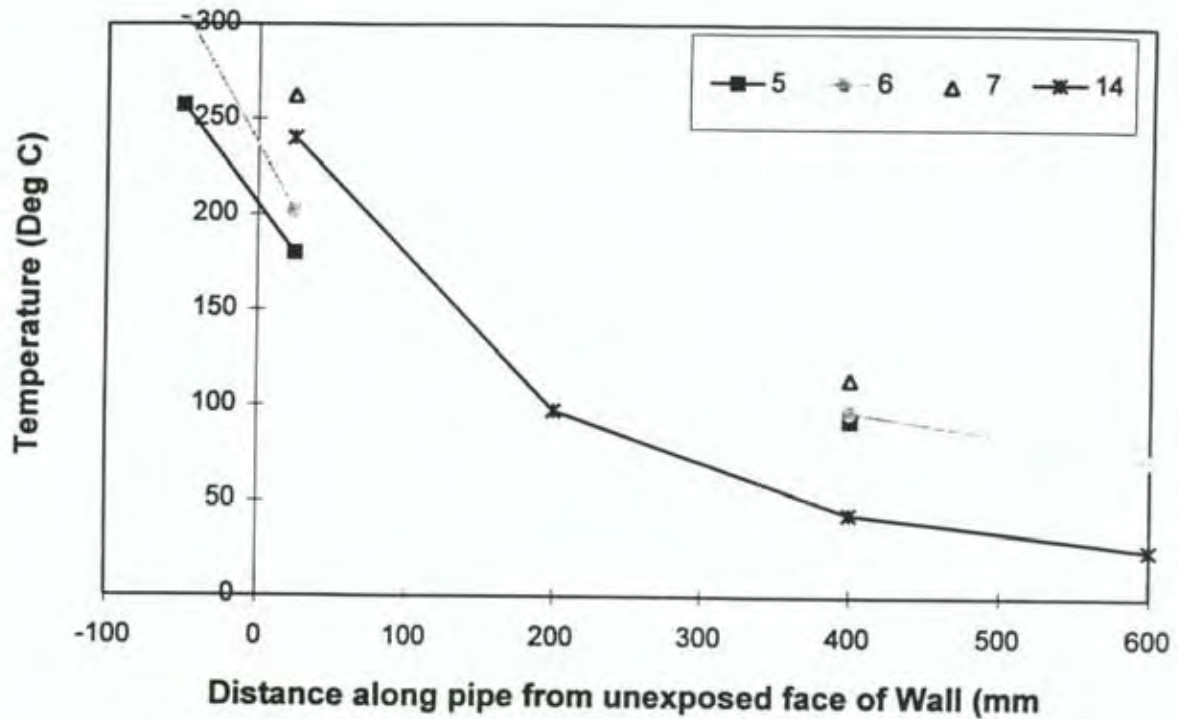
Temperature Profiles @ 30 mins, Pipes 1,2,3 & 4



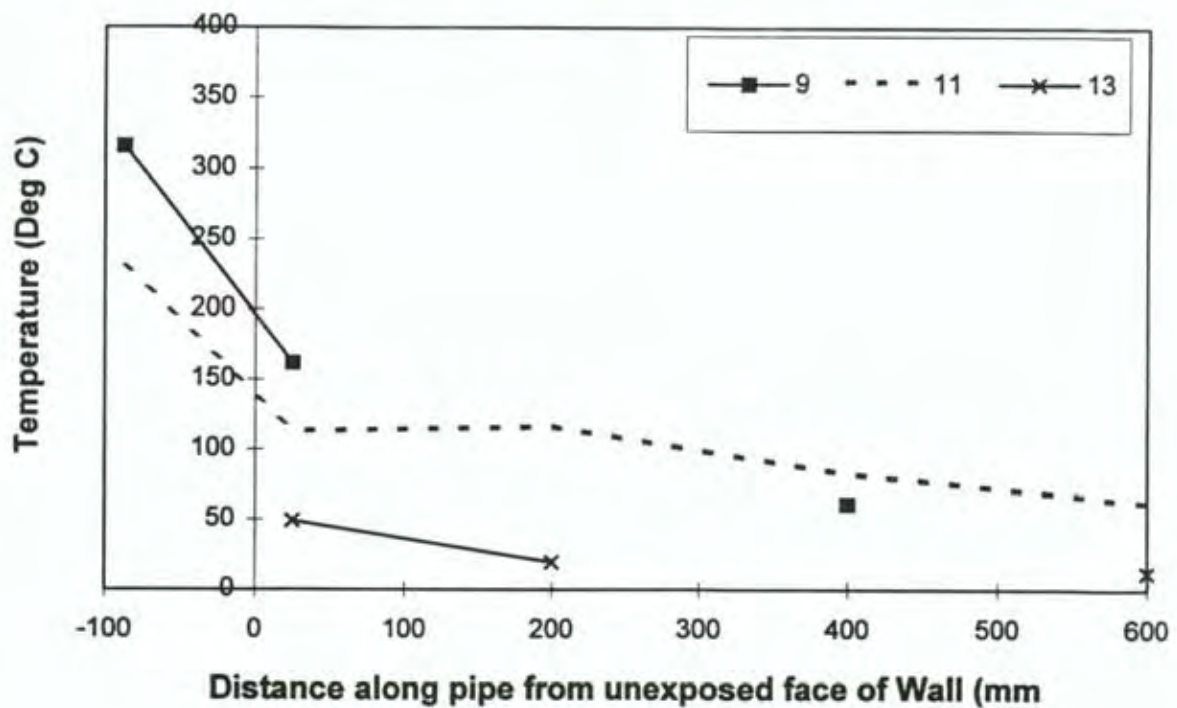
Temperature Profiles @ 30 mins, Pipes 1,8 & 12



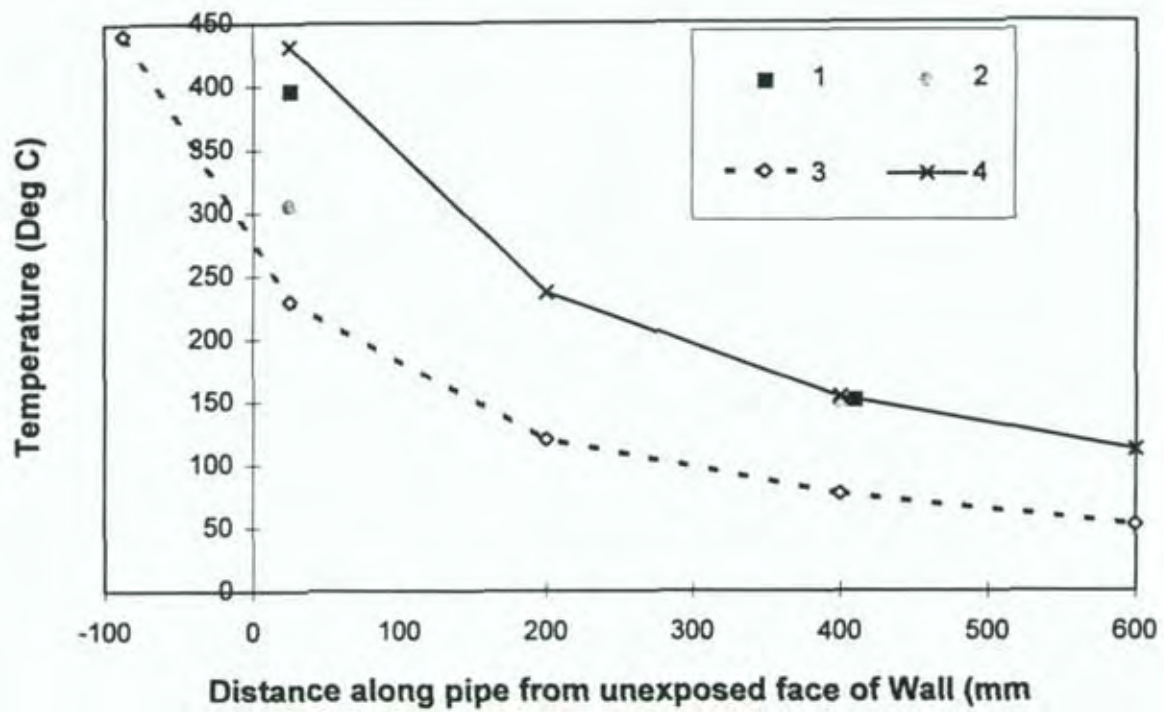
Temperature Profiles @ 30 mins, Pipes 5,6,7 & 14



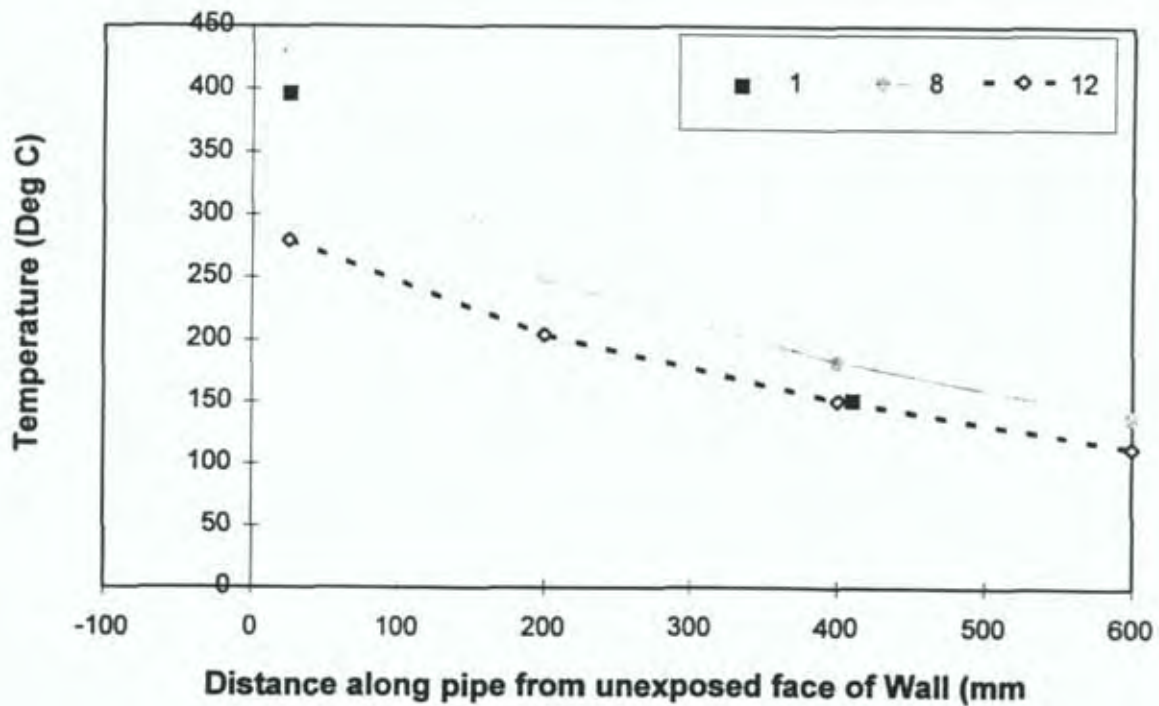
Temperature Profiles @30 mins, Pipes 9,11 & 13



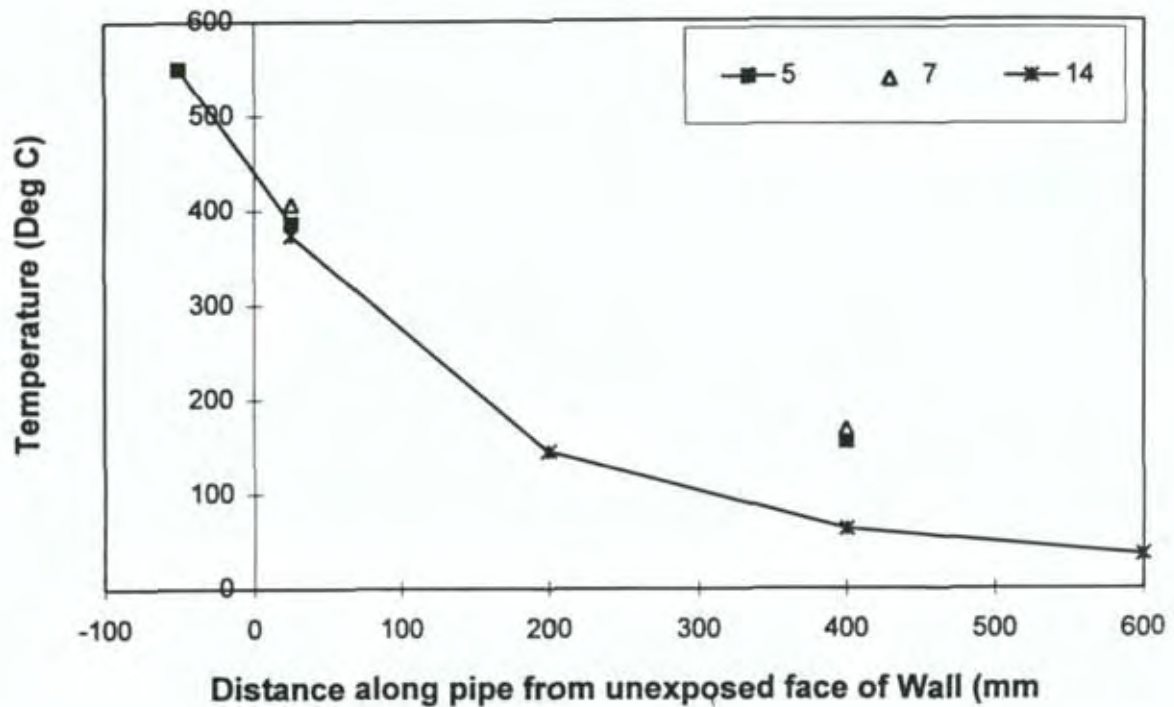
Temperature Profiles @ 90 mins, Pipes 1,2,3 & 4



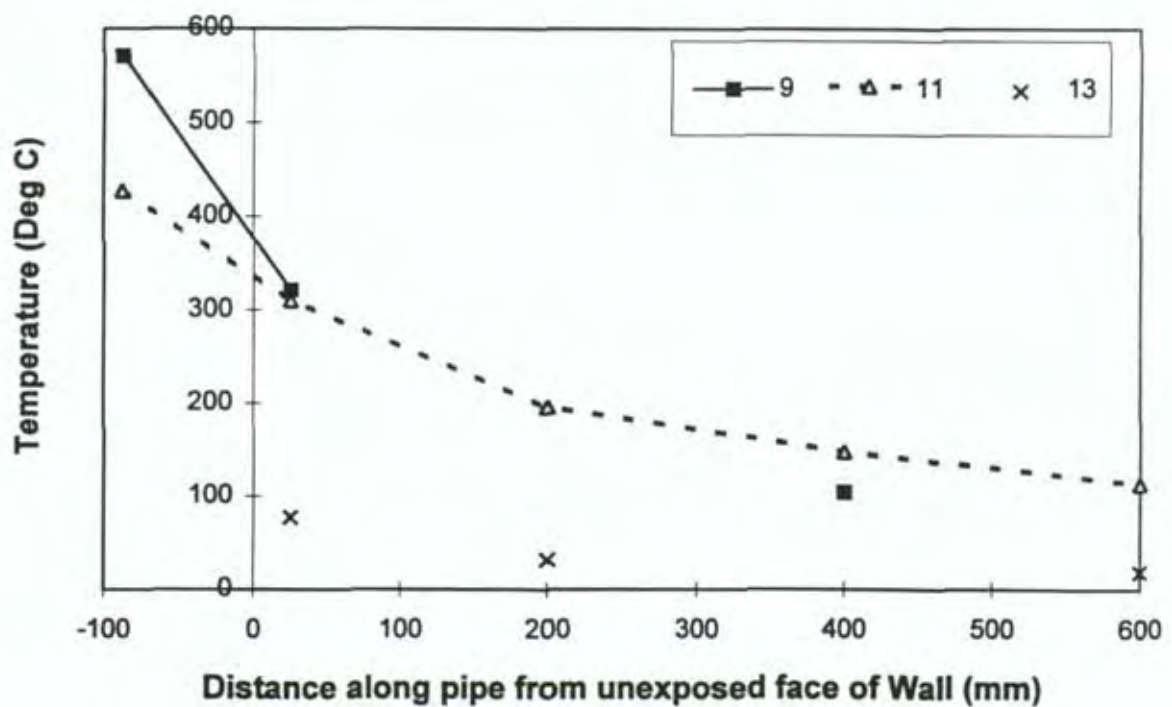
Temperature Profiles @ 90 mins, Pipes 1,8 & 12



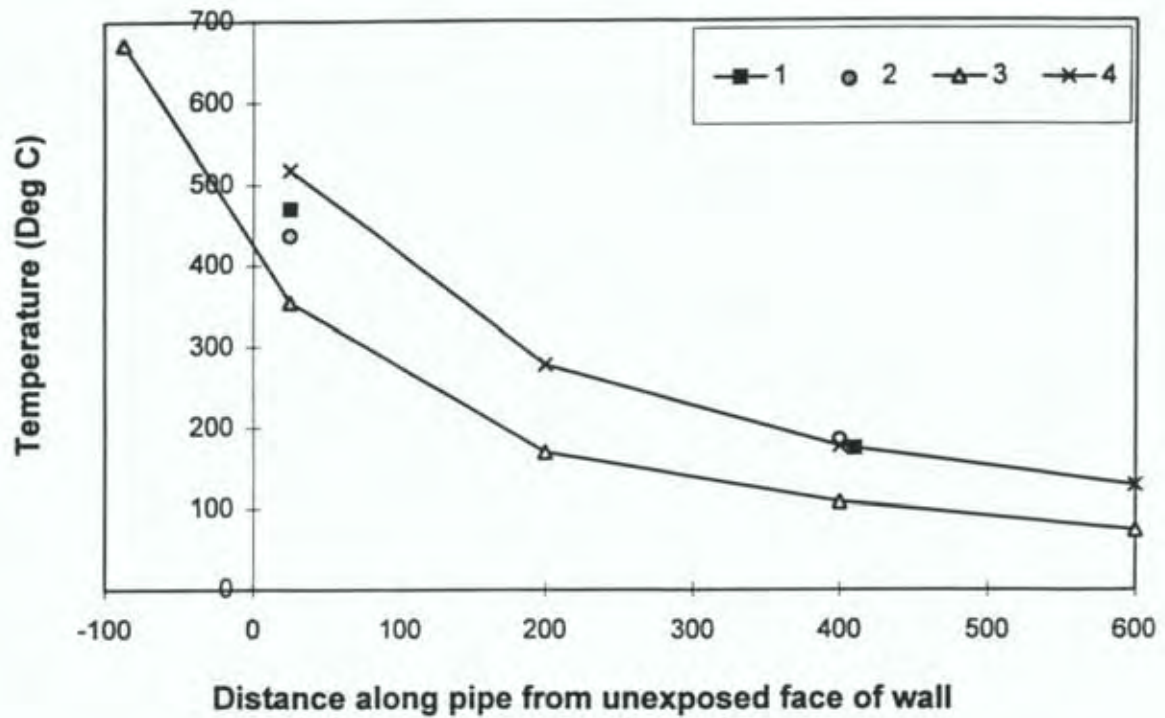
Temperature Profiles @ 90 mins, Pipes 5,6,7 & 14



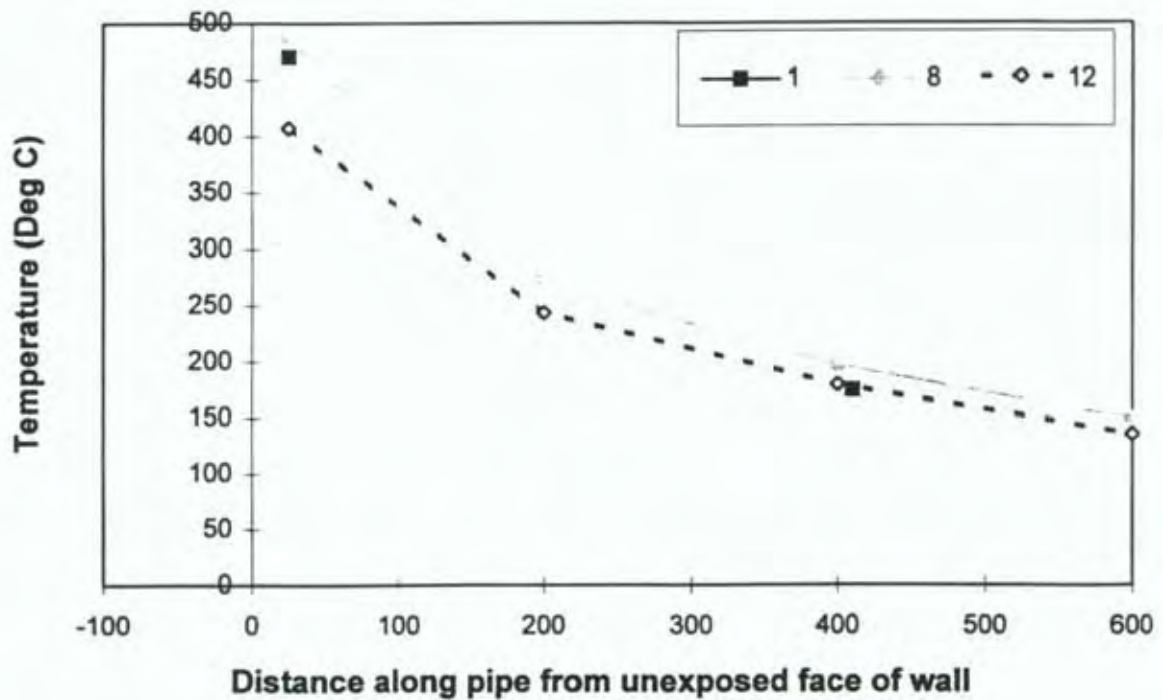
Temperature Profiles @ 90 mins, Pipes 9,11 & 13



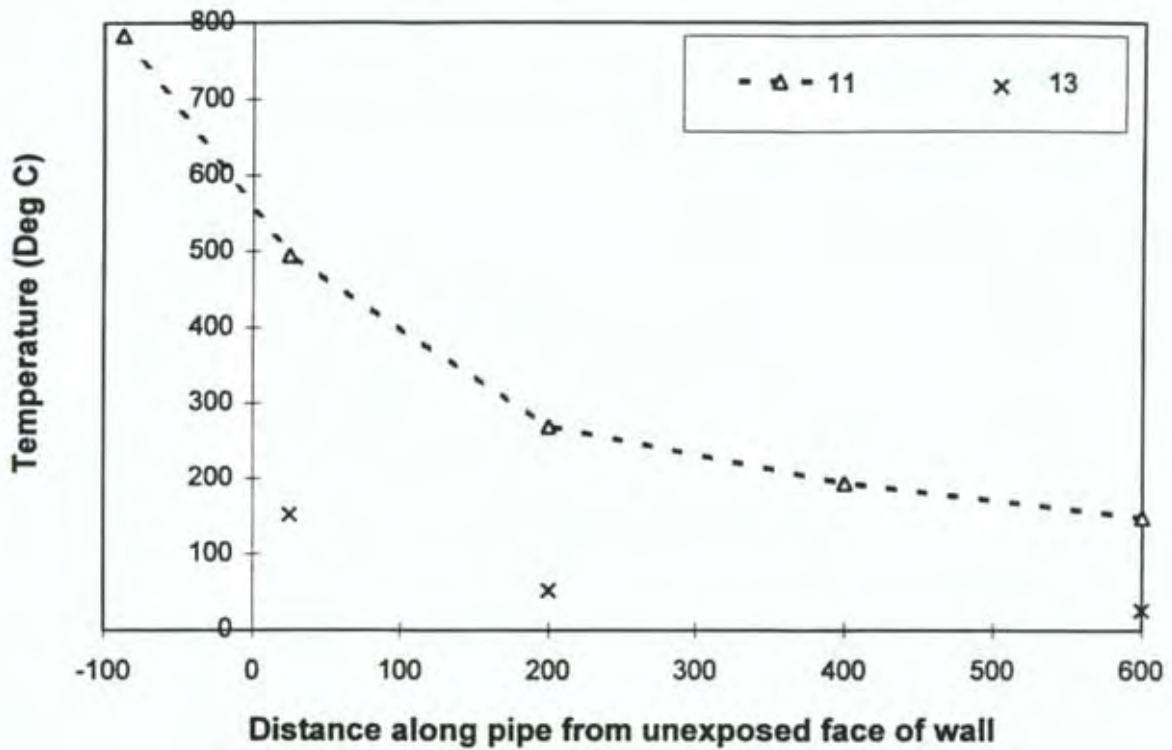
Temperature Profiles @ 210 mins, Pipes 1,2,3 & 4



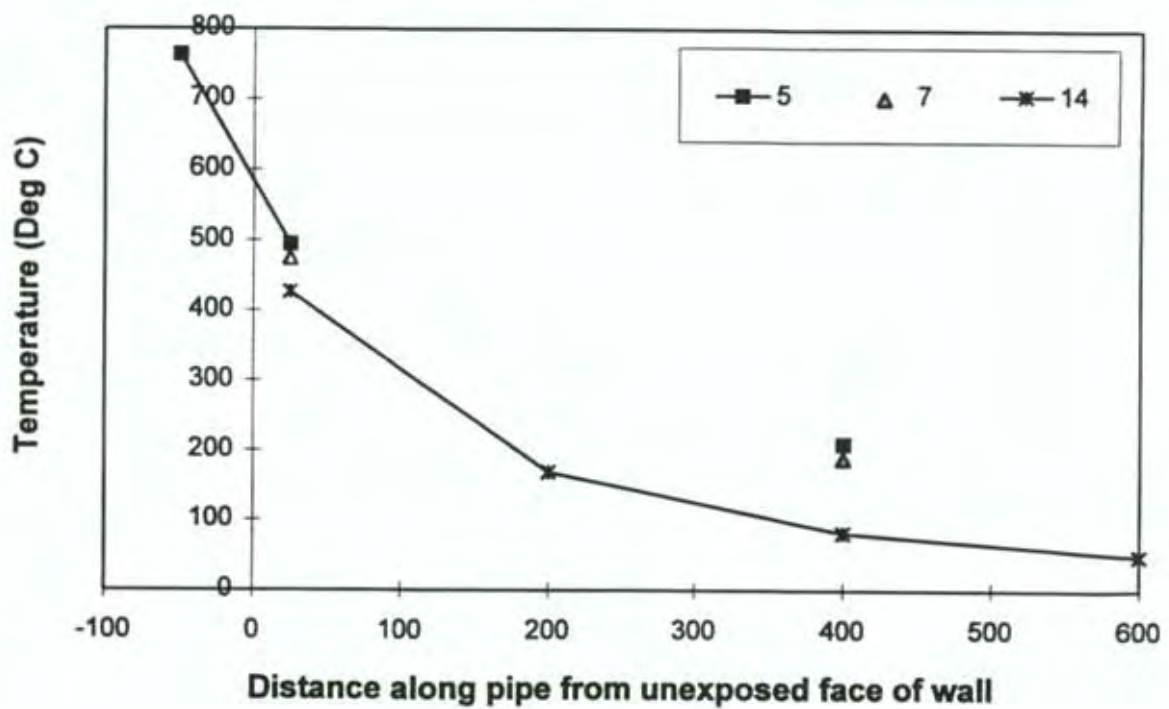
Temperature Profiles @ 210 mins, Pipes 1,8 & 12




Temperature Profiles @ 210 mins, Pipes 9, 11 & 13



Temperature Profiles @ 210 mins, Pipes 5,6,7 & 14





Modelling fire behaviour of metal pipe
penetrations through concrete walls
THURSTON, Stuart J.
Jul 1996 34859



BRANZ MISSION

To be the leading resource for the development of the building and construction industry.

HEAD OFFICE AND RESEARCH CENTRE

Moonshine Road, Judgeford
Postal Address - Private Bag 50908, Porirua
Telephone - (04) 235-7600, FAX - (04) 235-6070

REGIONAL ADVISORY OFFICES

AUCKLAND

Telephone - (09) 526 4880
FAX - (09) 526 4881
419 Church Street, Penrose
PO Box 112-069, Penrose

WELLINGTON

Telephone - (04) 235-7600
FAX - (04) 235- 6070
Moonshine Road, Judgeford

CHRISTCHURCH

Telephone - (03) 366-3435
FAX (03) 366-8552
GRE Building
79-83 Hereford Street
PO Box 496